8-22-2014

Proximal Aberrant Crypt Foci as a Surrogate Marker of Colorectal Cancer Risk

David Alden Drew
University of Connecticut - Storrs, dave@davidadrew.com

Proximal Aberrant Crypt Foci as a Surrogate Marker of Colorectal Cancer Risk

David Alden Drew, PhD

University of Connecticut, 2014

Colorectal cancer (CRC) prevention using screening colonoscopy relies upon the identification and removal of precancerous polyps or adenomas. Recently, an increase in CRC cases has been observed in individuals who have undergone screening colonoscopy before their next prescribed screening or surveillance interval, underscoring inherent limitations of routine colonoscopy as a complete preventive measure. Increasing evidence suggests that these "interval cancers" are most likely the product of missed or overlooked precancerous lesions. Specifically, interval cancers have a predilection for the proximal colon and their molecular features are associated with serrated polyps, lesions that due to their endoscopic morphology are difficult to detect and completely resect. To determine risk factors for precancerous lesions, especially those hard to detect endoscopically, we have performed a retrospective analysis of a gastroenterologist's endoscopy practice in central Connecticut. Using statistical models, we associate demographic and lifestyle factors with polyp occurrence, pathology and colonic location. Interestingly, we demonstrate a potent interaction between smoking history and daily aspirin use that predicts polyp incidence and multiplicity. This finding has important clinical implications, as aspirin is a putative chemoprevention agent for CRC, yet this protective effect may be limited to certain sub-populations of patients.

David Alden Drew – University of Connecticut, 2014

Aberrant crypt foci (ACF) are macroscopic epithelial abnormalities that occur within the human colon and may represent the earliest precancerous lesion detectable by high-definition chromoendoscopy. ACF exhibit pathologic and molecular abnormalities similar to those observed in advanced neoplasia. Therefore, they may serve as an important surrogate marker for CRC risk, but recently their reliability has been questioned and they have rarely been studied in the proximal colon. We describe a comprehensive clinical trial designed to characterize human ACF molecularly and pathologically, in context of colonic location. Novel techniques, combining microdissection with nanoproteomic and high-throughput mass spectrometry-based genotyping platforms, were established as effective methods to detect mutations and measure downstream signaling consequences within biopsy specimens. Proximal ACF are demonstrated to be frequently dysplastic, possess oncogenic mutations and associate with synchronous neoplasia and ACF multiplicity. As such, they may serve as a surrogate marker of the at-risk colonic mucosa and, importantly, may represent a subset of the missed lesions that contribute to interval cancers. With careful consideration of these studies, clinicians may identify individuals who may benefit from shorter surveillance intervals or advanced endoscopic approaches, such as high-definition chromoendoscopy.

Proximal Aberrant Crypt Foci as a Surrogate Marker of Colorectal Cancer Risk

David Alden Drew

B.S., Rensselaer Polytechnic Institute, 2009

A Dissertation

Submitted in Partial Fulfillment of the

Requirements for the Degree of Doctor of Philosophy

at the

University of Connecticut

2014

APPROVAL PAGE

Doctor of Philosophy Dissertation

Proximal Aberrant Crypt Foci as a Surrogate Marker of Colorectal Cancer Risk

Presented by

David Alden Drew, B.S

Major Advisor_____

Daniel W. Rosenberg, Ph.D.

Associate Advisor_____

Blanka Rogina, Ph.D.

Associate Advisor_____

Kevin Claffey, Ph.D.

Associate Advisor_____

Charles Giardina, Ph.D.

Outside Reader: Michael O'Brien, M.D., Boston University Medical College

University of Connecticut

2014

To my wife, Katelyn Dannheim Drew, for your never-ending love and support

and

In loving memory of those we have lost to cancer …

My grandfather, William “Grandad” Parker,

My aunt and godmother, Mary Parker

Patrick Johnston

ACKNOWLEDGEMENTS

I would like to thank Dr. Daniel Rosenberg for the opportunity to conduct my dissertation research in his laboratory, where I was given the support and direction to pursue this challenging thesis project. I greatly appreciate the respect and freedom given to me to pursue independent research theories as they arose, as well as the trust to manage such an important clinical trial.

My thanks goes to Drs. Joseph Anderson, Bruce Brenner, and, especially, Thomas Devers, our skilled gastroenterologists who tirelessly counted ACF specimens and to those individuals who volunteered for our study, whom without, this dissertation would not be possible. Special thanks to Dr. Devers for constantly challenging our understanding of the field and providing clinical guidance.

I would like to acknowledge the members of the Rosenberg laboratory, both past and present, for their support through the years, specifically Matthew Hanley, Nicole Horelik, and Allen Mo whom without the ACF clinical trial would be of little success.

I would like to further acknowledge, Dr. James Grady and Guhyeong Goh, for their statistical wisdom and patience, as well as Dr. Richard Stevens for his many helpful conversations and advice as I navigated an epidemiological study for the first time.

I extend my sincere gratitude to my committee members: Drs. Kevin Claffey, Charles Giardina and Michael O'Brien for their guidance during the course of this project, and especially to my committee chair, Dr. Blanka Rogina, for her constant support and guidance through the process.

And importantly, I'd like to thank my family and friends for their encouragement, understanding, and support on this journey. Specifically, a huge thank you to my parents, Jim and Debbie, and my brother, Kevin, for always encouraging me to challenge myself.

Table of Contents

LIST OF FIGURES

Page number for figure denoted, legends precede the figure by one page

LIST OF TABLES

CHAPTER 1

INTRODUCTION

1.1 OVERVIEW OF COLORECTAL CANCER

1.1.1 Colorectal cancer epidemiology

Colorectal cancer (CRC), or cancer of the large intestine, is currently the third most common cancer in the United States. In 2014, it is estimated 136,830 individuals will be diagnosed with CRC resulting in approximately 50,000 deaths. Age is strongly associated with CRC incidence, with more than a third of all CRC deaths occurring in the population aged 80 years or older. The death rates are higher in black populations and lowest in Asian individuals. Men have a slightly higher lifetime probability of receiving a CRC diagnosis (5.0%) compared to women (4.7%)[1].

In Connecticut, CRC incidence is approximately equivalent to the national average (50.2 and 50.9 cases per 100,000, respectively, in non-Hispanic, white males), but has the second lowest CRC mortality rates in the nation (16.2). The incidence trends compared to the national rates are similar for non-Hispanic white women. Nationally, incidence rates have been declining over the past two decades; and at a slightly higher rate over the last 10 years compared to the 1990s. This is largely believed to be due to improved access to screening methods and widespread-use of detailed surveillance guidelines. Still the public health concern remains as

CRC ranks third among all cancer deaths with only an approximate 65% five-year survival rate, necessitating further advances in cancer screening and early detection[1].

1.1.2. Colorectal carcinogenesis – pathways to cancer.

The majority of CRC cases are sporadic in origin, not inherited, despite the fact that family history of CRC is an established risk factor the disease. Vogelstein and Fearon provided a paradigm for sporadic CRC tumorigenesis in 1990 [2]. This 'traditional', or 'classical', pathway describes the step-wise accumulation of spontaneous or induced genetic alterations over the course of 10-15 years. Among cancer researchers, this adenoma-carcinoma sequence is also commonly called the 'Vogelgram' in reverence to its founding father. Mutational activation of oncogenes or inactivation of tumor suppressors leads to the formation of low-grade dysplastic tumors, or 'adenomas', that subsequently develop into high-grade dysplastic tumors, or 'carcinoma-*in-situ*' (CIS), and ultimately undergo malignant transformation. The majority (65-75%) of CRC is believed to develop via this pathway[3]. A detailed discussion of adenoma pathology and their endsoscopic morphology are provided in the next section.

Over the last two decades, an 'alternative' pathway for CRC tumorigenesis has been established. Under this model, CRC develops from pathologically distinct precancerous polyps and separate molecular mechanisms from those described by Vogelstein. Early oncogenic mutations or epigenetic aberrations lead to the formation of hyperplastic (non-dysplastic) lesions prior to malignant transformation. Many of these lesions' crypts display a 'serrated', or saw-tooth-like appearance, leading to the pathway being commonly called the 'serrated' pathway. This pathway may be responsible for up to 30% of CRC by the most liberal estimates; more

conservative estimates suggest the incidence is closer to a still significant, 20%[4]. A discussion of serrated polyps, their endoscopic morphology, and their distinct molecular mechanisms from traditional adenomas are provided in the following sections.

The minority (~5%) of CRC is the result of inherited germ-line mutations to key CRC-associated genes. The two most commonly inherited CRC disorders are familial adenomatous polyposis (FAP) and hereditary non-polyposis colorectal cancer (HNPCC), or Lynch syndrome. FAP is caused by inherited mutations to the *Adenomatous polyposis coli (APC)* gene, HNPCC is due to mutations in mismatch repair (MMR) genes including *hMLH1, hMSH2, hMSH3, hMSH6, hPMS1,* and *hPMS2* [5]. These cancers are still believed to follow the pathologic progressions laid out by the two distinct pathways. FAP CRCs distinctly follow the adenoma-carcinoma sequence, while Lynch syndrome lesions may follow either pathway depending on the early genetic mutations that occur.

1.1.3 Polypoid and nonpolypoid lesions of the colorectum.

Colorectal lesions fall under two broad categories that align with their pathways to CRC: traditional adenomas and serrated polyps (**Figure 1**). Traditional adenomas, or simply 'adenomas', are prevalent in a quarter of the population by age 50 and approximately half by age 70[6]. Traditional adenoma's main pathologic criteria are cellular hyperproliferation with the presence of cytologic dysplasia. Microscopically, crowded, hypercellular colonic crypts with elongated, enlarged, and pencil-shaped nuclei characterize this low-grade dysplasia **(Figure 2)**. Nuclei are also pseudostratified with hyperchromasia. The presence of other features such as complex crypt architecture, loss of cellular polarity and nuclear pleomorphism signify high-grade

Figure 1. Pathways to CRC. Two distinct pathways of CRC are defined by their precancerous lesions. *Left*; the traditional adenoma-carcinoma sequence as proposed by Vogelstein *et al.* and is believed to be responsible for approximately three-quarters of CRC cases. *Right*; the alternative serrated pathway to CRC as proposed by Jass *et al.* responsible for up to the remaining quarter of CRC cases. Less than five percent of CRCs are the result of an inherited CRC genetic disorder, but these CRCs will still follow one of the two pathways depending on their genetic alterations.

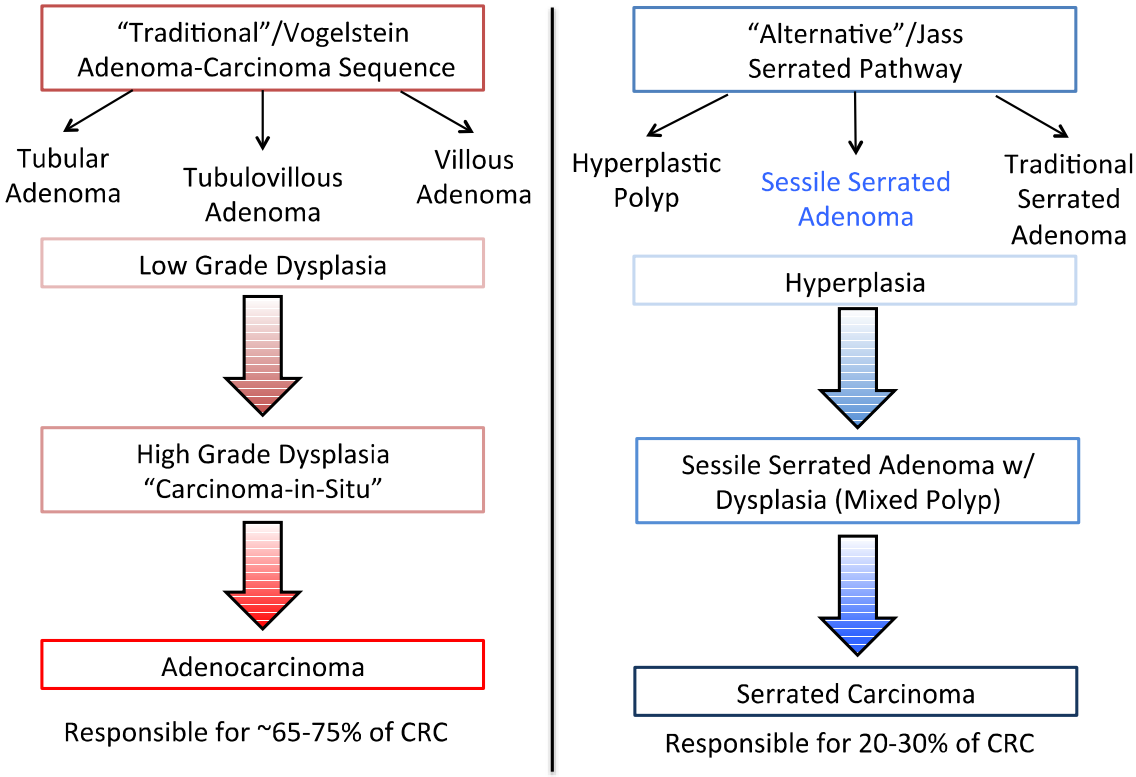
"Traditional"/Vogelstein
Adenoma-Carcinoma Sequence
Tubular Adenoma
Tubulovillous Adenoma
Villous Adenoma
Low Grade Dysplasia
High Grade Dysplasia
"Carcinoma-in-Situ"
Adenocarcinoma
Responsible for ~65-75% of CRC
"Alternative"/Jass
Serrated Pathway
Hyperplastic Polyp
Sessile Serrated Adenoma
Traditional Serrated Adenoma
Hyperplasia
Sessile Serrated Adenoma w/
Dysplasia (Mixed Polyp)
Serrated Carcinoma
Responsible for 20-30% of CRC

Figure 2. Representative photomicrographs (H&Es) of polyps and adenomas depicting characteristic cellular architectures.

A-C) Hyperplastic polyp (**A,** x100), showing simple tubular crypts oriented towards the muscularis mucosa (**A**) and a symmetrical proliferative zone at the base of the crypts with serration of the lining cells (**B,** x200; **C** x400, arrowheads**).**

D, E) Sessile serrated adenoma (**D,** x100), high power reveals a predominance of micro-vesicular cytologic features within the cells lining the crypts **(E,** x200, white arrowheads**)** and have complex crypt structure oriented towards the muscularis mucosa (**D**, black arrowheads) with an asymmetrical proliferative zone extending to the side-wall (**E**, black arrowheads).

F) Combined (mixed) dysplastic-sessile serrated adenoma (x100). Note a serrated lesion on the left side of the field without dysplasia (black arrowhead), combined with low-grade dysplasia tubular adenoma on the right side of the field (white arrowhead). Such lesions suggest possible progression of serrated lesions to dysplasia and carcinoma.

G, H) Tubular adenoma with low-grade dysplasia. Note smooth non-serrated lumen of the crypts and orientation in various directions. Details of cytologic dysplasia are evident (**H,** x200), characterized by elongated, cigar-shaped hyperchromatic nuclei with high N/C ratio.

K) Presence of the serrated pattern in a tubular adenoma (x100).

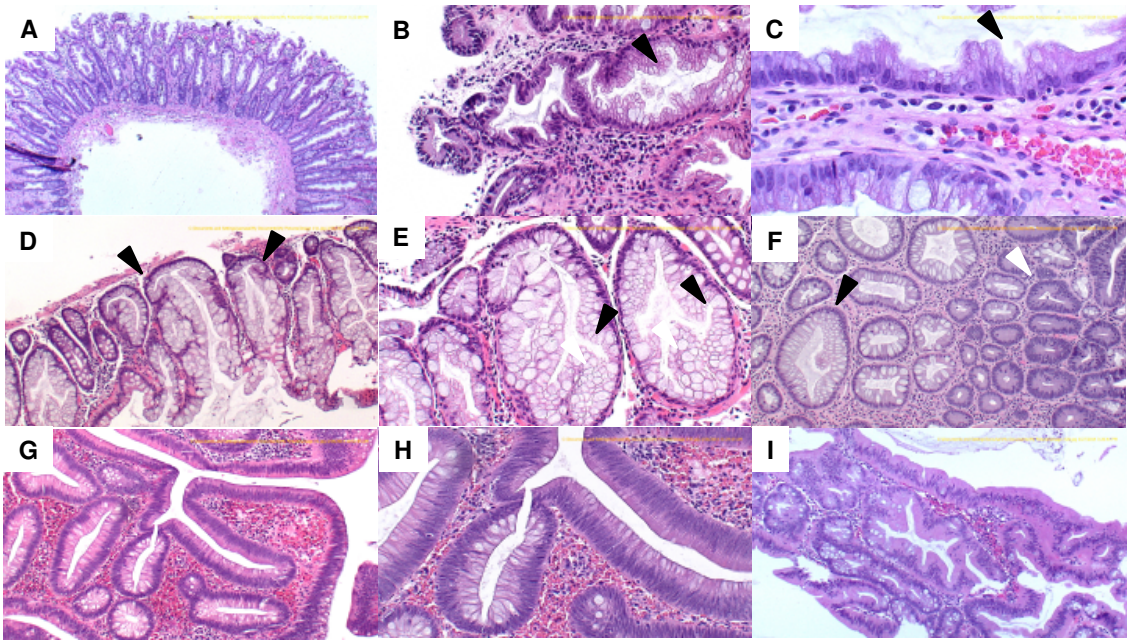
A
B
C
D
E
F
G
H
I

dysplasia or a CIS. Traditional adenomas are classified into three distinct pathologic sub-types: tubular adenomas (TA), tubulovillous adenomas (TVA), and villous adenomas (VA) (**Figure 1**, *left*). TAs have a distinct tubular-shaped crypt architecture that is more or less irregular or branched. VAs' crypts have villi- or finger-like projections of dysplastic epithelium with a thin fibro-vascular core. TVAs show both tubular and villous crypt architectures. A summary of the World Health Organization's (WHO) pathologic criteria for each of these lesions can be found in the appendix[7]. Endoscopically, tubular adenomas tend to be smaller, pedunculated polyps while villous adenomas tend to be larger and sessile (flat or non-polypoid)[8]. Cancers arising from these lesions are more prevalent in the distal colorectum (from splenic flexure to rectum, including the descending and sigmoid colon) [9].

Serrated polyps (SPs) have recently been recognized as a premalignant or neoplastic lesion. Originally thought to be benign due to their lack of dysplasia, they are now considered a precancerous lesion due to the presence of distinct CRC molecular signatures within these polyps. A discussion of the divergent molecular pathways between adenomas and SPs follows in the next section. With few examples of a clear histologic link between SPs and CRC, it remains unclear exactly when or how dysplasia develops in these lesions and how quickly they undergo malignant transformation. The pathologic guidelines for SP classification have been undergoing constant refinement for the past decade. Therefore, their prevalence in the population has been difficult to accurately quantify[10]. However, it is believed they account for approximately 25% of the polyps in the population[11]. SPs are currently classified by the WHO into three histologic categories: hyperplastic polyp (HP), sessile serrated adenoma/polyp with or without cytological dysplasia (SSA), or traditional serrated adenoma (TSA). Serrated refers to the microscopic

appearance of the crypt upon transverse section, where cellular hyperproliferation, or hyperplasia, leads to the appearance of a serrated or saw-tooth lumenal surface. Upon cross-section these crypts have a stellate or star-like luminal appearance[7]. Detailed pathologic descriptions of SPs can be found in the appendix.

HPs and SSAs both have elongated proliferative zones and the presence of serration. HPs are the most common of the SPs (~80% of all SPs) and typically have a lower degree of serration and a straight, non-distorted crypt architecture from the luminal surface to the muscularis mucosa (**Figure 2 A-C**). HPs are sometimes further classified into microvesicular hyperplastic polyps (MVHP), characterized by small droplet mucin within the epithelial cytoplasm with few goblet cells, and goblet cell hyperplastic polyps (GCHP), characterized by an overabundance of goblet cells and absence of cytoplasmic mucin. Endoscopically, HPs are typically flat or sessile, small (<5mm), more frequent in the distal colon and are mostly considered to be benign[11].

SSAs (~20% of all SPs) typically have a higher degree of serration extending throughout the crypt compared to HPs (**Figure 2 D&E**). They are specifically characterized by the presence of disorganized crypt architecture, resulting in crypts becoming dilated or branched, particularly in the base of the crypts (**Figure 2 D&E**, *black arrowheads*). Endoscopically, these lesions are sessile or flat, as their name implies, larger than 5 mm in size and are typically located in the proximal colon (from cecum through the transverse colon up to the splenic flexure, including the ascending colon and the hepatic flexure)[11]. Additionally, these lesions are commonly associated with the presence of a mucous coating or 'mucous cap'[12].

SSAs traditionally are non-dysplastic, but occasionally SSAs will have foci of traditional adenoma-like dysplasia (**Figure 2F**). These polyps were previously termed 'mixed polyps', but for the sake of clarity, should not convey that crypts of the polyp have both serrated and dysplastic features within the same crypt. Instead, within the polyp there are areas that resemble SSA histologically and immediately adjacent areas, with an abrupt transition, that resemble traditional adenomas. When crypts show both tubulovillous features and serrated lumenal surfaces within a polyp, the polyp is considered a TSA (**Figure 2 G&H**). These lesions are very rare, accounting for less than 2% of all SPs. Endoscopically, TSAs can be sessile or pedunculated, are usually larger than 5 mm in size and are distally located. They are, however, considered to be precancerous lesions [11].

1.1.4 Molecular mechanisms of carcinogenesis.

The adenoma-carcinoma sequence as originally described by Vogelstein provides a step-wise accumulation of genomic aberrations leading to the formation of malignant carcinomas. The process begins with an early inactivation mutation of the *APC* gene causing a truncation of the APC protein within a colonic epithelial cell. This is typically caused by a point or frameshift mutation in the "mutation cluster region", or the gene region between nucleotides 1263-1589 which encompasses the β-catenin binding motif [13]. The APC protein is an important negative regulator of β-catenin, an important downstream molecule of the canonical Wnt signaling pathway. β-catenin performs dual roles within a cell, supporting cell adhesion as well as transcriptional activation of the TCF/LEF family of transcription factors that are responsible for numerous cell processes including cell proliferation and differentiation. Under normal conditions, the cytoplasmic pool of β-catenin is stabilized through the action of the APC-Axin-

glycogen synthase-3β (GSK3β) complex, which phosphorylates β-catenin targeting it for ubiquitination and subsequent degradation. When the APC protein is truncated as a result of mutation, the APC-Axin-GSK3β destruction complex cannot be formed leading to cytoplasmic accumulation of β-catenin and its subsequent nuclear translocation driving aberrant transcription. These mutant cells can undergo monoclonal expansion causing focal dysplasia within the colonic epithelium [3].

Cellular proliferation is further accelerated through the constitutive activation the mitogen-activated protein kinase(MAPK) signaling cascade. The RAS/RAF/MAPK signaling pathway mediates cellular proliferation in response to extracellular growth factor receptor (*e.g.* EGFR, FLT3, ERBB2) signals. Oncogenic mutations to the RAS family – *KRAS, HRAS, and NRAS* – commonly occur within many different human cancers. Mutations to the RAS family of genes result in constitutive activation of downstream proteins (including MEK1/2 and ERK1/2) and aberrant cellular proliferation[14]. *KRAS* mutations (point mutations within codons 12 and 13) are commonly associated with traditional adenomas considered an early initiating event in the Vogelgram as they are found in ~40% of CRC[3].

As adenomas form from dysplastic foci, additional genomic and genetic aberrations will begin to accumulate as a result of the uncontrolled proliferation. As a result, many adenomas may develop a chromosome instability (CIN) phenotype leading to additional loss of gene function via mutation or chromosomal loss. It has been acknowledged that the order of early stage mutations are less important in terms of progression, but instead the quantity of molecular aberrations. The *TP53* gene is an important tumor suppressor gene implicated in the Vogelgram

and definitively believed to be one of the last events, just prior to the adenoma-carcinoma transition. p53 is activated in response to cell stressors causing cells to respond to damage by upregulating DNA repair pathways or inducing senescence or apoptosis. Mutations to p53 are detected in up to 70% of CRC[3].

The serrated pathway, while believed to be a step-wise progression like the adenoma-carcinoma sequence, has a distinct subset of associated molecular abnormalities specific to serrated carcinoma development[15]. The requirements for SP initiation and progression include MAPK pathway activation and aberrant genomic promoter methylation, termed CpG island methylator phenotype (CIMP). MAPK constitutive activation occurs primarily through mutations to *BRAF* (*V600E* mutation), but can also be the result of *KRAS* (codons 12 and 13) mutation. BRAF mutations primarily occur in MVHPs and SSAs, while KRAS mutations are primarily found in TSAs[4].

CIMP is determined by a panel of CpG islands, or regions of cytosine-guanine dinucleotide repeats, within CRC-associated tumor suppressor gene promoters that when hypermethylated lead to gene silencing[16,17]. Important CRC associated tumor suppressors, including p16 (*CDKN2a),* an important negative regulator of cyclin-dependent cell-cycle, and *MLH1* (as previously discussed with HNPCC) harbor CpG islands within their promoters and their loss may lead to serrated tumor progression. There are multiple degrees of CIMP depending on how many panel promoters exhibit hypermethylation, resulting in CIMP-high (CIMP-H) or CIMP-low (CIMP-L) classifications. Traditional adenomas tend to be CIMP negative ($CIMP^-$). The exact mechanism by which CIMP is acquired still needs to be determined, but upregulation

of DNA methyl-transferases (DNMTs) in response to increased proliferation or intake of dietary methyl donors (i.e. folate/folic acid) are putative explanations[4,16,17].

Microsatellite instability (MSI), is another feature commonly observed in serrated colorectal lesions, but infrequently described in traditional adenomas (microsatellite stable or MSS). MSI is determined by measuring the length of multiple mono-nucleotide repeats, or microsatellites, as a marker of genomic stability[18,19]. Patients with defects to MMR genes, not unlike those with Lynch syndrome, show high microsatellite instability. It is possible for this genomic instability to be acquired somatically, perhaps through methylation and subsequent loss of MLH1. MSI, like CIMP, has multiple classifications representative of the level of genomic instability, MSI-high (H) and MSI-low (MSI-L)[20]. Because MSI may be an acquired phenotype due to epigenetic silencing of MMR genes, it has been classified as an associated, but not required genetic abnormality for SP initiation [4].

As such serrated carcinomas are broadly classified into two categories: *BRAF* mutant, CIMP-H, and either MSS or MSI-H -or- *KRAS* mutant, CIMP-L, and MSS. The first class of carcinoma is strongly linked with the serrated pathway, making SSAs their likely precursor lesion. The second classification is presumed to arise from TSAs, which share these molecular characteristics. *BRAF* mutant, CIMP-H, MSI-H serrated carcinomas tend to be proximally located and may contribute significantly to interval colon cancers as discussed in the next section.[15,17,21,22]

1.2 PREVENTION OF COLORECTAL CANCER

In 1950, CRC was the most common cause of cancer death. Today it is the third leading cause of cancer deaths, in part because of changes in lifestyle, the introduction and widespread awareness of preventive measures, and advances in adjuvant therapies [1].

1.2.1. Colorectal cancer screening

Identification of precancerous lesions and routine polypectomy during endoscopy is credited with a subsequent lowering of CRC incidence[23,24]. However, despite increases in screening colonoscopy rates[25,26], CRC remains a leading cause of cancer deaths in the U.S. Standard preventive screening by total colonoscopy with bowel preparation is recommended for individuals who are aged 50+ years or have a history of CRC[27]. The traditional model of colon cancer pathogenesis provides a paradigm to explain the success of colonoscopy as a prevention tool. Because CRC develops slowly over decades, early neoplastic changes can be readily identified within the colon years before malignant transformation occurs[2]. Depending on the type of polyp removed during screening endoscopy, different surveillance intervals have been recommended by the American Gastroenterological Association **(Table 1)**[28].

Fecal occult blood tests are another widely used type of CRC screening. This method tests the stool for the presence of blood as a non-specific marker for CRC or advanced polyps or adenomas, but has been shown to significantly reduce CRC mortality in asymptomatic individuals[27,29].

Table 1. Surveillance interval guidelines based upon lesion pathology, size and multiplicity.

Lesions identified during baseline colonoscopy (most advanced finding)	Recommended Surveillance Interval* (in years, *assuming average risk)
No polyps	10
Small (<1 cm) HP in distal 20-cm of colon	10
1-2 small (<1 cm) TA	5-10
3-10 TA, regardless of size	<3
1+ TA, ≥ 1 cm	3
1+ VA, regardless of size	3
High-grade dysplasia or CIS	3
1+ Small SSA (<1 cm), no dysplasia	5
1+ SSA larger than ≥ 1 cm, no dysplasia	3
1+ SSA with dysplasia, regardless of size	3
1+ TSA	1

Table adapted from the American Gastroenterological Association's "Guidelines for Colonoscopy Surveillance after Screening and Polypectomy" (2012)[28]

Advanced screening techniques such as those that can enhance conventional endoscopy may be required to enhance screening efficacy and reduce CRC incidence and mortality. Technological advancement has provided clinicians with a number of tools including narrow band imaging, high-definition scopes, chromoendoscopy (the use of contrast dye during endoscopy) and virtual endoscopy (use of sonogram or radiography). All of which have been used in some clinical capacity but none have become widely used[11].

1.2.2. Interval or 'post-colonoscopy' CRC

During the past decade, there has been increased awareness of CRC cases that arise within the interval between colonoscopies[30,31]. Recently, it was demonstrated that the adenoma detection rate is inversely associated with these 'interval' colorectal cancers (iCRC), highlighting the importance of thorough index colonoscopies for CRC prevention and its inherent limitations[30]. As such, screening guidelines are continually reassessed as the spectrum of colonic polyps becomes more clearly defined, and as predictors for the development of these polyps are better understood[28].

Polyps contributing to iCRC may have an aggressive biological phenotype (i.e. those with multiple mutations or with CIMP-H and MSI-H), or are simply missed during screening colonoscopy, or a combination of both factors. In fact, recent studies have attributed more than 75% of iCRC to factors associated with inadequate colonoscopy rather than the rapid development of a new cancers,[24,32] highlighting the need for improved endoscopic observation. The growing consensus is that the majority of iCRC, especially in the proximal colon,[31,33,34] is the direct result of missed lesions during colonoscopy[24,32,35] as it inversely correlates with adenoma detection rates[30]. Therefore, in determining the risk factors

associated with iCRC, it is important to identify those risk factors that may be associated with the formation of colon lesions that most likely evade detection during colonoscopy.

The underlying pathology of missed precancerous lesions may partially explain why iCRC arises despite routine colonoscopic surveillance. The flat or depressed morphology of SPs make them difficult to detect endoscopically[11]. Recently, it was demonstrated that SPs have a number of additional morphologic characteristics that contribute to their evasiveness, including the presence of a mucous cap or a rim of debris or bubbles obstructing their detection during endoscopy[11,12,36]. Moreover, once detected, the sessile nature of these lesions makes their complete resection using snare polypectomy technically challenging due to the lack of defined visual borders. These morphological characteristics strongly implicate the presence of SPs, particularly in the proximal colon, as key contributors to iCRC. Therefore, more reliable predictors of all polyps, and specifically the serrated polyp subtype, require further investigation.

1.2.2 Risk Factors

Determinants of precursor lesions in the colon are presumably also risk factors for the development of cancer. Demographic factors including age, gender, and family history have been established as risk factors for polyps and subsequent cancer development[37]. The impact of smoking on CRC risk is of particular interest and has been studied for several decades[38]. Early epidemiological studies found conflicting risks from smoking, perhaps complicated by the particular population under study[39-42]. Overall, smokers have a modestly increased risk of CRC,[43] and of adenomatous polyps[44]. Importantly, smoking has been reported to be most strongly associated with the occurrence of serrated polyps[45,46]. Additional lifestyle factors

significantly increasing an individual's risk for CRC include alcohol consumption[47], obesity[48], and red meat consumption[49], among other dietary factors.

From a chemoprevention standpoint, natural agents or drugs may impact individual cancer risk. For example, aspirin and non-aspirin NSAIDs reduce the risk of CRC[50,51]. and also the occurrence of polyps[52], protective effects that may be mediated in large part through inhibition of cyclooxygenase activity[53]. Population-based studies have consistently shown benefit from long-term NSAID and, specifically, aspirin use for CRC and polyps[54-56]. Treatment of high-risk subjects with NSAIDs, such as ibuprofen, can also change the molecular features of adenomatous polyps as well[57].

1.3 ABERRANT CRYPT FOCI AS SURROGATE MARKERS OF COLON CANCER

Aberrant crypt foci (ACF) are the earliest morphologically distinct mucosal abnormality, a subset of which may be precancerous[58]. Endoscopically, ACF are defined as lesions that are typically flat, but may be depressed or slightly raised, <5 mm in diameter, and upon application of a contrast dye (e.g. indigo carmine or methylene blue) appear to have enlarged crypts with oval or slit-like lumens (**Figure 3**). Microscopically, ACF have multiple distinct pathologies that resemble those observed in advanced neoplasia[59,60]. They include a dysplastic subtype, most likely the dysplastic crypt focus as described by Vogelstein; as well as, two hyperplastic subtypes: serrated, similar to MVHPs, and non-serrated (distended), similar to GCHPs. Genetically, they share many of genetic abnormalities seen in advanced neoplasia and CRC, albeit with fewer molecular abnormalities found in a single lesion, consistent with a step-wise progression to CRC. To understand the earliest stages of CRC initiation, considerable effort has

Figure 3. Detection of ACF using high-definition chromoendoscopy. The use of contrast dye, either methylene blue (*top*) or indigo carmine (*bottom*) reveals the presence of foci of enlarged colonic crypts compared to the adjacent colonic epithelium. It is possible to biopsy single ACF for molecular and pathologic analyses with the use of biopsy forceps as shown by the single red arrow. In the foreground, (*two red arrows*) is an unbiopsied ACF, approximately 2 mm in diameter.

Methylene Blue

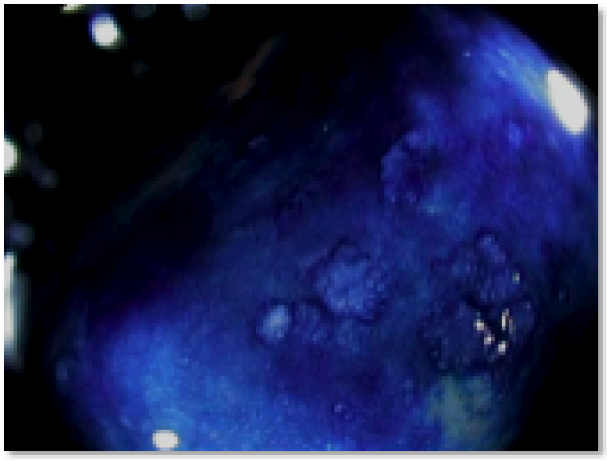

Indigo Carmine

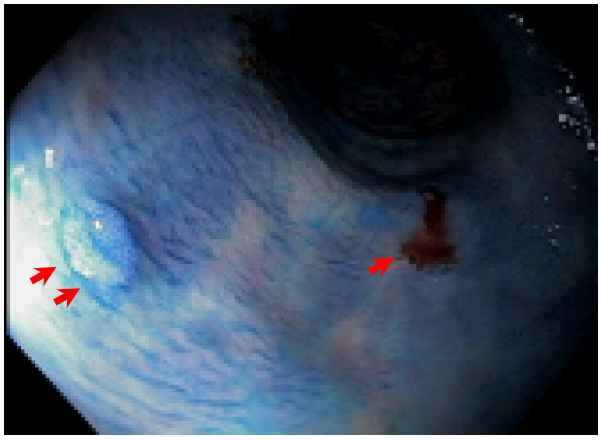

been focused on placing aberrant crypt foci within the context of both the traditional and serrated CRC pathways. The proposed role for ACF within CRC tumorigenesis is presented in **Figure 4**.

ACF were first described in 1987 within the murine colon following treatment with azoxymethane (AOM), a known colon carcinogen. Foci of aberrant crypts, with larger and thicker epithelial linings compared to adjacent normal crypts were described, with a multiplicity that associated directly with sensitivity to AOM and ultimately, tumor development. Upon their initial observation it was stated that "it will be important to investigate whether or not these crypts are present in human colons and if they are more frequent in populations possessing a higher risk for colon cancer than those at a lower risk".[58] At the time, they were postulated to be precursors to neoplastic lesions, at least within the murine colon[61]. A timeline of select findings for ACF is presented in **Figure 5**.

In 1991, human ACF were described for the first time in surgically resected colons [62,63]. Following their identification in human colons, it was postulated that "Since aberrant crypt foci appear to be the earliest identifiable putative precursors of colon cancer, they represent lesions that can be characterized further for the earliest genetic and biochemical alterations"[64]. This lead to many studies in the field aimed at molecularly characterizing ACF to determine their role in tumorigenesis. *APC* and *KRAS* mutations were among the first gene mutations to be detected in human ACF supporting their status as putative precursors of colorectal adenomas[65-67]. Evidence of microsatellite or genomic instability[68-70] and aberrant promoter methylation [71,72] has also been found in ACF. In 1997, the first report of ACF being detected endoscopically was described by Yokota *et al.*[73] It has been repeatedly demonstrated that *in*

Figure 4. Select highlights in the research of ACF between 1987 and 2008.

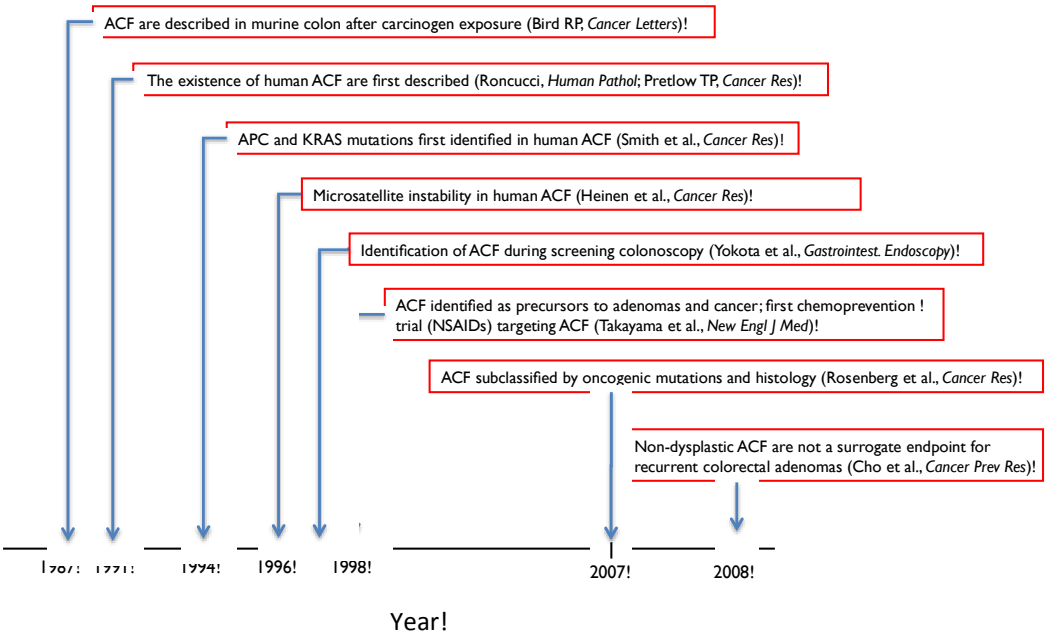
ACF are described in murine colon after carcinogen exposure (Bird RP, *Cancer Letters*)!
The existence of human ACF are first described (Roncucci, *Human Pathol*; Pretlow TP, *Cancer Res*)!
APC and KRAS mutations first identified in human ACF (Smith et al., *Cancer Res*)!
Microsatellite instability in human ACF (Heinen et al., *Cancer Res*)!
Identification of ACF during screening colonoscopy (Yokota et al., *Gastrointest. Endoscopy*)!
ACF identified as precursors to adenomas and cancer; first chemoprevention ! trial (NSAIDs) targeting ACF (Takayama et al., *New Engl J Med*)!
ACF subclassified by oncogenic mutations and histology (Rosenberg et al., *Cancer Res*)!
Non-dysplastic ACF are not a surrogate endpoint for recurrent colorectal adenomas (Cho et al., *Cancer Prev Res*)!
1996!
1998!
2007!
2008!
Year!

Figure 5. The proposed position of ACF within the pathways to CRC. ACF are the earliest putative precursor lesions on the pathway to CRC. Dysplastic ACF, or potential "microadenoma", most likely precede the formation of a traditional dysplastic adenoma (TA, TVA, or VA) and may ultimately be the precursors to 75% of CRC. Hyperplastic ACF, of which both serrated and distended (non-serrated) pathologic variants exist, are proposed precursors for SPs (HP, SSA, or TSA). It is unclear if hyperplastic ACF continue on to become SPs or potentially develop dysplasia and form micro-adenomas, as indicated by the *dashed arrow*.

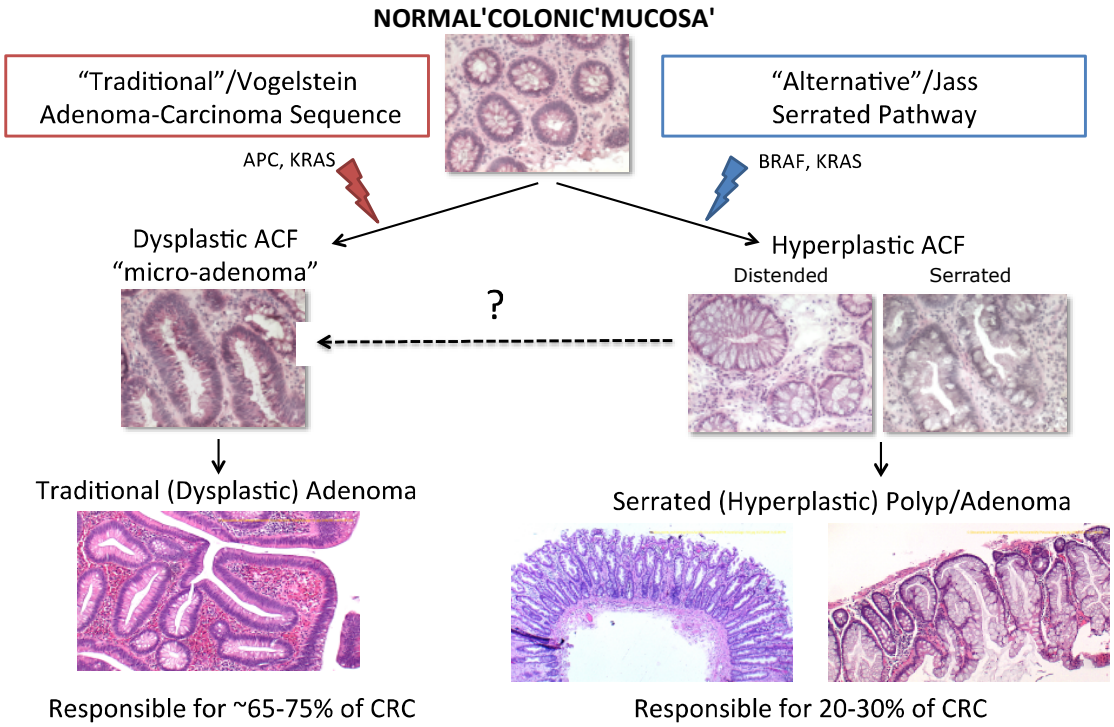
NORMAL'COLONIC'MUCOSA'
"Traditional"/Vogelstein
Adenoma-Carcinoma Sequence
"Alternative"/Jass
Serrated Pathway
APC, KRAS
BRAF, KRAS
Dysplastic ACF
"micro-adenoma"
Hyperplastic ACF
Distended
Serrated
?
Traditional (Dysplastic) Adenoma
Serrated (Hyperplastic) Polyp/Adenoma
Responsible for ~65-75% of CRC
Responsible for 20-30% of CRC

situ identification of ACF is possible with the use of dye-spray (e.g. indigo carmine or methylene blue) and magnifying or high-definition scopes (HD Chromoendoscopy)[60,73-75]. Evidence of BRAF mutations[60,76], the presence of multiple pathologies representative of neoplasia[59,60], and associations of ACF counts with known CRC risk factors[77] continued to compile over the decade, supplementing their precancerous potential.

ACF began to be widely used as endpoints in many chemoprevention studies or as measures of carcinogen exposure in dietary studies. The first study using ACF in a chemoprevention trial (NSAIDs including sulindac) as surrogate markers for adenomas and cancer was reported by Takayama *et al.* in 1998[78]. Many of the subsequent studies using ACF as endpoints focus on ACF multiplicity within the distal colorectum or the murine colon[79-82]. Despite the numerous evidence-based correlations between precancerous adenomas and CRC and ACF, their reliability as a biomarker of CRC began to be questioned[83]. One major concern limiting the acceptance of ACF as a surrogate marker was inter-rater variability and the overreliance on endoscopic counts of ACF[84]. Some in the field completely dismissed their utility as an accurate surrogate marker[85,86]; some came to the defense of ACF citing the need for more research before rendering a verdict on their fate[87,88]. Furthermore, many of the molecular studies of ACF, despite total colonic surveillance, restricted molecular and pathologic characterization of ACF to those removed from the distal colorectum.

1.4 EXPERIMENTAL DESIGN

Specific Aim 1. *To determine the risk factors associated with polyp incidence within a central Connecticut CRC screening practice.*

Screening colonoscopy is credited with a subsequent lowering of CRC incidence, yet despite wide-spread awareness for the benefits associated with regular screening, 180,000 individuals in 2014 will be diagnosed with CRC alone. The unexpected frequency of iCRC within individuals who have undergone routine screening underscores the inherent limitations of colonoscopy. There are specific limitations associated with the detection of proximal or serrated precancerous lesions. Through a retrospective study of a single gastroenterologist's clinical practice, a large sample set can be obtained to identify risk factors for polyp incidence and multiplicity. Furthermore, polyps can be stratified according to their colonic location or pathology, to determine site and pathway specific risk factors. These data will help provide clinical evidence used to identify high-risk individuals who may benefit from advanced endoscopic methods or shortened surveillance intervals to help reduce the incidence of iCRC.

Specific Aim 2. *To determine the downstream consequences of early BRAF and KRAS activation within human ACF.*

ACF represent the earliest putative precancerous lesions detectable by endoscopy. Previous studies have demonstrated a high frequency of hyperplastic ACF that harbor oncogenic mutations to the *KRAS* and *BRAF* oncogenes in the distal colorectum. However, ACF incidence is significantly higher across the population compared to precancerous polyps and especially CRC, suggesting that only a subset of ACF have the potential to progress through tumorigenesis. We hypothesize that ACF differentially activate the downstream MAPK signaling pathway.

Using an already established repository of ACF biopsy specimens, a nanoproteomic approach will be developed to quantify ERK1/2 phosphorylation in microdissected ACF with known *BRAF* and *KRAS* mutation status. These data will reveal insight into downstream signaling consequences of early oncogenic activation and perhaps provide evidence of ACF's tumorigenic potential.

Specific Aim 3. *To assess the utility of proximal ACF as a surrogate marker of the colonic mucosa at risk for CRC development.*

ACF though widely studied, have rarely been studied in context of colonic location. The role of Proximal ACF will be assessed through a prospective endoscopic clinical study. Subjects enrolled in the study will undergo total high-definition chromoendoscopy at John Dempsey Hospital at the University of Connecticut Health Center. Proximal (cecum to hepatic flexure) and distal (distal 20 cm) colorectal ACFs will be counted and a subset will be biopsied for downstream molecular and pathologic characterization. Comprehensive patient demographic information will also be collected to associate potential risk factors with proximal ACF incidence and multiplicity. We hypothesize that proximal ACF represent the presence of a field defect within the colonic mucosa and may be a distinct surrogate marker of CRC risk compared to their distal counterparts. The clinical study will provide a large sample size to study potential interactions between CRC risk factors and ACF incidence. In order to molecularly characterize these ACF, a high-throughput sensitive genetic screen will be developed that is capable of detecting somatic mutations in microdissected biopsy specimens.

CHAPTER 2

POLYP OCCURRENCE WITHIN A CENTRAL CONNECTICUT SCREENING POPULATION[1]

2.1 Introduction

The goal of this retrospective clinical study was to identify risk factors associated with polyp number, including those lesions that constitute the evasive subtypes that may contribute to iCRC within a central Connecticut screening population. The clinical goal was to identify subsets of the population that would benefit from modified screening intervals or the addition of enhanced screening techniques, such as high-definition chromoendoscopy, to potentially reduce the incidence of iCRC.

2.2 Materials and Methods

2.2.1. Patient selection

Patients were identified from an ongoing gastroenterological practice at the University of Connecticut Health Center (UCHC). This practice draws patients from a catchment area in central Connecticut, and is well-defined in terms of socioeconomic and other demographic

[1] The majority of this work has been submitted for publication in *Gut* with the title "*Impact of Smoking and Daily NSAID use on Occurrence of Colonic Polyps: Analyses by Location and Pathology*"

variables. Included were all patients undergoing a colonoscopy performed by one experienced endoscopist (TJD) between January, 2011 and June, 2013. Data was obtained on each patient by querying the electronic medical record (EMR) and recording results from endoscopy reports, admitting charts and associated pathology reports. Data was routinely entered into the EMR by an RN as a direct query to each patient immediately prior to the colonoscopy procedure in a uniform manner across the GI endoscopy unit. The following items are routinely obtained: age, gender, ethnicity, height, weight, smoking status, family history ('hx' in Tables) of CRC, statins and aspirin use. Smoking was coded as never, former, and current, and further reduced to ever/never for the statistical analysis. Subjects with missing variables were excluded from the analysis (n=67), with the exception of patients with an unknown family history of CRC (n=119) that were coded as 'no'. Sensitivity analyses for the family history of CRC parameter showed no significant changes to the estimate when including these subjects ($\Delta_{\text{p-value}}$ = -0.0004; Δ_{estimate} = +0.0137) Additionally, it was noted whether the patient was undergoing colonoscopy for cancer screening purposes, for some indication secondary to preventative cancer screening, or surveillance colonoscopy. Human subjects approval was obtained from the Institutional Review Board at UCHC. Due to the risk of bleeding post-polypectomy, it was a priority to accurately determine NSAID use prior to the procedure. This was determined by asking each patient upon admission the following set of questions and recording responses in the EMR: 1. "Do you take aspirin?" 2. "What dose do you take?" 3. "Do you take it every day?" 4. "When did you take it last?" 5. "Do you take other NSAIDs like Advil, Motrin, Aleve?" If the answer to question 5 is yes, questions 2-4 were repeated for each additional NSAID.

2.2.2. Colonoscopy procedure

High-definition colonoscopy was performed using an Olympus PCF-190 endoscope (Olympus Corp., Center Valley, PA). A customized magnesium citrate, split-dose bowel preparation was used, providing excellent visualization of the entire colon in almost all cases. All procedures were photo-documented and lesion morphology and colonic location carefully recorded in the endoscopy report prior to removal. Polypectomies were completed using cold-snare in the majority of cases or snare and cautery, if necessary. Propofol was most commonly used for general anesthesia. The colon was divided into proximal and distal segments at the splenic flexure, with lesions occurring within the splenic flexure considered to be proximal. Colorectal polyps were classified according to the Paris-Japanese criteria[89]. Flat, non-polypoid lesions were classified as such when the width of the polyp was greater than half of the height[90]. Lesions were retrieved and sent for standard histological assessment by the Pathology Department at UCHC.

2.2.3. Pathologic analysis

Colonic polyp tissues were collected prospectively at John Dempsey Hospital from January, 2011 through June, 2013. As described by Bettington et al.[91], only polyps that were identified during the colonoscopy procedure have been included in the study. Polyp location was determined from the colonoscopy report and assigned to proximal, distal and rectal positions[91]. Further location details are provided as follows: proximal (cecum, ascending colon, hepatic flexure, transverse colon, splenic flexure), distal (descending colon, sigmoid colon, rectum). Polyp diagnoses were based on current WHO criteria[7] for serrated polyps (includes hyperplastic polyp, sessile serrated adenoma and traditional adenoma) and traditional polyps (includes low-grade dysplasia lesions: tubular adenoma, tubulovillous adenoma, villous adenoma

(none in this study) and high-grade dysplasia or "carcinoma-in-situ"). Serrated polyps were grouped together because of the evolving pathologic recommendations regarding representative sessile serrated adenoma histology over the last five years[10]. Representative pathologies are shown in **Figure 2**. A detailed pathologic discussion of polyp sub-types has been included in the appendix, based on the WHO classifications[7].

2.2.4. Statistical analysis

For group comparisons, t-test and Cochran-Mantel-Haenszel χ^2 test, respectively, have been conducted for numerical responses (e.g., Age, BMI) and categorical responses (e.g., Gender, Smoker, Family History CRC, etc). To uncover the association of potential risk factors with polyp characteristics, negative binomial regression models were used. Statistical significance thresholds were defined at $p<0.05$ for main effects and $p<0.1$ for interaction terms. In general, Poisson or negative binomial regression models can be used to analyze count data (= the number of polyps per subject). However, in the presence of over-dispersion (i.e., the variance is greater than the mean) as is the case with our data set, the Poisson model is inappropriate due to the assumption that the mean is equal to the variance. Therefore, a negative binomial regression model was used as an alternative, where it is assumed that the mean and variance are unequal and over-dispersion is accounted for as a parameter in the model.[92] In this study, all estimated dispersion parameters are significantly larger than zero, thereby validating the use of negative binomial regression models.

From a clinical perspective, while negative binomial models do not necessarily provide readily accessible interpretation of odds ratios, they do in fact offer a measure of severity.

Individual risk clearly falls within a spectrum and the number of polyps, among other factors, is an important variable when determining surveillance intervals as described in the American Gastroenterological Association's 2012 *Guidelines for Surveillance Colonoscopy* (**Table 1**). By using the negative binomial model, it is possible to distinguish between individuals at lower risk (less polyps) and those at higher risk (more polyps), while also taking into account the contribution of other risk factors. However, parallel logistic regression analyses (no polyps vs. one or more polyps) were also performed to provide clinically interpretable odds ratios. All analyses were conducted in Statistical Analysis Systems v. 9.4 (SAS 9.4).

2.3 Results

2.3.1. Baseline Characteristics of the Cohort

A total of 1,988 patients underwent colonoscopy over the 30-month study period. **Table 2** presents descriptive statistics of the patient population, with and without polyps. These subjects had a mean age of 57.6 ± 11.8 years, were primarily Caucasian (79%) and had an average BMI of 29.4 ± 7.3. The majority of subjects were never smokers (84%) and undergoing the colonoscopic procedure for screening (76%) rather than surveillance. Twenty-nine percent were taking statins and 37% were taking an NSAID (85% of whom were taking aspirin). Fifteen percent of the subjects had a known family history of CRC. Forty-four percent (n = 876) of patients had at least one detectable polyp identified and removed during the procedure; this is the widely used Polyp Detection Rate (PDR). The PDR depends upon at least two important considerations; quality of the colonoscopy and true prevalence of polyps in the specific patient

Table 2. Comparison of characteristics for the patients with and without polyps.

Variable	Patients			*P* value†
	Total (n = 1988)	No Polyps (n = 1112)	≥1 Polyp (n = 876)	
Age, mean (SD)	57.6 (11.8)	56.1 (12.7)	59.6 (10.4)	0.0001, t-test
Gender, n (%)				
Male	980 (49)	504 (51.4)	476 (48.6)	0.0001
Female	1008 (51)	608 (60.3)	400 (39.7)	
Smoker, n (%)				
Never	1660 (84)	960 (57.8)	700 (42.2)	0.0001
Ever	328 (16)	152 (46.3)	176 (53.7)	
BMI, mean (SD)	29.4 (7.3)	29.1 (7.8)	29.7 (6.5)	0.0571, t-test
Family History of CRC, n (%)				
No	1691 (85)	961 (56.8)	730 (43.2)	0.0553
Yes	297 (15)	151 (50.8)	146 (49.2)	
Indication, n (%)				
Screening	1505 (76)	890 (59.1)	615 (40.9)	0.0001
Surveillance	483 (24)	222 (46.0)	261 (54.0)	
Statin User, n (%)				
No	1413 (71)	827 (58.5)	586 (41.5)	0.0003
Yes	575 (29)	285 (49.6)	290 (50.4)	
Daily NSAID User, n (%)				
No	1427 (72)	807 (56.6)	620 (43.4)	0.4996
Yes, 81 mg Dose Aspirin	473 (24)	256 (54.1)	217 (45.9)	
Yes, >81 mg Dose Aspirin	63 (3)	35 (55.6)	28 (44.4)	
Yes, Other NSAID	25 (1)	14 (56.0)	11 (44.0)	

†Denotes Cochran-Mantel-Haenszel χ^2 test statistic, unless otherwise noted

population being examined; 46% is typical in high quality settings[93]. Recently, it was demonstrated that the adenoma detection rate is inversely associated with iCRC, highlighting the importance of thorough index colonoscopies for CRC prevention[30].

2.3.2. Predictors of Total Polyp Number and Identification of a Smoking/Aspirin interaction

A group of eight variables was included in the negative binomial regression model for total number of detected polyps in each patient: age, gender, smoking, BMI, family history of CRC, indication (screening vs. surveillance), statin use and daily NSAID use. One of the primary objectives in this inquiry was the potential association of smoking with polyp occurrence, and whether other factors might modify any association. We therefore included interaction terms for smoking with each of the other 7 variables in separate models. Only one model yielded a statistically significant interaction with smoking, and that was daily NSAID use ($p=0.0355$) (**Table 3**).

Daily NSAID users included in the previous model reported use of any NSAID daily regardless of type or dose; therefore, daily NSAID users were separated into daily aspirin users (95% of daily NSAID users) and daily other NSAID users (**Table 4**). The statistical analysis revealed that seven variables [age, gender, smoking history (all $p<0.0001$); BMI, family history of CRC, indication (all $p<0.01$); and statin use, $p=0.0313$] were significantly associated with increased polyp number, and one, daily aspirin use ($p<0.01$), was significantly associated with reduced polyp number (**Table 4**). Daily use of other NSAIDs was not significantly associated with polyp number ($p=0.7145$). Importantly, the smoking interaction with daily aspirin use remained significant at alpha = 0.10 ($p=0.0795$).

Table 3. Negative binomial model of total polyps with grouped daily NSAIDs**.**

Variable	Estimate (95% CL)	S.E.	*P* value	(*)
Age	0.03 (0.02, 0.03)	0.003	<0.0001	***
Gender (M)	0.35 (0.22, 0.48)	0.07	<0.0001	***
Smoker (Ever)	0.52 (0.33, 0.70)	0.09	<0.0001	***
BMI	0.01 (0.003, 0.02)	0.005	0.0079	***
Family History CRC (Y)	0.30 (0.13, 0.47)	0.09	0.0006	***
Indication (Surveillance)	0.23 (0.08, 0.38)	0.07	0.0016	***
Statin User (Y)	0.16 (0.01, 0.30)	0.08	0.0391	**
Daily NSAID User (Y)	-0.23 (-0.40, -0.07)	0.09	0.0064	***
Smoking*Daily NSAID User	0.40 (0.03, 0.77)	0.19	0.0355	**

Intercept = -2.48 (-2.97, -1.98), SE = 0.25, p<0.0001; Dispersion = 0.77 (0.63, 0.94), SE = 0.08
* = 0.05≤ p <0.10; **= 0.01≤ p <0.05; ***= p < 0.01

Table 4. Negative binomial model of total polyps.

Variable	Estimate (95% CL)	S.E.	*P* value	(*)
Age	0.03 (0.02, 0.03)	0.003	<0.0001	***
Gender (M)	0.34 (0.21, 0.48)	0.07	<0.0001	***
Smoker (Ever)	0.52 (0.33, 0.70)	0.09	<0.0001	***
BMI	0.01 (0.003, 0.02)	0.005	0.0083	***
Family History CRC (Y)	0.30 (0.13, 0.47)	0.09	0.0005	***
Indication (Surveillance)	0.24 (0.09, 0.38)	0.07	0.0015	***
Statin User (Y)	0.16 (0.01, 0.31)	0.08	0.0313	**
Daily Aspirin User (Y)	-0.24 (-0.40, -0.07)	0.09	0.0059	***
Daily Other NSAID User (Y)	-0.14 (-0.86, -0.59)	0.37	0.7145	
Smoking*Daily Aspirin User	0.35 (-0.04, -0.74)	0.20	0.0795	*
Smoking*Daily Other NSAID User	0.72 (-0.44, 1.89)	0.60	0.2237	

Intercept = -2.48 (-2.97, -1.98), SE = 0.25, p<0.0001; Dispersion = 0.77 (0.63, 0.94), SE = 0.08
* = 0.05≤ p <0.10; **= 0.01≤ p <0.05; ***= p < 0.01

To illustrate the impact of the smoking and aspirin interaction, the predicted number of polyps from the model is shown in **Figure 6**; among non-smokers, aspirin use significantly reduces the expected number of polyps, whereas among ever smokers, aspirin use significantly increases the expected number of polyps. Logistic regression models of the population of subjects with no polyps versus those with one or more polyps reveal statistically significant odds ratios for all variables ($p<0.05$) with the exception of statin use ($p = 0.1434$) (**Figure 7**). Subjects who smoke and use aspirin daily are significantly more likely to have polyps than those who do not smoke and do not take aspirin (OR = 2.1 [95% CI: 1.2,3.8]). Non-smokers who take aspirin regularly are less likely to have polyps (OR = 0.7 [95% CI: 0.5-0.9]), while smokers who do not take aspirin are more likely to have polyps (OR =1.6 [95% CI: 1.2-2.1]).

2.3.2. Predictors of Polyp Colonic Location and Pathology

The location and pathology of polyps are important both in terms of malignant potential andlikelihood to evade detection. Each polyp's colonic location and underlying pathology was carefully recorded (**Table 5**). The distribution of polyps by location in proximal or distal colon (**Table 6**, Cochran-Mantel-Haenszel χ^2 = <0.0001) and by serrated or traditional pathologies (**Table 7**, Cochran-Mantel-Haenszel χ^2 = 0.6518) was also recorded. In order to determine location and pathology specific risk factors, we applied the same negative binomial regression models to distal and proximal polyps separately, and to serrated and traditional polyps separately (**Tables 8** and **9,** respectively).

A summary of these findings (**Table 10**) shows that smoking is significantly associated with the occurrence of both serrated and traditional subtypes, and with polyps found in proximal

Figure 6. Expected total number of polyps by gender, smoking history, and daily aspirin use illustrate smoking and aspirin interaction. Using negative binomial modeling (**Table 4**), expected number of polyps are generated according to gender (female, left; male right), smoking status (non-smokers, blues; smokers, reds) and aspirin use (non-users, light colors; daily users dark colors). Other variables were kept constant at baseline or average value: Age = 57 yrs; BMI = 29; Family History of CRC = No; Indication = Screening; Statin Use = No.

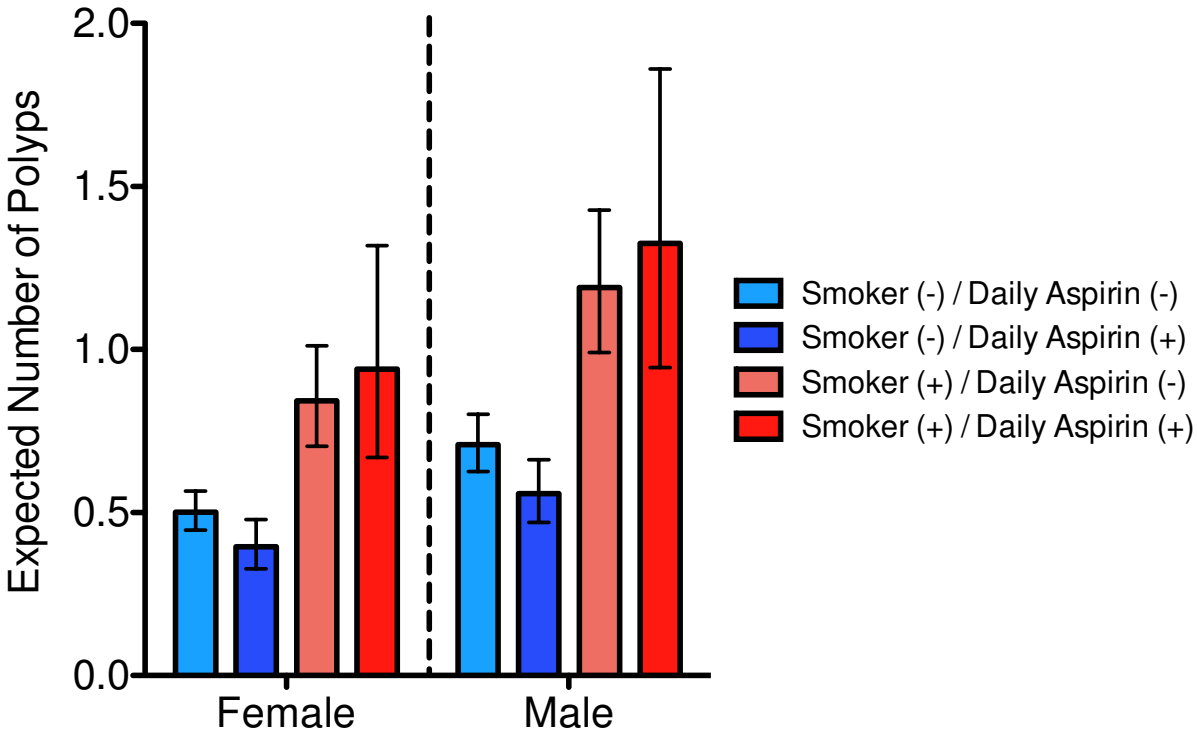
Expected Number of Polyps
2.0
1.5
1.0
0.5
0.0
Female
Male
Smoker (-) / Daily Aspirin (-)
Smoker (-) / Daily Aspirin (+)
Smoker (+) / Daily Aspirin (-)
Smoker (+) / Daily Aspirin (+)

Figure 7. Odds ratios generated from logistic model of polyp occurrence confirm smoking and aspirin interaction. Logistic modeling for polyp occurrence (individuals with no polyps versus those with one or more polyp) reveal significant ORs ($p < 0.05$) for all risk factors with the exception of statin use, including the interaction between smoking and aspirin as revealed by negative binomial model. ORs are representative of listed unit changes for continuous variables and listed category for categorical variables. Boxed numbers appearing on the graph represent calculated OR and the respective 95% confidence limits.

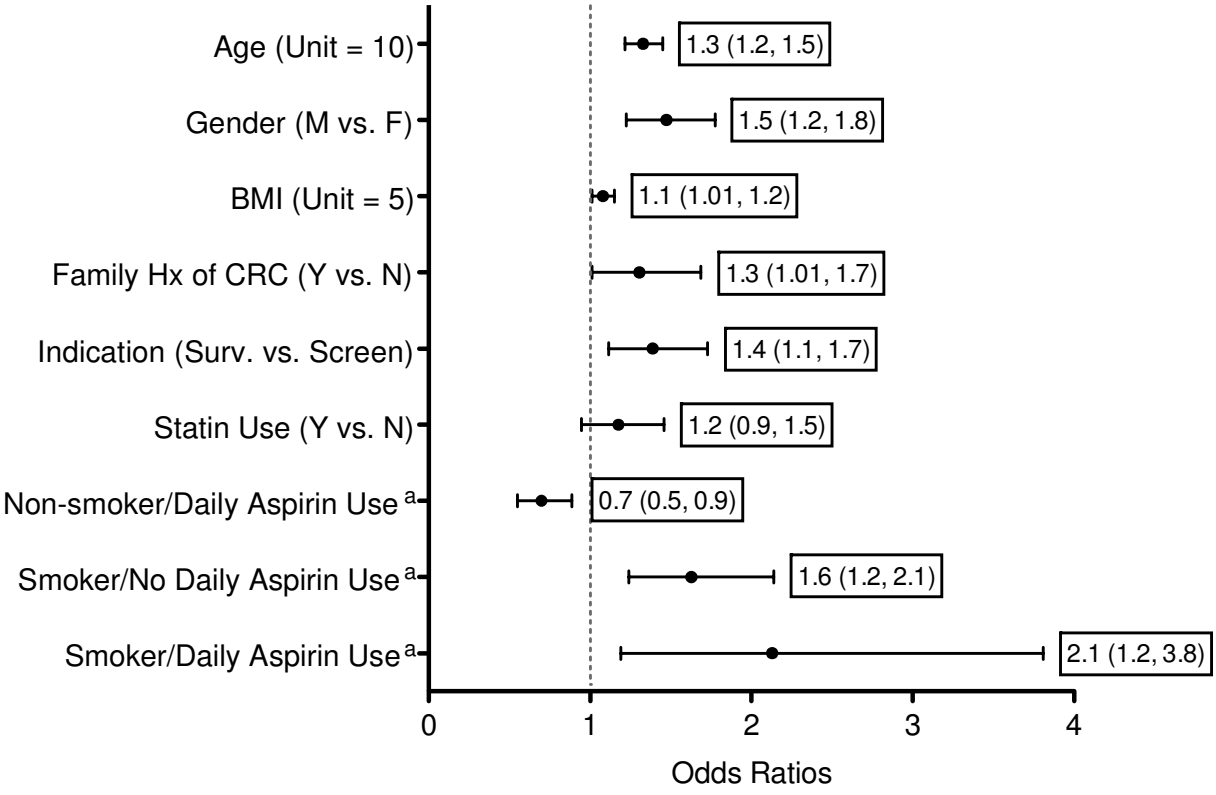

[a] Referent: Non-smoker, No Daily Aspirin Use

Table 5. Distribution of polyp pathologies. Number of polyps (number of subjects with polyps)

	Serrated Polyps			*Traditional Polyps*		
Location	Hyperplastic Polyps	Sessile Serrated Adenomas	Traditional Serrated Adenomas	Tubular Adenomas	Tubulovillous Adenomas	Carcinoma-in-situ
Proximal Colon	118 (103)	56 (47)	0	545 (365)	7 (7)	8 (6)
Distal Colon	238 (181)	38 (31)	0	318 (252)	11 (10)	13 (7)

Table 6. Distribution of polyps by location. Proximal and distal location are not independent (CMH χ^2 = <0.0001)

		Distal Polyps						
	Frequency	**0**	**1**	**2**	**3**	**4**	**≥5**	**Total**
Proximal Polyps	**0**	1118	230	65	13	4	4	1434
	1	250	86	30	8	2	1	377
	2	63	29	8	10	0	0	110
	3	30	9	5	1	1	1	47
	4	8	3	3	0	0	0	14
	≥5	1	4	1	0	0	0	6
	Total	1470	361	112	32	7	6	1988

Table 7. Distribution of polyps by pathway. Serrated and traditional pathways are independent (CMH $\chi^2 = 0.6518$)

		Traditional Polyps						
	Frequency	**0**	**1**	**2**	**3**	**4**	**≥5**	**Total**
Serrated Polyps	**0**	1207	279	105	45	15	13	1664
	1	178	35	19	7	2	0	241
	2	40	10	0	3	2	1	56
	3	11	5	1	0	0	0	17
	4	3	3	0	0	0	0	6
	≥5	3	1	0	0	0	0	4
	Total	1442	333	125	55	19	14	1988

Table 8. Negative binomial models of proximal and distal polyps. (* = 0.05 ≤ p < 0.10; **= 0.01 ≤ p < 0.05; ***= p<0.01)

	*Proximal Polyps**					*Distal Polyps*†			
Variable	Estimate (95% CL)	S.E.	*P* value	(*)	Variable	Estimate (95% CL)	S.E.	*P* value	(*)
# Distal Polyps	0.25 (0.15, 0.35)	0.05	<0.0001	***	# Proximal Polyps	0.22 (0.13, 0.31)	0.05	<0.0001	***
Age	0.03 (0.02, 0.04)	0.004	<0.0001	***		0.02 (0.01, 0.02)	0.004	0.0005	***
Gender (M)	0.24 (0.06, 0.41)	0.09	0.0077	***		0.38 (0.20, 0.55)	0.09	<0.0001	***
Smoker (Ever)	0.34 (0.10, 0.60)	0.13	0.0065	***		0.59 (0.35, 0.82)	0.12	<0.0001	***
BMI	0.002(-0.01, 0.01)	0.01	0.7415			0.02 (0.01, 0.03)	0.01	0.0014	***
Fam Hx CRC (Y)	0.37 (0.14, 0.59)	0.11	0.0012	***		0.19 (-0.04, 0.42)	0.12	0.1059	
Indication (Surveillance)	0.20 (-0.005, 0.39)	0.10	0.0445	**		0.25 (0.06, 0.45)	0.10	0.0111	**
Statin User (Y)	0.25 (0.06, 0.44)	0.10	0.0118	**		0.02 (-0.18, 0.22)	0.10	0.8303	
Daily Aspirin (Y)	-0.19 (-0.41, 0.04)	0.11	0.0990	*		-0.21 (-0.44, 0.02)	0.12	0.0779	*
Daily Other NSAID (Y)	0.07 (-0.83, 0.96)	0.49	0.8804			-0.62 (-1.84, 0.61)	0.62	0.3247	
Smoking*Aspirin	0.06 (-0.47, 0.60)	0.27	0.8141			0.46 (-0.03, 0.95)	0.25	0.0630	*
Smoking*Other NSAID	0.74 (-0.71, 2.18)	0.74	0.3174			0.52 (-1.22, 2.26)	0.89	0.5576	

*Intercept = -3.00 (-3.65, -2.34), SE = 0.33, p<0.0001; Dispersion = 1.07 (0.83, 1.39), SE = 0.14

†Intercept = -2.98 (-3.63, -2.32), SE = 0.33, p<0.0001; Dispersion = 0.92 (0.67, 1.25), SE = 0.15

Table 9. Negative binomial model of serrated and traditional polyps (* = 0.05 ≤ p < 0.10; **= 0.01 ≤ p < 0.05; ***= p<0.01)

	*Serrated Polyps**					*Traditional Polyps*†			
Parameter	Estimate (95% CL)	S.E.	*P* value	(*)	Parameter	Estimate (95% CL)	S.E.	*P* value	(*)
# Trad. Polyps	-0.02 (-0.15, 0.10)	0.06	0.7003		# Serrated Polyps	-0.01 (-0.15, 0.13)	0.07	0.8681	
Age	0.01 (-0.004, 0.02)	0.01	0.1890			0.04 (0.03, 0.05)	0.005	<0.0001	***
Gender (M)	-0.003 (-0.24, 0.23)	0.12	0.9821			0.56 (0.38, 0.74)	0.09	<0.0001	***
Smoker (Ever)	0.71 (0.43, 0.99)	0.14	<0.0001	***		0.51 (0.28, 0.74)	0.13	<0.0001	***
BMI	0.02 (0.004, 0.04)	0.01	0.0170	**		0.01 (-0.004, 0.02)	0.01	0.1802	
Fam Hx CRC (Y)	0.27 (-0.04, 0.58)	0.16	0.0850	*		0.27 (0.04, 0.51)	0.12	0.0220	**
Indication (Surveillance)	0.25 (-0.02, 0.52)	0.14	0.0689	*		0.27 (0.08, 0.48)	0.10	0.0057	***
Statin User (Y)	-0.05 (-0.32, 0.23)	0.14	0.7468			0.25 (0.05, 0.45)	0.10	0.0130	**
Daily Aspirin (Y)	-0.15 (-0.34, 0.23)	0.15	0.7211			-0.24 (-0.45, -0.03)	0.11	0.0275	**
Daily Other NSAID (Y)	-1.74 (-3.81, 0.33)	1.06	0.0995	*		0.58 (-0.09, 1.25)	0.34	0.0907	*

*Intercept = -2.75 (-3.62—-1.88), SE = 0.44, p<0.0001; Dispersion = 2.31 (1.73–3.08), SE = 0.34

†Intercept = -3.81 (-4.51—-3.11), SE = 0.36, p<0.0001; Dispersion = 1.44 (1.16-1.79), SE = 0.16

Table 10. Summary of significant risk factors according to polyp pathology and location.

Risk Factor	+/–	Total Polyps	*Location*		*Pathology*	
			Proximal	Distal	Serrated	Traditional
Age	+	***	***	***		***
Male	+	***	***	***		***
Ever-smoker	+	***	***	***	***	***
BMI	+	**		***	**	
Family History of CRC	+	***	***		*NS	**
Undergoing Surveillance Colonoscopy	+	***	**	**	*NS	***
Statin User	+	**	**			**
Daily Aspirin User	–	***	*NS	*NS		**
Daily Other NSAID User	NS				*NS	
*Smoking * Daily Aspirin User*	+	*		*		
*Smoking * Daily Other NSAID User*	NS					

NS = Not significant (* = $0.05 \leq p < 0.10$; **= $0.01 \leq p < 0.05$; ***= $p<0.01$)

as well as distal colon (all p<0.0001). The interaction effect between smoking and aspirin use was only observed among distal polyps (p=0.0630). Neither smoking interaction term (aspirin or other NSAID) was significant (p>0.10) in the pathology models so the parameters were excluded from these analyses. In our patient population, males were at greater risk of distal and traditional polyps than females (p=<0.0001 for both). The number of traditional polyps increased with age (p<0.0001) in both the distal (p=0.0005) and proximal colon (p<0.0001), but not in the serrated polyp group (p=0.1890). BMI was associated with distal location (p<0.01) and serrated histology (p=0.01). The opposite is true for family history of CRC which was only associated with proximal location (p<0.01) and traditional histology (p<0.05). Surveillance colonoscopy was a significant predictor of polyps in both colon locations(both p<0.05) and was specifically associated with traditional polyps (<0.01).

In addition to the eight explanatory variables for analysis of pathology and location (**Tables 8** and **9**), we included in the model for each location the number of polyps in the other location (i.e., the model for proximal location included the number of distal polyps), and in the model for each pathology, the number of polyps of the other pathology was included. We found that number of proximal polyps was a significant predictor of the number of distal polyps (p<0.0001) and *vice versa* (p<0.0001) (**Tables 6 & 8)**. However, the number of serrated polyps was not a predictor of the number of traditional polyps, nor was the reverse true (**Tables 7 & 9)**. Statin use was associated with traditional polyp occurrence (p=0.0130), but not serrated, and with proximal location (p=0.0181) but not distal.

2.4 Discussion

The primary goal of this study was to identify risk factors associated with colon polyp number within a typical screening population. Secondary to this goal was the identification of risk factors of specific polyp pathology and location that may contribute to risk of developing iCRC. In this cross-sectional study of 1,988 colonoscopy patients, it was found that the total number of colon polyps was associated with male gender, smoking, BMI, and family history of CRC, and inversely with daily aspirin use, consistent with previous studies.[37,52,56] A direct association of statin use and polyp number was observed. The relationship of statin use and colonic polyps has been inconsistent in the literature, with some published studies reporting a protective effect of statins,[94-96] whereas other studies indicate little to no effect[97-100] and even a potentially harmful effect.[101]

Among those factors examined, only smoking was associated with proximal location and serrated morphology, the type of polyp most likely to be missed upon endoscopic examination.[31,102] Interestingly, the number of distal colon polyps of any pathology predicted the presence of proximal polyps in our study sample. However, the presence of one subtype (serrated or traditional) did not predict the presence of the other form of polyp. Dodou and de Winter (2012) conducted a meta-analysis of 32 studies and found that any type of distal lesion predicted increased risk for a proximal lesion,[103] consistent with our observation with respect to large intestinal location.

There have been a number of studies that have examined the relationship of daily NSAID or aspirin use[52,54-56,104] or of smoking[38,43,44] with the development of colon polyps, but

only recently has the possible interaction of these two important modifiers been described.[105] As recently reported by Ishikawa et al. (2014), the use of baby aspirin in a high-risk Asian population resulted in an increased risk of CRC recurrence in active smokers. Although the findings were *post hoc*, the interaction of smoking with any NSAID use in the present study was very strong, and remained significant when specifically examining aspirin use, which is consistent with the recent results from Japan.[105] The data suggest that the interaction may be limited specifically to aspirin, but additional subjects who regularly take non-aspirin NSAIDs such as ibuprofen would be required to test these potential interactions. In addition, our study population was not confined to those patients at high-risk for CRC, nor weighted towards surveillance colonoscopies, and the effect was seen in subjects with any history of smoking (rather than only active smokers), adding additional broad applicability to our results. If this finding is confirmed, it has important implications especially for active smokers, a population that still comprises approximately 20% of the adult population in the United States, but also potentially for those who have quit smoking. A mechanism to explain how smoking could alter so dramatically the effect of daily aspirin use on development of polyps is not readily apparent. While speculative, it is possible to envision a potential synergistic relationship between smoking and the negative side effects of habitual aspirin intake in some individuals that may result in increased mucosal injury. Additional molecular studies are needed to clarify these important relationships.

In summary, the strengths of this study include a patient base from one gastroenterologist at an academic hospital in a relatively stable population of central Connecticut over a well-defined period of time. The polyp detection rate is consistent with those widely reported by

other institutions.[30,93] and several of the epidemiological findings are consistent with results already reported in the literature, including the recently reported interaction between cigarette smoking and baby aspirin use. In addition, several new and significant findings in this study contribute to our progress on understanding the predictors and risk factors for colonic polyps, and therefore colon cancer risk in general. A potential limitation is that the patient population is 'real-world' and not part of an existing research study *per se*; however, this may also be viewed as a key strength of this study. These results, combined with previous studies, provide information that may facilitate the identification of subjects who would benefit most from the application of shorter screening intervals or modified endoscopic procedures, such as intensive bowel preparation,[106] increased withdrawal time,[107] or the use of high-definition chromoendoscopy[75]. With careful consideration of risk factors discussed in this study, gastroenterologists may see increases in both their proximal adenoma and serrated polyp detection rates and subsequently a decrease in the incidence of interval colon cancers. Finally, we believe that the strong effect modification we observed, in which daily aspirin intake among non-smokers protected against the formation of polyps in a dose-dependent manner, yet increased polyp numbers among ever smokers, is of significant concern and should be investigated in further studies.

CHAPTER 3

MAPK SIGNALING CONSEQUENCES OF RAF AND RAS ACTIVATION IN HUMAN ABERRANT CRYPT FOCI[2]

3.1 Introduction

While significant advances have been made in our understanding of the molecular events that accompany the progression of normal colonic mucosa to adenocarcinomas, the precise role of ACF within the adenoma-carcinoma sequence has not yet been conclusively established. Identifying genetic and molecular abnormalities that may contribute to their formation and expansion within the colonic mucosa are necessary for establishing their utility as surrogate cancer markers. As it has been previously reported [60], ACF from the distal colorectum almost always show histological features of hyperplasia, and these lesions often harbor somatic mutations to key proto-oncogenes, including *BRAF* and *KRAS*. Because of their limiting sample size, however, molecular characterization of ACF has proven to be technically challenging beyond the available routine histological and immunohistological analyses.

An ultra-sensitive platform for protein quantification has been developed that enables capillary-based nanofluidic isoelectric focusing and antibody-based chemilluminescence analyses on only nanogram quantities of total protein[108]. This nanofluidic proteomic

---

[2] The majority of this work has been previously published in *Proteomics* (vol. 13; issue 9; pages 1428-1436) in December 2013 with the title "*Nanoproteomic analysis of extracellular receptor kinase-1/2 post-translational activation in microdissected human hyperplastic colon lesions*" (PMID:23467982)

immunoassay (NIA) has been used primarily to examine changes in signaling activity in response to drug treatment [109,110]. To date, however, these applications have relied primarily on whole tissue or cell culture lysates[111]. Since it is impossible to generate a sufficient concentration of protein lysate from small (< $1mm^2$) biopsy specimens for traditional IEF/Western blotting, we developed a new methodology combining the use of tissue microdissection with nanofluidics to study protein modifications in limiting numbers of cells.

In the following study, we demonstrate the use of NIA to examine the downstream consequences of RAS and RAF activation in ultraviolet-infrared (UV/IR) captured ACF removed from normal human colonic mucosa during screening colonoscopy. We have examined the phosphorylation states of ERK1 and ERK2 in UV/IR microdissected ACF and adjacent normal colonic mucosa. The significance of this experimental approach is that we can quantitatively determine the levels of individual ERK isoforms within the cellular context of oncogenic mutations.

3.2 Materials and Methods

3.2.1. Subject selection

All patients included in this study underwent a total colonoscopy at the University of Connecticut Health Center (UCHC) at John Dempsey Hospital (JDH) in accordance with Institutional policies. All patients who met the Amsterdam criteria for familial adenomatous polyposis (FAP) or hereditary non-polyposis CRC (HNPCC) were excluded from this study. This study was performed following Institutional Review Board approval and after receiving written informed consent from the subjects.

3.2.2. ACF collection and characterization

ACF were identified and isolated from grossly normal-appearing colonic mucosa by biopsy *in situ* during high-resolution, close-focus magnifying chromoendoscopy as previously described [60]. Briefly, the distal 20-cm of the colorectum (encompassing parts of the rectum and sigmoid colon) were stained with 40 mL of 0.2% indigo carmine. ACF were visualized and photographed using an Olympus close-focus colonoscope (XCF-Q160ALE; Olympus Corp., Center Valley, PA) capable of 60x magnification over a longer visualizing distance (100 mm). A finding was accepted as an ACF if, under magnification, two or more crypts had increased lumen diameter, thick crypt walls or abnormally shaped lumens. Biopsies of individual ACF and normal mucosa were immediately embedded in optimum cutting temperature (OCT) freezing medium, flash-frozen, and stored at -80°C.

Histological analyses were performed on coded hematoxylin and eosin (H&E) stained sections using light microscopy by T.V.R, a board-certified human pathologist who was blinded to clinical and molecular findings, according to previously described characteristics [60]. Briefly, hyperplastic ACF are characterized by the same criteria applied to hyperplastic polyps [112]. Serrated hyperplastic ACF are defined by their stellate luminal shape (serrated on oblique or cross-section) and the prominent component of columnar cells with microvesicular cytoplasm. Distended hyperplastic ACF lack crypt serration and have prominent goblet cell populations. In addition, hyperplastic ACF frequently have tufting of the surface epithelium. H&E slides were visualized using a BX60 upright bright-field microscope with 10x occulars/20x UPlanFl objectives (Olympus), a CoolSNAP imager and RSImage software, v.1.9.2 (RoperScientific, Ottobrunn, Germany)

3.3.3. Laser capture microdissection, DNA extraction and mutation analyses for BRAF^{V600E} and KRAS codons 12/13

Laser capture microdissection, DNA extraction and subsequent analyses for mutations to *BRAF* and *KRAS* were performed as previously described [60,112]. Briefly, frozen serial sections of ACF were prepared at 5- to 7-μm thickness on glass slides and microdissection was performed on these sections using the Veritas microdissection instrument (Applied Biosystems, Inc., Foster City, CA). Whenever possible, cells from the adjacent normal mucosa (ANM) directly abutting the aberrant crypts were collected separately by laser-capture. On average, approximately 3,000 cells were collected from each sample.

DNA (25 ng) was extracted from micro-dissected aberrant crypts and ANM using the PicoPure DNA Extraction Kit (Applied Biosystems). Mutations were detected by amplifying a 189-bp fragment of the *BRAF* gene spanning codon 600 using the following primers: forward, 5'-CCTAAACTCTTCATAATGCTTGCTC-3' and reverse, 5'-CCACAAAATGGATCCAGACA-3'. Similarly, a 205-bp fragment of *KRAS* spanning codons 12 and 13 was amplified using the following primers: forward, 5'-GTACTGGTGGAGTATTTGAT-3' and reverse, 5'-TCTATTGTTGGATCATATTC-3'. Amplified products were confirmed by gel electrophoresis and enzymatically purified with 2 μL of EXO SAP-IT (U.S. Biochemical Corp., Cleveland, OH). 2.5-μL aliquots of product were sequenced using the forward primer with an ABI BigDye TerV3.1 Cycle Sequencing kit on an ABI 9700 thermocycler (Applied Biosystems). Fifteen microliters of ethanol-precipitated reaction product was sequenced by capillary electrophoresis using a 3100-avant Genetic

Analyzer (Applied Biosystems). The data were analyzed using ABI DNA Sequencing Analysis Software (ver. 3.7). Positive controls for *BRAF* (human colon carcinoma sample with a known mutation at codon 600) and *KRAS* (SW480 cells) and a negative control (placental DNA; Sigma, St. Louis, MO) were used in these analyses.

3.3 Results

3.3.1. KRAS and BRAF mutational status in ACF

172 distal colon ACF were stratified according to their molecular genotype into the following three categories: KRAS, BRAF, or wild-type for both loci (referred to as WT). ACF were independently classified as hyperplastic-serrated or hyperplastic-distended (**Figure 8**). Approximately half (51%) of distended ACF exhibit a missense mutation in the KRAS gene at either codon 12 or 13 (**Table 11**). Interestingly, the presence of a *BRAF* mutation in distended ACF is rare (3%) and 31% of distended ACF are WT for both *KRAS* and *BRAF*. These results correlate with our previously reported frequencies for distended crypts (KRAS: 42%; BRAF: 3%; WT 55%)[60]. In comparison, a large percentage of serrated ACF harbor a $BRAF^{V600E}$ mutation (36%) consistent with our previous results[60]. However, the frequency of *KRAS* mutations in serrated ACF (40%) is greater than we previously reported (19%)[60]. In addition, the frequency of specific *KRAS* missense mutations, including G12A, G12C, G12D, G12V, and G13M, occur at equivalent frequencies between serrated and distended ACF, with G12D being the predominant mutation (**Table 11**).

Figure 8: Experimental approach for NIA analysis of microdissected ACF. The combined use of UV/IR microdissection with NIA increases the informative potential of size-limited human biopsy specimens. The use of fresh-frozen tissues, cryosectioning and microdissection enables the acquisition of histological, genetic and proteomic data. Histopathological scoring shows H&E staining of representative normal colonic mucosa, distended and serrated hyperplastic ACF (all images shown at 200x magnification).

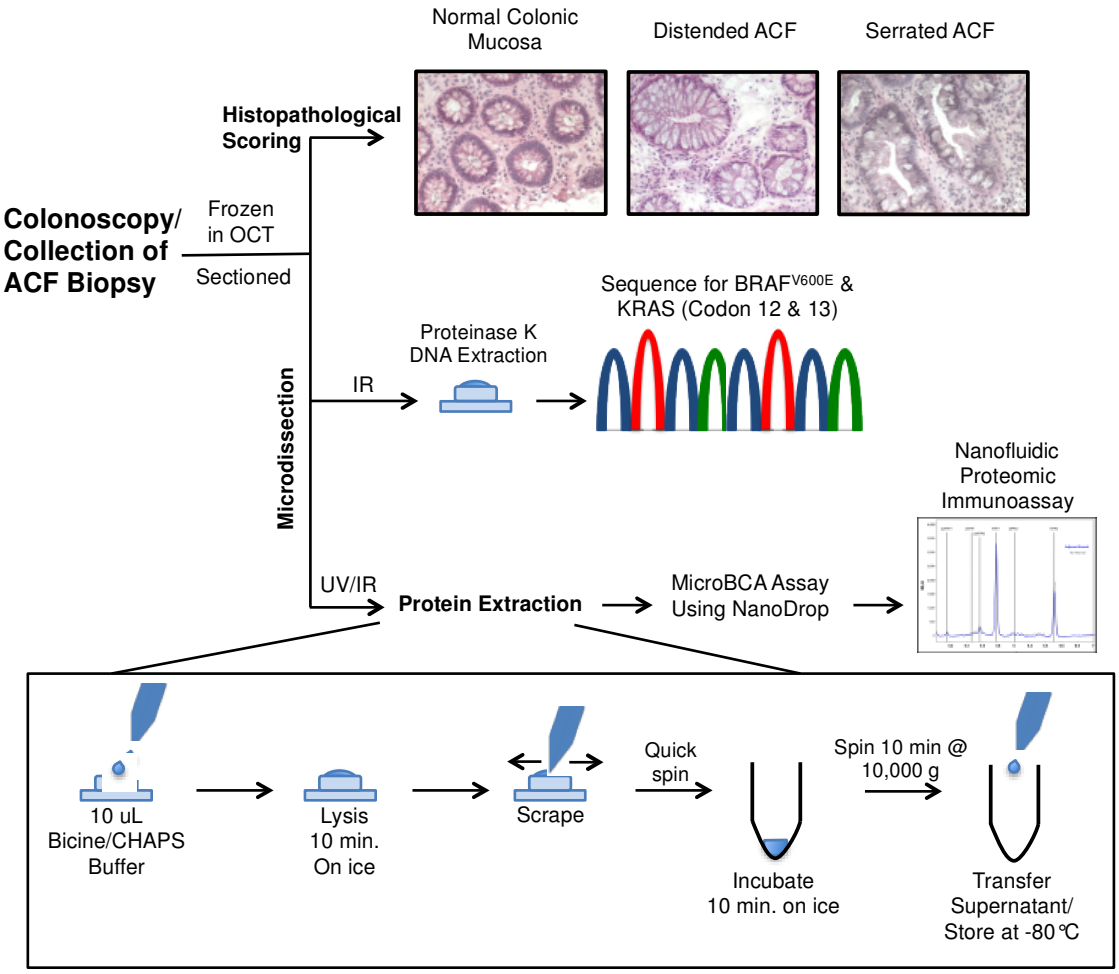
Normal Colonic Mucosa
Distended ACF
Serrated ACF
Histopathological Scoring
Colonoscopy/ Collection of ACF Biopsy
Frozen in OCT
Sectioned
Microdissection
IR
Proteinase K DNA Extraction
Sequence for BRAF V600E & KRAS (Codon 12 & 13)
Nanofluidic Proteomic Immunoassay
UV/IR
Protein Extraction
MicroBCA Assay Using NanoDrop
10 uL Bicine/CHAPS Buffer
Lysis 10 min. On ice
Scrape
Quick spin
Incubate 10 min. on ice
Spin 10 min @ 10,000 g
Transfer Supernatant/ Store at -80℃

Table 11. *BRAF* and *KRAS* mutation frequency in distal hyperplastic ACF.

		Hyperplastic ACF	
Mutation Status	Mutation	Distended (%)(n = 67)	Serrated (%)(n = 105)
Wild-Type	***N/A***	31 (46.27)	22 (20.95)
KRAS	*G12A*	1 (1.49)	0
	G12C	4 (5.97)	2 (1.90)
	G12D	16 (23.88)	26 (24.76)
	G12V	12 (17.91)	16 (15.24)
	G13M	1 (1.49)	0
	ALL	34 (50.75)	44 (41.90)
BRAF	***V600E***	2 (2.99)	39 (37.14)
			TOTAL ACF = 172

3.3.2. MAPK activation in ACF

Based on our findings of a distinct ACF histology that is related to the underlying oncogenic alterations, we hypothesized that *KRAS* or *BRAF* mutations may be associated with differential ERK-1/2 activation. In order to test this hypothesis, a pan-ERK1/2 antibody was examined in frozen tissue sections. As shown in **Figure 9**, ACF displayed a modestly elevated nuclear accumulation of ERK1/2 compared to adjacent NCM. However, immunostaining was highly variable across the panel of ACF that were tested, compromising our ability to quantify the staining intensity. Thus to more accurately assess the potential differential activation of ERK signaling in these hyperplastic lesions, we developed a new method combining the high cellular resolution of tissue microdissection with the sensitivity afforded by a nanofluidic proteomic immunoassay. Our initial approach was to optimize the microdissection method to maximize protein yield. It was determined that the use of UV/IR microdissection followed by an on-cap protein extraction in limited sample buffer was essential (**Figure 8**). Furthermore, we determined that the lower limit of detection is 12 ng of total protein for the NIA analysis, requiring at least 1 mm^2 of captured tissue from 12-μm sections.

Using this approach, the relative concentrations of unphosphorylated ERK-1 and -2, singly phosphorylated ERK-1 and -2 (pERK1/2), and the activated dually phosphorylated ERK-1 and -2 (ppERK1/2) isoforms were measured in ACF. HeLa cell lysates were used as controls to determine the relative pIs of the individual isoforms: ERK1 = 5.78 ± 0.059; pERK1 = 5.42 ± 0.059; ppERK1 = 5.10 ± 0.059; ERK2 = 6.50 ± 0.059; pERK2 = 6.03 ± 0.059; ppERK2 = 5.55 ± 0.059. As shown in **Figure 10**, colon crypts isolated from adjacent normal mucosa (N=8)

Figure 9. ERK1/2 analysis in human colonic mucosa. Immunofluorescence analysis of ERK1/2 was determined in frozen tissue sections as described under Materials and methods. ACF show evidence of nuclear accumulation of ERK1/2 (*white arrowheads*) suggesting its activation compared to normal colonocytes (200x). Blue, DAPI nuclear stain (1:10,000); Green, 1° mouse mAb anti-human β-catenin for membrane visualization (*Sigma*, 1:1,000), 2° Alexa 488 goat anti-mouse IgG (*Invitrogen,* 1:200). Red, 1° rabbit pAb anti-human ERK1/2 (*Novus,* 1:200), 2° Alexa 568 goat anti-rabbit IgG (*Invitrogen*, 1:200). Rabbit IgG Isotype control shows no positive staining (data not shown).

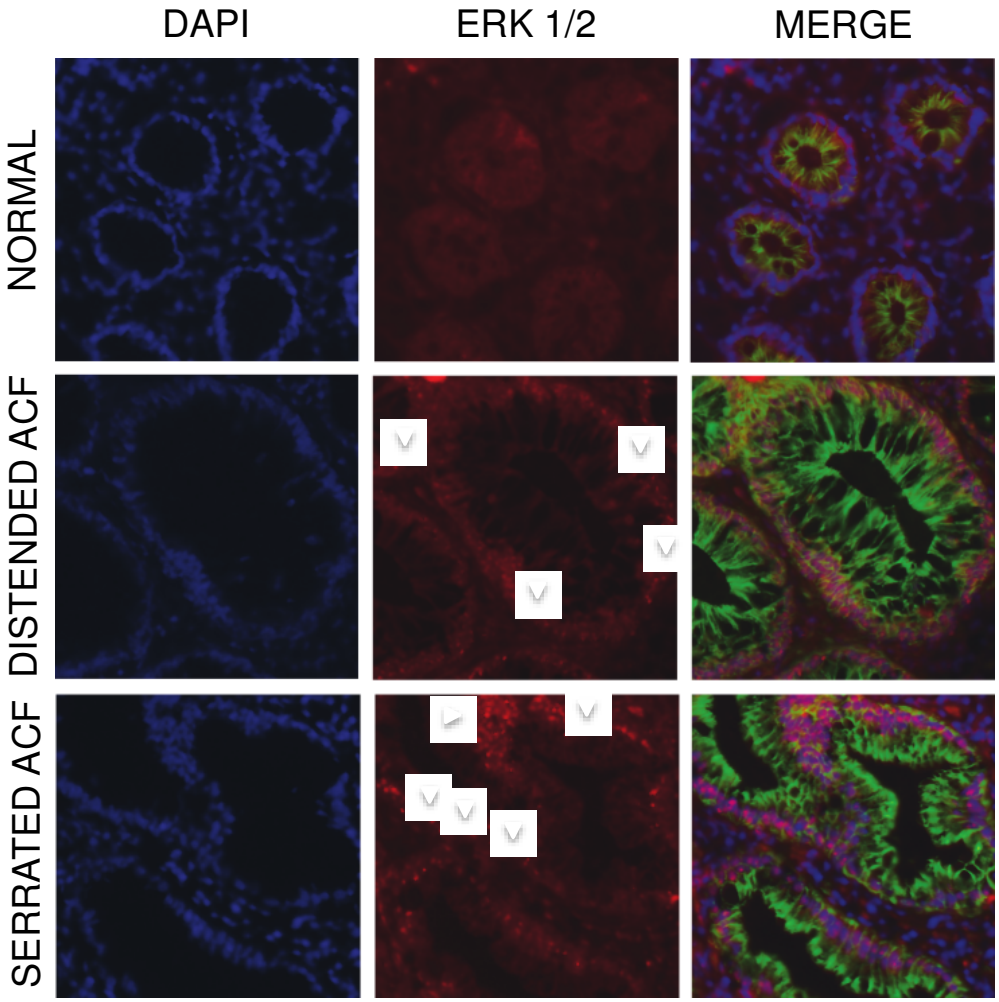
DAPI
ERK 1/2
MERGE
NORMAL
DISTENDED ACF
SERRATED ACF

Figure 10. ERK activation state in normal colonocytes. Microdissected colonocytes were prepared from frozen sections as described under Materials and methods. Normal-appearing crypts were microdissected from distant normal biopsies (gray) and from adjacent normal areas within ACF biopsies (*blue*) and subjected to NIA analyses. A) Representative electrophoretograms of ERK1/2 isoforms. B) Electrophoretograms were quantified for ERK1/2 phosphoforms using Compass software to measure the area under the curve. There are no significant differences in ERK activation between normal crypts according to their proximity to hyperplastic crypts. Error bars represent one standard deviation of the mean.

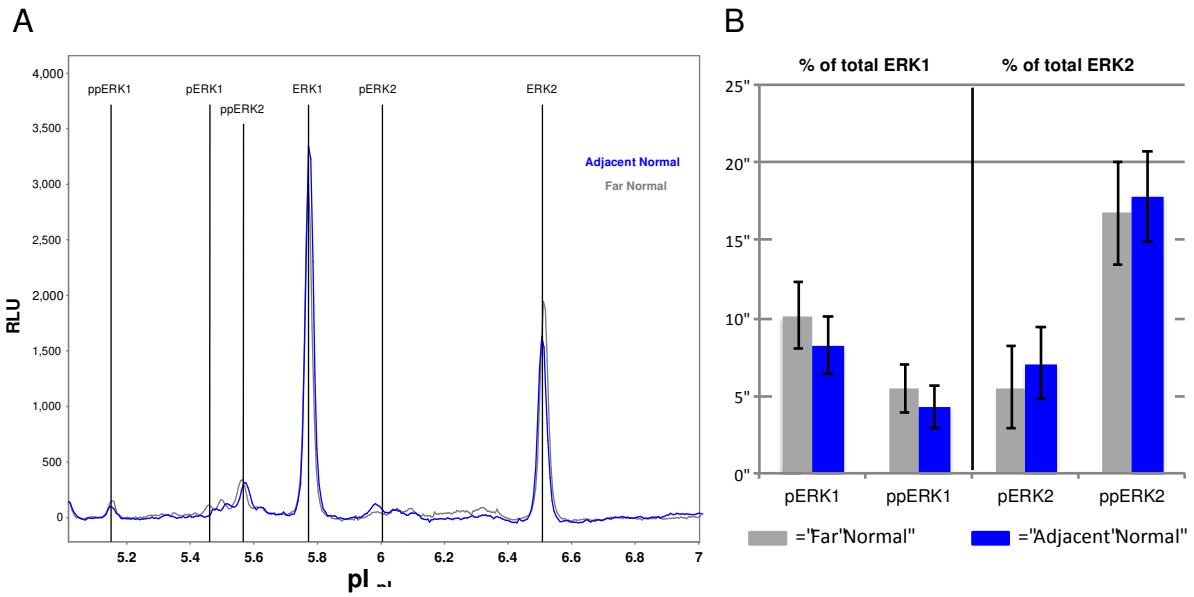
A
ppERK1
pERK1
ppERK2
ERK1
pERK2
ERK2
Adjacent Normal
Far Normal
RLU
4,000
3,500
3,000
2,500
2,000
1,500
1,000
500
0
5.2
5.4
5.6
5.8
6
6.2
6.4
6.6
6.8
7
B
% of total ERK1
% of total ERK2
25"
20"
15"
10"
5"
0"
pERK1
ppERK1
pERK2
ppERK2
='Far'Normal"
='Adjacent'Normal"

showed no significant differences in the extent of ERK activation when compared to colonocytes prepared from independent biopsy specimens histologically confirmed as normal mucosa (N=6).

While a total of 172 ACF were used for the mutational analysis, a subset of 32 samples were sectioned and analyzed for ERK activation status using the NIA. The subset was chosen so as to maximize the use of the most recently obtained human tissues, thus minimizing the extent of protein degradation during sample storage. Of the 32 specimens that were selected, 20 were determined to provide a sufficient quantity of protein for the NIA analysis. Ultimately, colonocytes were micro-dissected from four ACF biopsies that were wild-type for *BRAF* and *KRAS* mutations, nine ACF positive for *KRAS* codon 12 or 13 mutation, and seven ACF positive for the $BRAF^{V600E}$ mutation. Samples were analyzed for ERK activation signatures and compared to colonocytes isolated from adjacent normal mucosa **Figure 11**. Relative concentrations of activated ERK 2 are significantly elevated in all ACF compared to normal crypts. However, only KRAS and WT ACF have significantly increased ERK1 activation. Distal colon ACF with constitutively activated *KRAS* activate ERK1/2 to the greatest extent, suggesting that these mutations are a more potent activator of the MAPK signaling cascade compared to the $BRAF^{V600E}$ mutation.

3.4 Discussion

The 'classical pathway' of colon carcinogenesis describes the step-wise formation of CRC resulting from the accumulation of genetic mutations, specifically those occurring within the *APC*, *KRAS*, and *p53* genes[3,113]. An alternative pathway that has been refined over the past decade results in a spectrum of hyperplastic lesions, ranging

Figure 11. ERK activation state in ACF. Microdissected colonocytes were prepared from frozen sections as described under Materials and methods. Nanofluidic proteomic immunoassays for ERK1/2 result in distinct electrophoretogram signatures (A,C,E) for ACF when compared with adjacent normal crypts (purple). Signatures shown represent three ACF genotypes: WT for *BRAF/KRAS* (A, green), *KRAS* mutant (C, blue), and *BRAF* mutant (E, red). Areas under the curve for each ERK1 and ERK2 phosphoform are quantified as a percent of the total ERK1 or ERK2 (B,D,F). Only WT for *BRAF/KRAS* ACF (B) and *KRAS* mutant ACF (D) have significantly elevated levels of pERK1 and ppERK1, while *BRAF* mutant ACF (F) have only slightly elevated (not significant) pERK1 and ppERK1 levels. All ACF significantly activate ppERK2. **: Significant using Tukey's HSD procedure, two-sided alpha level of significance of 0.05. Error bars represent one standard deviation of the mean.

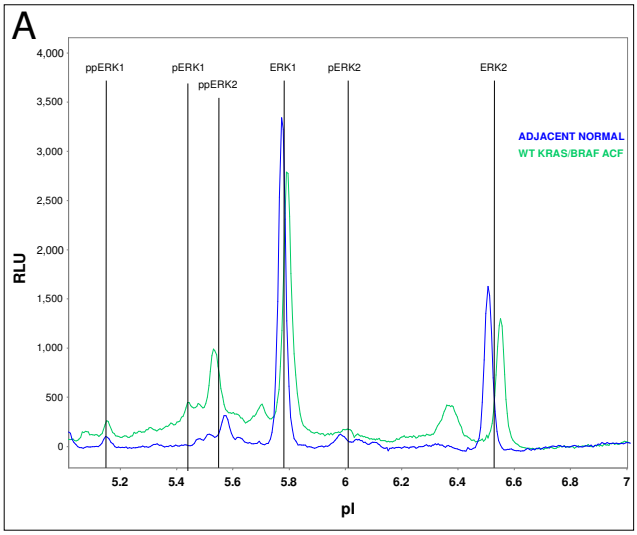
A
ppERK1
pERK1
ppERK2
ERK1
pERK2
ERK2
ADJACENT NORMAL
WT KRAS/BRAF ACF
RLU
pI

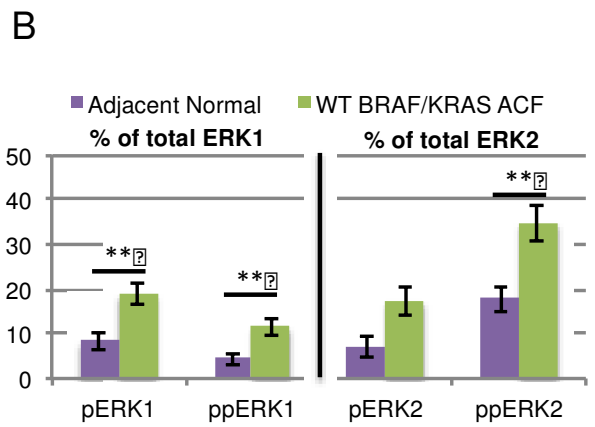
B
Adjacent Normal
WT BRAF/KRAS ACF
% of total ERK1
% of total ERK2
pERK1
ppERK1
pERK2
ppERK2

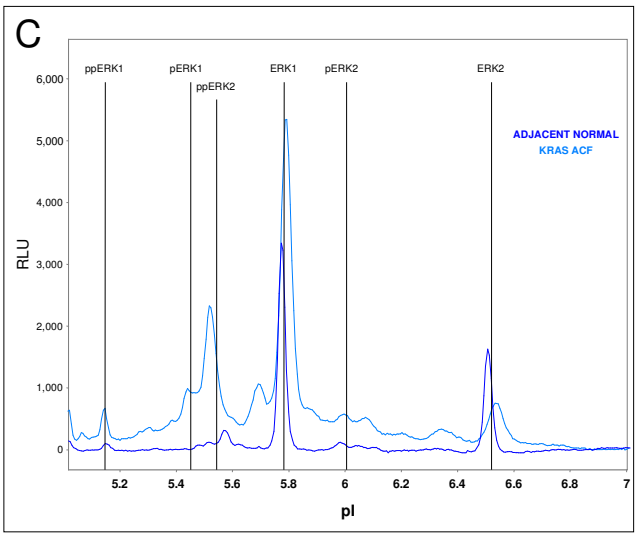
C
ppERK1
pERK1
ppERK2
ERK1
pERK2
ERK2
ADJACENT NORMAL
KRAS ACF
RLU
pI

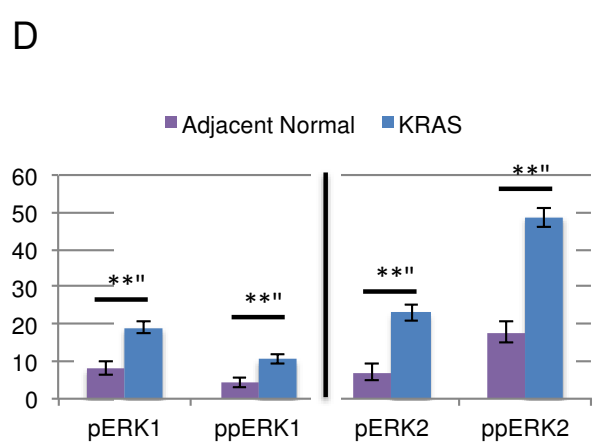
D
Adjacent Normal
KRAS
pERK1
ppERK1
pERK2
ppERK2

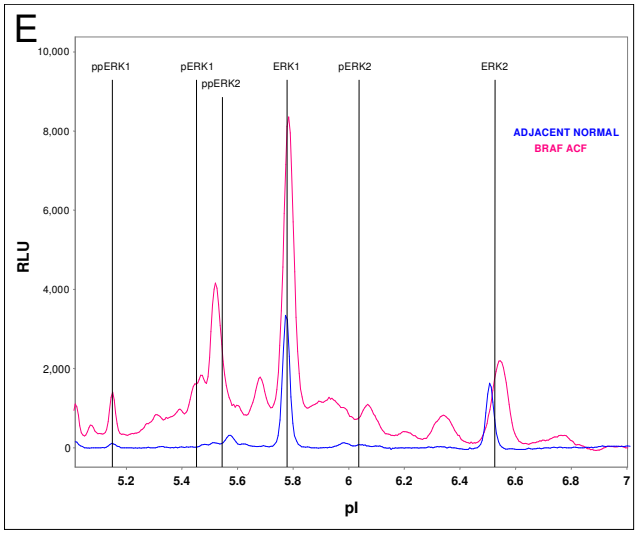
E
ppERK1
pERK1
ppERK2
ERK1
pERK2
ERK2
ADJACENT NORMAL
BRAF ACF
RLU
pI

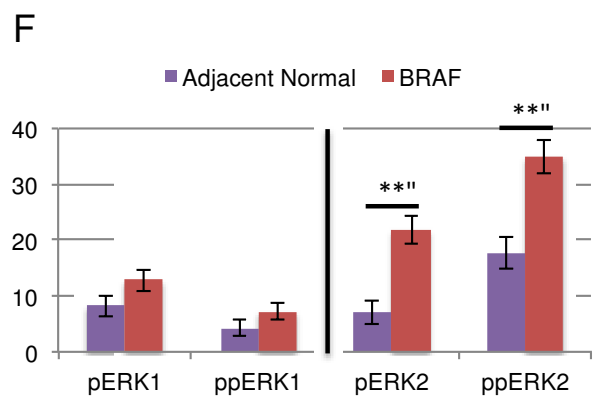
F
Adjacent Normal
BRAF
pERK1
ppERK1
pERK2
ppERK2

from hyperplastic polyps (HP) to sessile serrated adenomas (SSA)[114,115]. The molecular features of the HPs vary with respect to their colonic location. For example, HPs and SSAs occurring in the proximal colon tend to have a higher frequency of BRAF mutations, microsatellite instability (MSI) and CpG island methylator phenotype (CIMP) in comparison to similar hyperplastic lesions found in the distal colon[17,116]. In addition, these lesions generally lack *APC* mutations [9].

We believe that a subset of ACF described in the present study may represent precursor lesions to this alternative pathway. We show that mutations to either *KRAS* or *BRAF* are associated with the development of early hyperplasia within the distal colon. Consistent with the molecular aberrations that accompany this alternative pathway [17], we have also identified MSI and hypermethylation of Ras-association domain family 1a (*RASSF1a)* in 24% of hyperplastic ACF [70]. Because of their limiting sample size, however, it has not been technically feasible to combine genetic and proteomic analyses within the same specimen. The novel methods described in this report have begun to establish a robust approach that minimizes the amount of sample required per assay (**Figure 8**), thus directly increasing the informative potential of a single biopsy specimen. By using this technique, it may ultimately be possible to understand the biological outcome of these early colonic lesions.

The equivalent distribution of *KRAS* and *BRAF* mutations within the serrated ACF observed in the present study, where we have greatly increased our sample size, differs somewhat from our previous findings [60]. While *KRAS* mutations occur at a greater frequency in serrated ACF than previously reported (41.9 vs. 18.8%), we have confirmed the rare

occurrence of *BRAF* mutations in hyperplastic-distended crypts [60]. Although we still cannot determine with certainty whether these lesions occur in sequence or represent parallel pathways, the similar frequency of *BRAF* and *KRAS* mutations in serrated ACF and the infrequent occurrence of *BRAF* mutations in distended ACF raises the interesting possibility that distended lesions precede serrated ones. It is possible that the acquisition of a *BRAF* mutation favors its rapid growth into a serrated histological phenotype. On the other hand, *KRAS*-mutated distended crypts may activate several key inhibitory pathways, such as *RASSF1/2*, that may impede their progression to the serrated phenotype [117]. This mechanism may be bypassed in the event of a *BRAF* mutation [117]. Understanding the downstream signaling consequences of these oncogenic mutations will shed new insights into the relationship between serrated and distended ACF and their potential role within the alternative pathway to carcinogenesis.

Using our NIA approach, we have been able for the first time to evaluate the extent of ERK activation in biopsy specimens obtained from the human colon. Our results show that both *KRAS* and *BRAF* mutations result in elevated levels of the activated, dually-phosphorylated ERK2 isoform (**Figure 11**). Interestingly, ACF that are wild-type for *BRAF* and *KRAS* also demonstrate ERK2 activation, suggesting that other mechanisms can stimulate this proliferative pathway, possibly including members of the EGFR family or other mutations within the Ras-Raf-Mek pathway that have not yet been uncovered. A relatively high frequency of *ErbB2/3* and *NRAS* mutations in human CRC were recently described; their status in ACF, however, has not been established[118]. Nevertheless, our results demonstrate the importance of ERK2 activation in stimulating mucosal hyperplasia, especially since directly adjacent normal crypts do not appear to have increased ERK activation (**Figure 10 & 11**). The high level of ERK2 activation

compared to ERK1 is not surprising, given its known role in mediating cell proliferation and its typically higher level of expression[119,120]. Interestingly, only WT and *KRAS*-mutant ACF showed a significant activation of ERK1, while *BRAF*-positive ACF demonstrated only a modest (< 2-fold) increase. It has been suggested that activated ERK1 may actually act as a competitive inhibitor of ERK2, thereby blocking its activity[120,121]. These functional distinctions among the ERK isoforms and their differential activation in ACF of varying histologies again support the idea that the formation of distended crypts may precede the appearance of serrated ACF. Of course, determining the activation status of the ERK isoforms within these very small epithelial lesions would not have been possible using conventional immunohistochemistry, and further underscores the advantages of this novel experimental approach.

An additional consideration is the potential role of oncogene-induced senescence in determining the biological outcome of ACF. Several recent mouse genetic studies have examined the effects of these early oncogenic alterations within the intestinal mucosa. Carragher et. al[122] showed that *LSL-BRAF*^{V600E} *x AhcreER*$^{T+/o}$ mice with an activating mutation of the *BRAF* oncogene develop serrated hyperplasia within three days after tamoxifen activation of the *Cre* recombinase. The mice developed small intestinal tumors by twelve weeks following *BRAF* activation, but this only occurred with a concurrent inactivation of *p16*^{INK4a} *via* promoter methylation. Similarly, Bennecke et. al[123] showed that *LSL-KRAS*^{G12D} x *villin-Cre* mice develop serrated, hyperplastic colon crypts accompanied by increased *p16*^{INK4a} expression. After crossing these mice with *Ink4a/Arf*$^{-/-}$ mice, which are deficient for *p16* expression, > 50% of these mice developed tumors resembling traditional serrated adenomas by twelve weeks of age. These studies in mice highlight the important role of p16-mediated senescence in reducing the

transformative potential of these oncogenic mutations[124]. In the present study using IF analysis, although p16 was consistently expressed within the colonic mucosa, its levels were not significantly different between hyperplastic and normal crypts (**Figure 12**). However, it is possible that the activation state of p16 is differentially affected by *BRAF* or *KRAS* mutations. It has been shown that p16 is phosphorylated at four different serine residues, two of which may have different effects on its activation state; *i.e.*) Ser8 (inactivating)[125] and Ser152(activating)[126]. In future studies, it may be possible to develop NIA-based assays to examine these post-translational modifications of p16 to overcome the inherent limitations of IF analysis.

In summary, we describe a new methodology that will increase the informative potential of extremely small human biopsy specimens. By combining precise tissue microdissection of early hyperplastic lesions with subsequent proteomic analysis, it is now possible to examine post-translational modifications to specific signaling proteins within the context of underlying genetic and histological changes. The results highlight the advantages of this approach over conventional immunohistological methods by focusing on two ERK isoforms and their relative activation states. Combining UV/IR microdissection with the NIA assay has made it possible to obtain quantitative proteomic information within the context of histological changes and upstream genetic abnormalities.

Figure 12. p16 expression in normal colonic mucosa and *KRAS* and *BRAF* mutant ACF. Expression of senescenc-associated p16 expression measured by immunofluorescence of frozen tissue sections. Mutant ACF show positive nuclear staining of p16, while less nuclei show positive staining in normal colonic mucosa (pink, example areas indicated by arrows). However, this staining is variable across the study and difficult to quantify, therefore no conclusions can be made at this time. Blue = DAPI nuclear stain(1:10,000); Green = 1° mouse mAb anti-human β-catenin for membrane visualization (*Sigma*, 1:2,000), 2° Alexa 488 goat anti-mouse IgG (*Invitrogen,* 1:200). Red = 1° rabbit pAb anti-human p16 (*Epitomics,* 1:200), 2° Alexa 568 goat anti-rabbit IgG (*Invitrogen*, 1:200). *Rabbit IgG Isotype control shows no positive staining (pictures not shown).*

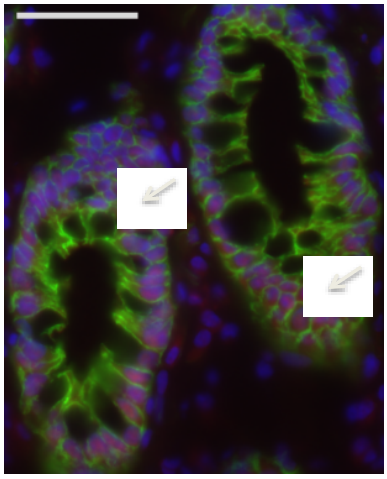

Normal Colonic Mucosa

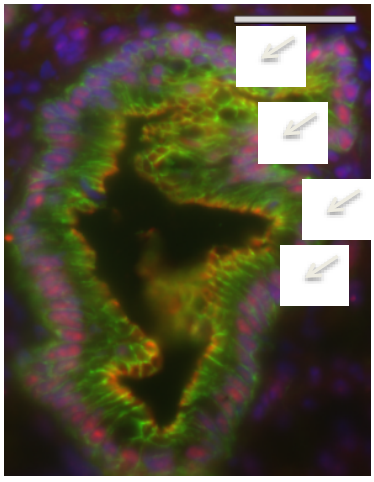

BRAF Serrated ACF

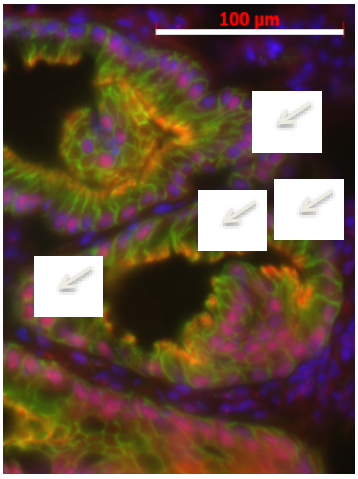

KRAS Distended ACF

CHAPTER 4

A DNA MASS SPECTROMETRY-BASED HIGH-THROUGHPUT METHOD TO GENOTYPE HUMAN MICRODISSECTED ABERRANT CRYPT FOCI[3]

4.1 Introduction

Screening colonoscopy has been established as an effective strategy to reduce the risk of colorectal cancer [127]. However, recent evidence suggests that protection may be most successful in the distal colorectum since the incidence of proximal colon cancer has not been significantly reduced by the implementation of widespread screening colonoscopy [128]. The frequency of interval colon cancers, or those cancers developing between screening procedures, raises the possibility that proximal tumors in particular may have accelerated growth characteristics that limits the effectiveness of colonoscopy [129]. This lack of protection afforded by colonoscopy, in particular within the proximal colon, underscores the need for advanced endoscopic techniques that may be used to identify small precursor lesions that would otherwise be missed by traditional screening approaches.

The following study was undertaken to more accurately define the molecular alterations that are present within colonic ACF. Using DNA mass spectrometry (DNA-MS) combined with

---

[3] The majority of this work has been previously published in *Molecular Cancer Research* (vol. 12; issue 6; pages 823-829) in June 2014 with the title "*HD Chromoendoscopy Coupled with DNA Mass Spectrometry Profiling Identifies Somatic Mutations in Microdissected Human Proximal Aberrant Crypt Foci*" (PMID:24651453)

laser capture microdissection (LCM), we report a highly sensitive method to interrogate the mutational spectrum of microscopic biopsies following their removal from the human colon. A limited number of somatic mutations have been identified, including mutations to APC^{R876*} and $FLT3^{I836M}$, as well as an insertion/deletion within the *EGFR* gene, underscoring the biological significance of ACF within the context of CRC and in particular within the proximal colon.

4.2 Materials and Methods

4.2.1. Subject Selection

All subjects underwent a total screening colonoscopy at the University of Connecticut Health Center (UCHC) in accordance with Institutional policies. Patients who met the Amsterdam criteria for familial adenomatous polyposis (FAP) or hereditary non-polyposis CRC (HNPCC) were excluded from the study. This study was performed only following Institutional Review Board approval and receipt of written informed consent from the subjects.

4.2.2. ACF Collection and Characterization

ACF were identified *in situ* and biopsied from grossly normal-appearing colonic mucosa during high-definition, close-focus magnifying chromoendsocopy. The proximal colon from the cecum to the right hepatic flexure, in addition to the distal 20-cm of the colorectum, were sprayed with a freshly prepared solution of 1% indigo carmine. ACF were visualized and photographed using a close-focus colonoscope (Olympus, PCF-H190L; Olympus Corp., Center Valley, PA) with visualization from 2-100 mm at 60x magnification. A finding was accepted as an ACF if 5 or more crypts have an increased lumen diameter (1.5-2x), thick crypt walls, or abnormally shaped lumens relative to the surrounding mucosa. In addition, the lesion must be

less than 5 mm in diameter to be considered an ACF. Biopsies were immediately embedded in freezing medium (OCT), flash-frozen, and stored at -80°C [130].

Frozen sections were stained with hematoxylin and eosin (H&E) and routine histological analyses were performed by two independent, board-certified human gastrointestinal pathologists blinded to clinical findings according to our previously established criteria (11). Dysplastic ACF are characterized histologically by enlarged upper cryptal regions of irregular shape with stratified, elongated nuclei and a general dysplastic appearance. Hyperplastic ACF are characterized according to the same criteria applied to hyperplastic polyps[112]. These hyperplastic ACF are sub-classified into serrated and distended (non-serrated) pathologies as previously described [130]. Briefly, serrated ACF are defined as ACF that show stellate luminal shape upon cross-section with a prominent component of columnar crypts with microvessicular cytoplasm. Distended ACF lack serration, prominently feature goblet cells, and frequently exhibit tufting of the surface epithelium.

4.2.2. Laser capture microdissection and DNA purification

A Veritas microdissector was used to capture ~5,000 cells (or the equivalent of approximately one mm^2 of collected tissue area) from 12-μm thick frozen serial sections of ACF prepared on PEN membrane glass slides (Applied Biosystems, Foster City, CA). Genomic DNA was extracted from aberrant crypts (isolated from surrounding stroma and normal mucosa by LCM) using the PicoPure DNA extraction kit (Applied Biosystems). Samples were then cleaned using the DNA Wizard protocol (Promega, Madison, WI)

4.2.3. Somatic mutation screening using DNA mass-spectrometry

Mutation screening was performed at the Yale Center for Genome Analysis using the Sequenom MASSArray DNA-MS approach. This method uses a matrix assisted laser desorption ionization-time of flight mass spectrometry (MALDI-TOF MS) platform to detect single base mutations with increased sensitivity[131]. Extracted DNA was amplified using multiplexed OncoCarta PCR primers targeting 105 mutations across 22 known tumor suppressor and proto-oncogenes (v.3.0, Sequenom Inc., San Diego, CA; **Table 12**). The DNA concentration per reaction approached 1 ng of gDNA, a concentration that is within the limits of detection for the Sequenom platform[131]. DNA mass-spectrometry was carried out as previously described [131]. Briefly, target regions are amplified through multiplex PCR reactions. Shrimp alkaline phosphatase is added to the reaction to dephosphorylate unincorporated dNTPs and an extension reaction mix is added. A post-PCR primer extension reaction creates a single nucleotide extension using mass-modified terminators and the reactions are desalted using 6 mg of CLEAN Resin. Reaction products are then printed onto a SpectroCHIP to be read by MALDI-TOF MS. Mass spectrometry data is then analyzed using Typer4.0 software to identify sample genotype with respect to the assayed mutation.

Somatic mutations were confirmed by extracting DNA from whole blood using the DNAeasy Blood and Tissue Kit standard protocol (Qiagen; Venlo, Netherlands) and sequenced by GeneWiz, Inc. (South Plainfield, NJ). To determine mutation status in adenomas, DNA was extracted from two 10-micron FFPE curls using the QIAamp DNA FFPE Tissue Kit standard protocol and sequenced (GeneWiz, Inc.) Primer sequences for PCR amplification and Sanger sequencing were: EGFR F: 5’-CCCCAGCAATATCAGCCTTA-3’

Table 12. Somatic mutations included in DNA-MS screen. 105 mutations to 22 known tumor suppressors and proto-oncogenes were screened for each sample.

Gene	Mutations Screened
ABL1	M244V
APC	R876*, R1114*, E1309fs*4, Q1338*, Q1429*, S1465fs*3, T1661fs*9
BRAF	V471F, N581S, V600M
CDKN2A	R58*, E61*, E69*, H83Y, D84Y
CSF1R	L301S, Y969F/C/H/*
CTNNB1	A13T, V22A, W25-D32Del, S45A
EGFR	G719D, L730F, G735S, V742A, L747-P753>S, L747-T751>P, H773R, G810D/S, L858M
ERBB2	D769H, V777L
FLT3	D835Del, I836M
HRAS	G12C, G12R
JAK3	P132T, A572V, V722I
KRAS	Q22K
MET	T1010I, H1112R/Y, M1268T, Y1248C/H
MLH1	V384D
MYC	P57S, A59V, T731, N101T, A260A
PDGFRA	D842-D846>E/N, D846>G, D842-M844Del, D842-S847>EA, D842I/Y, R841-D842Del, S566-E571>R
PTEN	K6fs*4, R130fs*4, R130G, R173C/H, R233*, P248fs*5, K267fs*9, V317fs*3, N323fs*2, N323fs*21
RB1	E137*, L199*, R320*, R455*, R556*, R579*, L660fs*2, C706F, E784*
RET	A883F, C634R, D631-L633>E, D631G, D898-E901Del, E632-A640>VRP, E768D, F612-C620Del
STK11	Q37*, Q170*, D194V, G196V, F264fs*22, P281fs*6, P281L, W332*
TP53	R306*
VHL	L85P, F148fs*11, L158Q, R161*, R167W

R: 5'-ATGAGGTACTCGTCGGCATC-3' ; APC F: 5'-GCATGCTCAAGAACCTCATTC-3' R: 5'-TAGGTCGGCTGGGTATTGAC-3' ; FLT3 F: 5'-AGAACTGCAGCCACCATAGC-3' R: 5'-ACCTCATGATCTGCCCTCCT-3' (Integrated DNA Technologies, Coralville, IA). Sanger sequencing for BRAF and KRAS mutations was performed as previously described [60].

4.2.4. Immunohistochemistry

Immunohistochemistry (IHC) was performed on frozen ACF prepared at 7-μm thickness. Sections were treated with 3% hydrogen peroxide, blocked and incubated in anti-β-catenin primary antibody (1:2,000; Sigma-Aldrich Co, St. Louis, MO). Sections were incubated in ImmPRESS anti-mouse Ig (Vector Laboratories, Burlingame, CA). Signal detection was achieved using a 3,3'-diaminobenzidine solution (Vector Laboratories) and tissues were counterstained with methyl green nuclear stain.

4.3 Results and Discussion

4.3.1. High-definition chromoendoscopy positively identifies ACF in the proximal colon

Using high-definition chromoendoscopy, we and others have previously demonstrated the ability to identify ACF within the distal colon[72,73]. We have recently expanded our analysis to include the identification of ACF within the proximal colon, a region of the colon that includes the cecum to the splenic flexure (**Figure 13A**). A total of 96 patients have been screened and 88 proximal ACF and 1,010 distal ACF have been identified (**Figure 13B**). The majority of the subjects were undergoing a screening colonoscopy (n=70/96; 73%) and approximately half of the subjects (n = 47/96; 49%) had at least one polyp identified and removed during the procedure.

Figure 13. Clinicopathological features of proximal ACF. A, High-definition magnifying colonoscopy combined with dye-spray reveals diminutive flat lesions of the proximal colorectum, including ACF and flat adenomas. B, Frequency of ACF according to colonic location identified during screening chromoendoscopy. C, Histologic appearance of normal colonic mucosa and ACF procured from the proximal colon. Proximal lesions display the same type of morphologies commonly associated with distal colon ACF, including dysplasia and hyperplasia (distended and serrated) (200x magnification; bar = 60 μm).

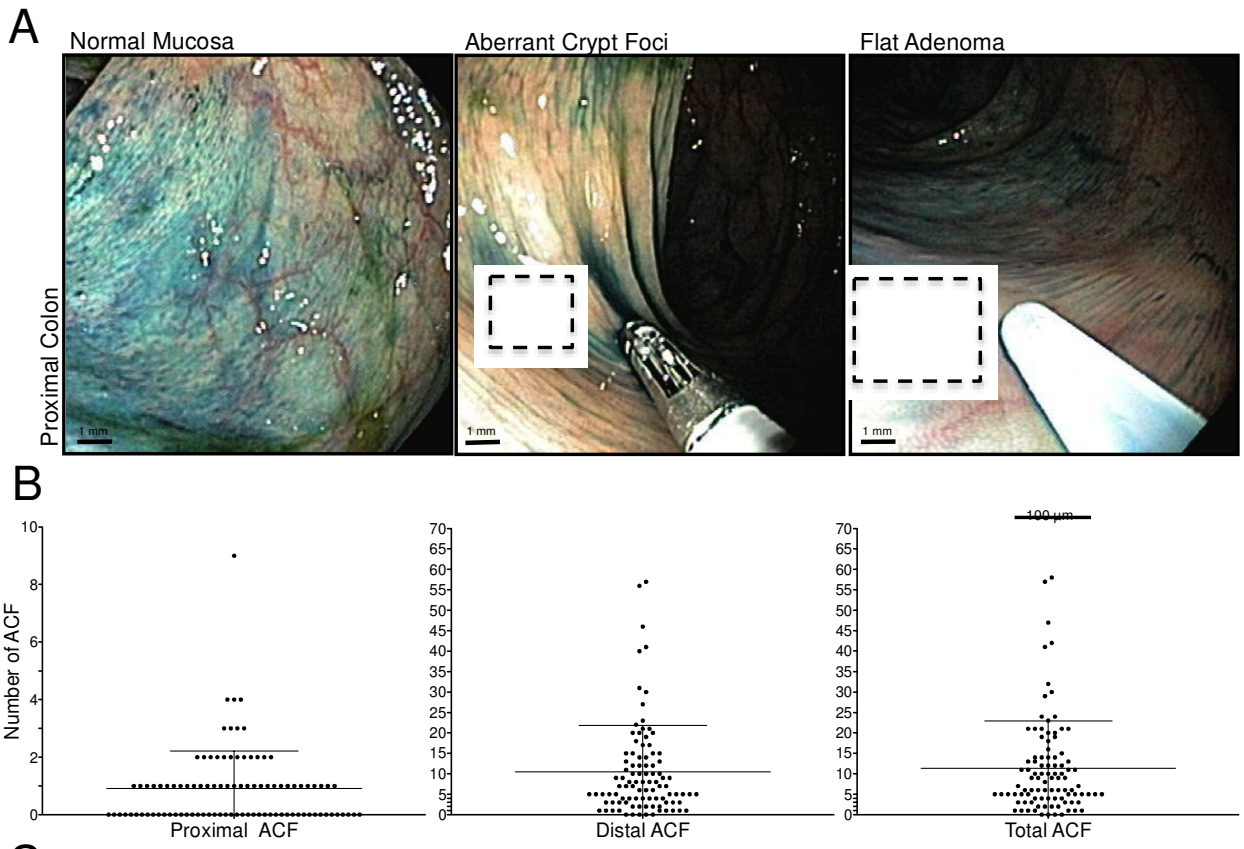
A
Normal Mucosa
Aberrant Crypt Foci
Flat Adenoma
Proximal Colon
1 mm
1 mm
1 mm
B
Number of ACF
Proximal ACF
Distal ACF
Total ACF
100 µm
C
Normal Mucosa
Dysplastic ACF
Distended ACF
Serrated ACF

Histologic evaluation reveals that proximal ACF harbor the full spectrum of established histologic abnormalities present within distal ACF, including hyperplasia (serrated or distended) and dysplasia (**Figure 13C**).

ACF within the distal colon share many genetic and histologic abnormalities associated with more advanced colonic neoplasia. For example, hyperplastic ACF commonly harbor *BRAF or KRAS* mutations[60], resulting in increased ERK activation[130]. The presence of ACF with dysplastic histological features, however, is uncommon within the distal colon, although in one case a dysplastic ACF was found to carry a novel somatic mutation to the *APC* gene[60]. A high frequency of *APC* mutations has been reported previously in dysplastic ACF[67], but the inclusion of patients with FAP disease in this study may have exaggerated the prevalence of *APC* mutations. In an earlier study, we found that, a significant percentage of ACF (~ 40%) do not harbor mutations to *BRAF* or *KRAS*[130]. Thus in the present study, a broader genetic screen was undertaken to identify additional mutations that may contribute to early neoplastic changes in the colon.

4.3.2. Application of DNA-MS for high-throughput genotyping of ACF

Comprehensive mutation profiling of early neoplasia may provide insight into future colon cancer risk[118]. However, there are a number of technical challenges associated with the application of high-throughput screening strategies to the analysis of small mucosal biopsy specimens. In addition, the number of morphologically abnormal colonic crypts within an ACF biopsy is limited, necessitating the use of LCM to enrich for subpopulations of aberrant and normal-appearing colonocytes. Recent advances in DNA-MS technology using MALDI-TOF

have provided a high-throughput, multiplexed approach to allow somatic mutational profiling with as little as 1 ng of input genomic DNA[131]. To examine the feasibility of performing DNA-MS analyses on micro-dissected ACF samples, DNA was extracted from approximately 5,000 colonocytes and subjected to the MASSArray PCR standard protocol. Amplification of genomic loci was achieved with less than 1 ng of input genomic DNA (**Figure 14**). A total of twenty-six micro-dissected ACF were then subjected to DNA-MS analyses. This group included seven proximal ACF, nineteen distal ACF, and four normal colon biopsies.

As shown in **Figure 15A**, a proximal, serrated hyperplastic ACF was positive for the in-frame insertion/deletion, *c.2239_2251delTTAAGAGAAGCAAinsC* (AA:L747_T751>P) in the *EGFR* gene (19.6% deletion: 80.4% wild-type) as detected by MASSArray This mutation was not present in the subject's blood, confirming that it was somatically acquired While EGFR mutations occur in approximately 6% of colorectal cancers (COSMIC, n = 3,102), they are much more frequent in lung adenocarcinomas (25.2%, COSMIC, n = 26,293). This specific mutation has not been previously detected in colorectal cancer and accounts for <1% of lung EGFR mutations, but is associated with a gain of EGFR function [132].

Additionally, a distal, distended hyperplastic ACF was positive for a *FLT3 c.2508C>G (I836M)* mutation (24.0% mutant: 76.0% wild-type) and confirmed by Sanger-sequencing to be somatic (**Figure 15B**). *FLT3* mutations have widely been implicated in cases of acute myeloid leukemia (23.5%, COSMIC, n = 63,213) and mutations to *FLT3* occur in 4.8% of colorectal cancers (COSMIC, n = 1,003). To our knowledge, the c.2508C>G mutation found in this study

Figure 14. Sequenom-based PCR amplification of LCM genomic DNA. Suitable amplification of genomic loci from three microdissected ACF samples was accomplished using the Sequenom standard PCR protocol. Microdissected ACF DNA achieved the equivalent amplification levels obtained using 1 ng of input DNA. The loci amplified is a 462 nt region of *RRBP1* using the following primers: F (exon): 5'-AGATGGCGAAAACTCACCACC-3' and R (intron): 5'- GCCTTTTTGCCCTGAGTAGT-3'. The primers span an intron-exon border to restrict amplification to the genomic DNA template.

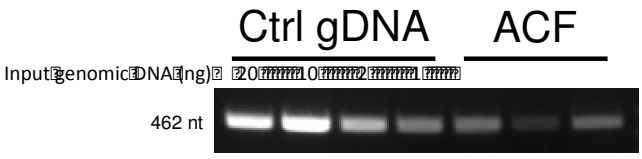
Ctrl gDNA
ACF
462 nt

Figure 15. DNA-MS identifies *FLT3*^{I836M} and a deletion to *EGFR* gene in hyperplastic ACF. A, DNA-MS identification of an insertion/deletion to the *EGFR* gene in a serrated hyperplastic proximal colon ACF. B, DNA-MS detection of a G>C missense mutation resulting in *FLT3*^{I836M} somatic mutation in a distended hyperplastic distal colon ACF. *UEP=unextended primer*

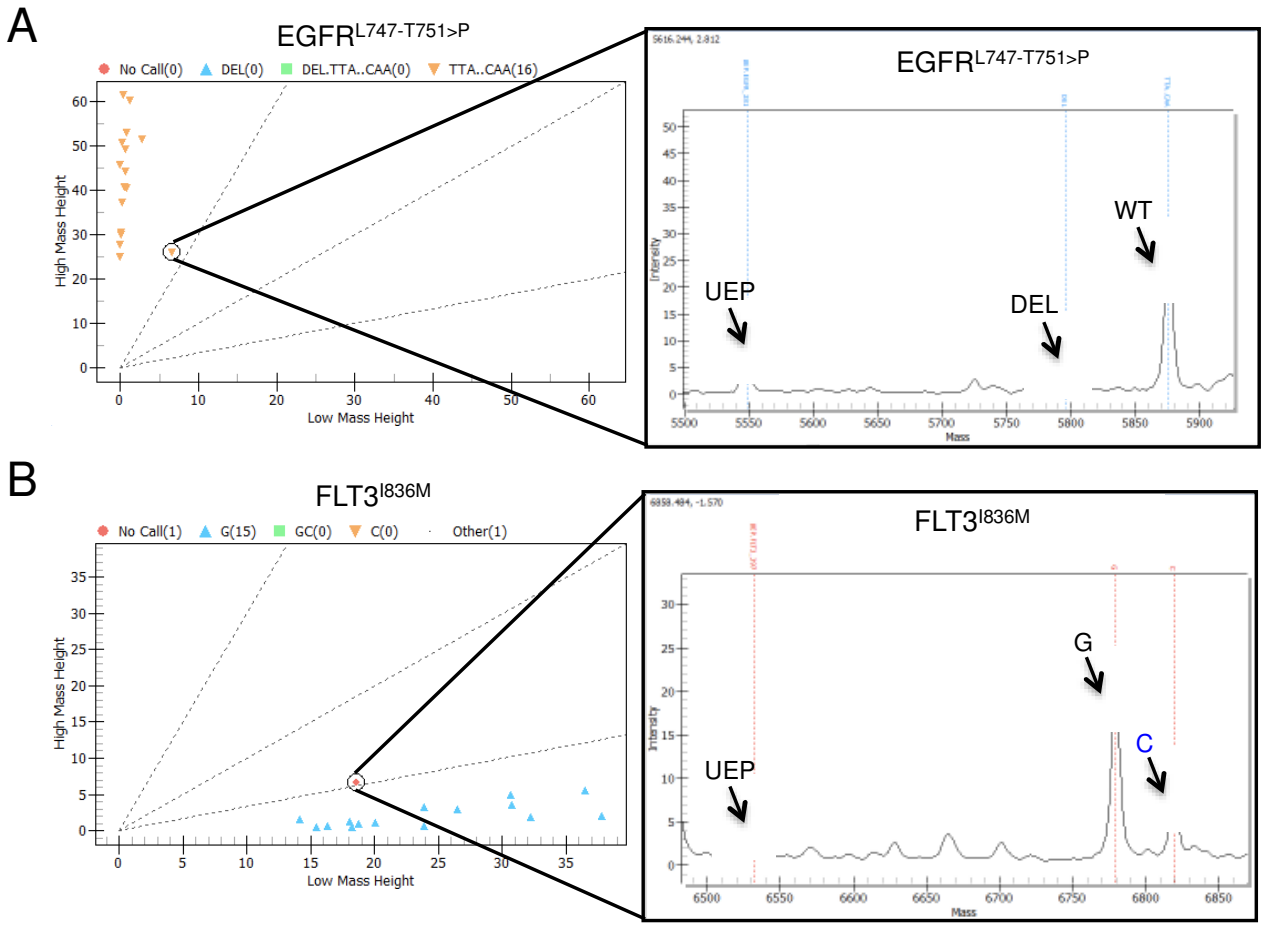
A
EGFR L747-T751>P
No Call(0)
DEL(0)
DEL.TTA..CAA(0)
TTA..CAA(16)
High Mass Height
Low Mass Height
EGFR L747-T751>P
UEP
DEL
WT
Intensity
Mass
B
FLT3 I836M
No Call(1)
G(15)
GC(0)
C(0)
Other(1)
High Mass Height
Low Mass Height
FLT3 I836M
UEP
G
C
Intensity
Mass

has never before been reported in colorectal cancer. The I836M missense mutation has been shown previously to cause constitutive activation of the receptor tyrosine kinase and subsequent downstream signaling[133]. Constitutive activation of these two receptor tyrosine kinases, not previously implicated in ACF formation, may contribute to the aberrant activation of MAPK signaling reported earlier in hyperplastic lesions[130].

While the commercially available panel used in this study does not include *KRAS* or *BRAF*, we have previously reported a high frequency of mutations to these protooncogenes in distal hyperplastic ACF using conventional PCR-based sequencing [60,130]. Thus to establish the presence of $BRAF^{V600E}$ and *KRAS* (codons 12 and 13) mutations, Sanger-sequencing was performed on seven randomly selected ACF that had no other somatic mutations detected by the OncoCarta panel. Four of the seven ACF were positive for *KRAS* mutations and none of the ACF had $BRAF^{V600E}$ mutations.

4.3.3. DNA mass spectrometry identifies a rare somatic APC mutation in a proximal colon ACF

An APC^{R876*} mutation, a c.2626C>T (30.4% mutant T: 69.6% wild-type C), was identified in a proximal dysplastic ACF (**Figure 16A**) In order to determine the function of this rare mutation, immunolocalization of the Wnt target protein, β-catenin, was performed on the dysplastic ACF. As shown in **Figure 16B**, there was an increase in nuclear accumulation of β-catenin in the dysplastic colonocytes compared to adjacent normal crypts. While mutations to *APC* are frequently detected in colorectal cancers (42%; COSMIC, n=3,982), the APC^{R876*} mutation is relatively rare, accounting for approximately 2.5% of all *APC* mutations. The

Figure 16. DNA-MS reveals *APC*^{R876*} somatic mutation in a proximal dysplastic ACF. A, DNA-MS reveals a c.2626C>T substitution resulting in an *APC*^{R876*} mutation in a proximal dysplastic ACF. *UEP = unextended primer.* B, IHC demonstrates an accumulation of nuclear β-catenin (black arrowheads) in dysplastic crypts positive for the *APC*^{R876*} mutation compared to adjacent normal crypts. (400x magnification; bar = 30 μm) C, Sanger sequencing confirms that the *APC*^{R876*} mutation is somatically acquired. Blood and synchronous tubular adenomas are wild-type at codon 876 of *APC*.

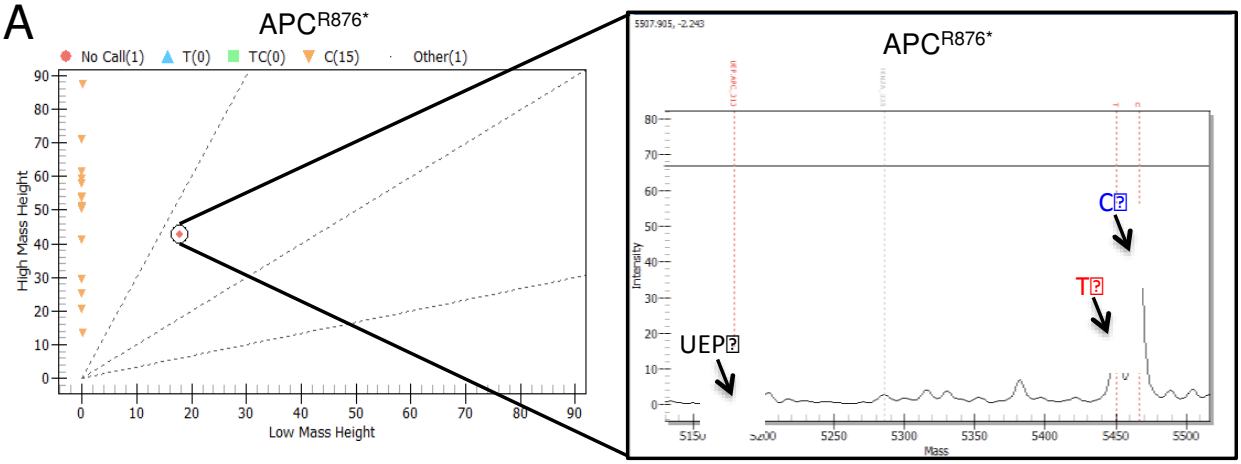
A
APC^R876*
No Call(1)
T(0)
TC(0)
C(15)
Other(1)
High Mass Height
Low Mass Height
APC^R876*
C?
T?
UEP?
Intensity
Mass

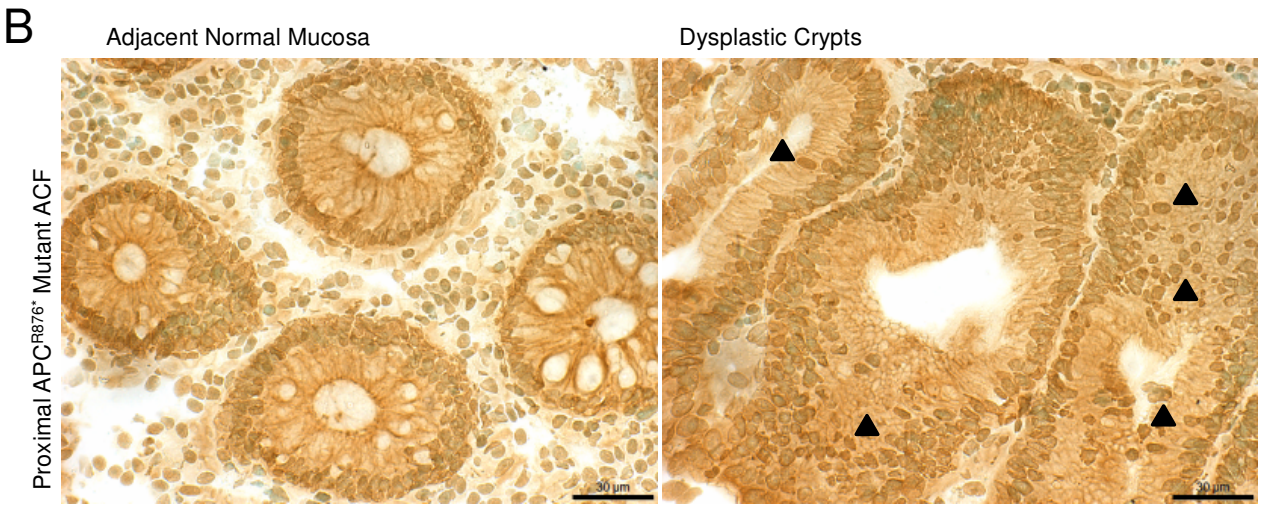
B
Adjacent Normal Mucosa
Dysplastic Crypts
Proximal APC^R876* Mutant ACF
30 µm
30 µm

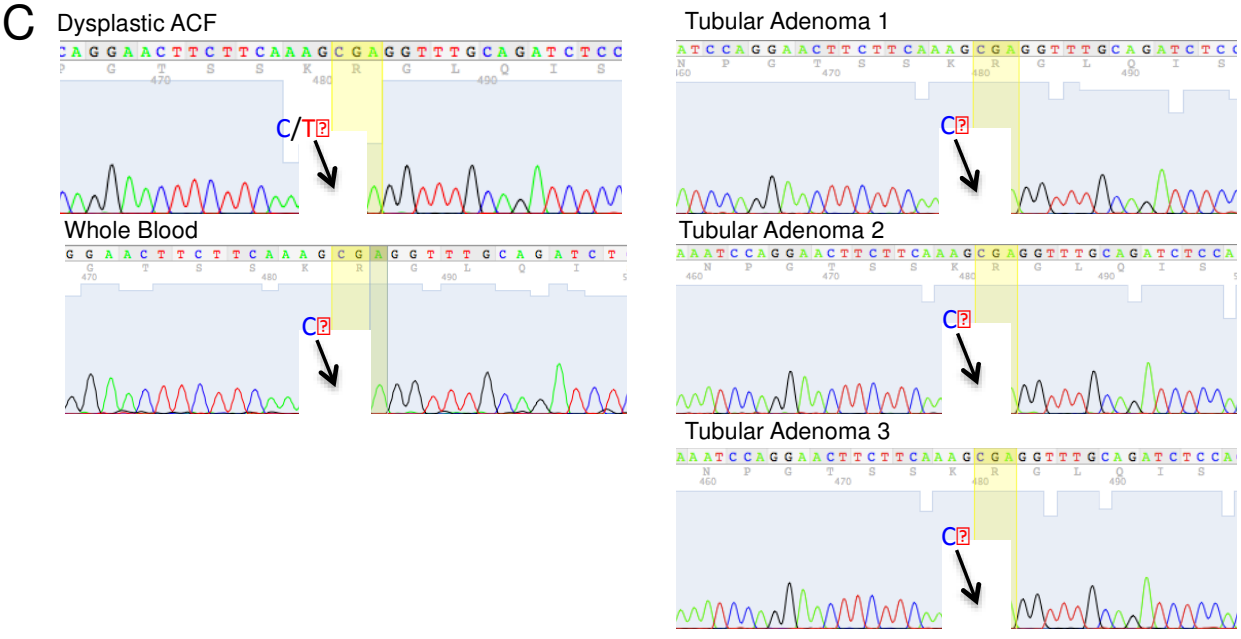
C
Dysplastic ACF
C/T?
Whole Blood
C?
Tubular Adenoma 1
C?
Tubular Adenoma 2
C?
Tubular Adenoma 3
C?

c.2626C>T non-sense mutation is most commonly somatically acquired[134], although it has occasionally been detected in FAP pedigrees [134-136]. In the present study, however, this mutation was confirmed to be somatic, as it was not detected in a matched blood sample (**Figure 16C**), thereby ruling out the possibility of underlying FAP disease. Interestingly, this mutation was not detected in any of the three synchronous tubular adenomas removed during the chromoendoscopy procedure (**Figure 16C**).

Sporadic forms of CRC are most likely the result of early somatic mutations resulting in the clonal expansion of initiated progenitor cells. ACF have been shown to be monoclonal and as such are likely the direct consequence of this initial clonal expansion [137]. Polyps and adenomas are presumed to arise from these lesions following the accumulation of multiple genetic alterations within this initiated cell population. Clearly, additional somatic mutations must occur to drive neoplastic progression [113]. Additional changes have been identified in early stages of CRC that contribute to carcinogenesis, including the acquisition of aberrant promoter methylation [72] and microsatellite instability [70]. Therefore, it is reasonable to anticipate that only a small percentage of ACF may sustain multiple oncogenic mutations at this early precancerous stage. In fact, in the present study there was no evidence for the presence of multiple somatic mutations, at least within the cancer panel that was tested.

The *in situ* identification of colonic ACF, and in particular those from the proximal colon, is dependent upon the use of dye-spray and high-definition magnifying endoscopy and we believe that in some cases this additional clinical effort is warranted. For example, the identification of the *APC* mutation, APC^{R876*}, associated with the formation of aggressive,

invasive carcinomas[138], in a commonly missed mucosal lesion underscores the potential preventive benefit of implementing this clinical approach to larger patient populations. It is possible that ACF that harbor this and other significant somatic mutations have the capacity to rapidly progress to a more advanced neoplasia, perhaps representing a subset of "missed lesions" that may be responsible for interval colon cancers. Expanded molecular classification of proximal ACF with a DNA-MS panel designed specifically for CRC, as well as establishing detailed associations of proximal ACF with known CRC risk factors, as explored in the next chapter, will be necessary to firmly establish their pre-malignant potential and utility as a surrogate marker for future cancer risk.

CHAPTER 5

PROXIMAL ABERRANT CRYPT FOCI AS A MARKER OF COLONIC MUCOSA AT RISK

5.1 Introduction

In the following study, we describe the routine study of ACF in both the proximal (including the cecum, ascending colon and hepatic flexure) and distal colorectum (distal 20-cm of the sigmoid colon, including the rectum) in a large screening population over a two-year period. We utilized high-definition chromoendoscopy to characterize these ACF for their clinicopathologic and molecular features. To do this we developed a custom high-throughput DNA mass spectrometry (DNA-MS) panel with coverage of 112 mutation targets in 12 CRC-related tumor suppressors and proto-oncogenes. In addition, detailed demographic information was collected on these patients and statistical models were used to associated proximal ACF with known CRC risk factors. This study is a direct follow-up to pilot study presented in Chapter 4. We demonstrate here that proximal ACF, in particular, may represent missed lesions that contribute to interval CRC and as such act as an important marker of 'at-risk' colonic mucosa.

5.2 Materials and Methods

5.2.1. Subject selection

168 patients underwent total colonoscopy at the University of Connecticut Health Center in accordance with Institutional policies. Patients were excluded from the study if they had

previously undergone screening or surveillance colonoscopy at another Institution or were suspected to have an inherited CRC genetic disorder such as familial adenomatous polyposis (FAP) or hereditary non-polyposis colon cancer (HNPCC). The study was performed after receiving approval from an Institutional Review Board, and all subjects provided written informed consent prior to all procedures.

5.2.2. ACF collection and characterization

ACF were isolated from grossly normal-appearing colonic mucosa as previously described[75]. Briefly, the proximal (the cecum and ascending colon, including the hepatic flexure) and distal 20-cm of the colorectum were sprayed with 1% indigo carmine solution administered through a spray catheter. ACF were visualized and photographed using Olympus high-definition endoscopes (PCX-190, Olympus Corp., Center Valley, PA) capable of 60x magnification with a focal length of 2 to 100 mm. Up to ten ACF per subject were biopsied using forceps and colonic location, diameter and endoscopic appearance were recorded. Normal biopsy specimens, one each from both the proximal and distal colon, were routinely collected. Biopsy specimens were immediately embedded in OCT, flash frozen and stored at -80°C.

A systematic pathologic analysis of ACF and normal biopsies was performed by a human gastrointestinal (GI) pathologist (T.V.R) blinded to endoscopic findings and a skilled technician, as previously described[75]. A subset of ACF (n=96) was analyzed by a second human GI pathologist (M.J.O'B) with good inter-rater agreement across the four possible pathologies (77.1% agreement, Kappa = 0.689 [S.E.=0.055; 95% CI: 0.58 – 0.80]). Blinded biopsies were confirmed to be either dysplastic or hyperplastic ACF or normal mucosa. Hyperplastic ACF were

further sub-classified into serrated and non-serrated (distended) pathologies. Biopsy specimens with the presence of 'pseudo' hyperplasia or dysplasia-like pathologic appearance due to the presence of a lymphoid follicle are not representative of a classic ACF and were considered "false-positive" [59,139].. ACF biopsy specimens that showed no histologic evidence of hyperplasia or dysplasia were considered a 'missed biopsy' and also not counted.

5.2.3 Laser capture microdissection and DNA purification

Frozen serial sections of colon biopsies were prepared on Arcturus PEN membrane glass slides (Applied Biosystems, Foster City, CA). Slides were dehydrated with ethanol and xylenes and LCM was performed using a Veritas microdissection instrument (Applied Biosystems). Morphologically distinct aberrant crypt populations, consisting of approximately 3-5,000 cells (the equivalent of 1 mm^2 of collected tissue area), were isolated on CapSure Macro LCM caps (Applied Biosystems) from adjacent normal mucosa and the surrounding stroma. Adjacent normal mucosa was separately collected when available. Genomic DNA was extracted on cap according to the PicoPure DNA extraction kit (Applied Biosystems) and cleaned using the DNA Wizard (Promega, Madison, WI) standard protocols.

5.2.4. DNA-MS mutation profiling

DNA-MS profiling was performed at the Yale Center for Genome Analysis on the MASSArray platform (Sequenom, Inc., San Diego, CA). The MASSArray platform uses matrix-assisted laser desorption ionization time-of-flight (MALDI-TOF) mass spectrometry to detect single base mutations with increased sensitivity as previously described (Drew MCR 2014). A custom panel of 112 mutations to 12 known CRC-related tumor suppressors and proto-

oncogenes was created using pilot study data[75], COSMIC and TCGA database mutation frequencies.

5.2.5. MSI analysis

MSI analysis was performed using five mononucleotide repeat microsatellite targets (BAT-25, BAT-26, NR-21, NR-24, and NR-27) in a pentaplex PCR assay. Primer sequences have been previously described[18,19]; each primer pair was fluorescently labeled with one of two markers: 6-FAM or NED. Pentaplex PCR was performed in a T100 Thermal Cycler (Biorad, Hercules, CA) with 1 μL of purified DNA using a touchdown thermal cycling profile. The PCR conditions consisted of an initial 10 minute denaturation step at 95°C, followed by 16 cycles at 95°C for 30 s, 60°C for 45 s (-0.5°C/cycle), 72°C for 30 s, followed by 34 cycles at 94°C for 30 s, 40°C for 45 s and 72°C for 30 s with a final extension at 72°C for 10 min. Amplified PCR products were sent to Genewiz, Inc., where a fluorescent size standard (LIZ) was added and samples were diluted 1:3 with formamide, and run on an Avant automated capillary electrophoresis DNA sequencer (Applied Biosystems). Peaks were analyzed using the PeakScanner Software v1.0 (Applied Biosystems). Samples that demonstrated no instability in any loci were considered microsatellite stable (MSS), instability in one of five loci were considered to have a microsatellite instability low phenotype (MSI-L), and instability in two or more loci were considered to have a microsatellite instability high phenotype (MSI-H).

5.2.6. Statistical analysis

Standard t-test and Cochran-Mantel-Haenszel χ^2 (CMH) tests were used for group comparisons for numerical responses (e.g. age, BMI) and categorical responses (e.g. gender,

smoking history, endoscopist), respectively. Negative binomial models were used to adjust for known risk factors age, BMI, gender, and smoking history. Current and former smokers were grouped together as "ever" smokers and compared to never smokers. To control for intra-observer variation, we also adjusted for endoscopist, as TJD (63% of all cases) vs. others (JCA 27%; BB 10%). Negative or Poisson binomial regression models are more appropriate for count data like the data in this study rather than logistic or linear regression models. Due to the presence of overdispersion (the variance is greater than the mean) in the data, use of the Poisson model is inappropriate as the negative binomial model accounts for this overdispersion as a variable in the model. All dispersion parameters from the models were significantly larger than zero, validating the use of the negative binomial model. All analyses were conducted using Statistical Analysis Systems v.9.4 (SAS 9.4).

5.3 Results

5.3.1. Baseline Characteristics of the Cohort

Between January 2011 and June 2013, a total of 168 subjects were enrolled and underwent the ACF screening procedure. **Table 13** presents descriptive statistics of the study population. These subjects had a mean age of 56.4 ± 7.8 years and were primarily male (60.1%) and Caucasian (80.3%). The majority of the subjects were never smokers (53.0%) and only 10.7% were current smokers. The mean BMI was 29.5 and the subjects were stratified by the BMI categories normal (<25.0; 23.8%), overweight (25.0 - <30; 39.9%), and obese (≥30; 36.3%). The majority of subjects did not have a family history of CRC (69.1%) and were undergoing screening colonoscopy (74.4%).

Table 13. Characteristics of the Subjects with and without proximal ACF.

Variable	Subjects			*P* value
	Total (n =168)	No Proximal ACF (n = 77)	≥1 Prox. ACF (n = 91)	
Age, mean ± SD	56.4 ± 7.8	54.9 ± 8.4	57.6 ± 7.1	0.0245*, t-test
Sex, n (%)				
Male	101 (60.1)	44 (43.6)	57 (56.4)	0.4700, CMH†
Female	67 (39.9)	33 (49.2)	34 (50.8)	
Smoker, n (%)				
Current	18 (10.7)	8 (44.4)	10 (55.6)	0.3210, CMH
Former	61 (36.3)	25 (41.0)	36 (59.0)	
Never	89 (53.0)	44 (49.4)	45 (50.6)	
BMI, mean ± SD	29.5 ± 6.1	29.1 ± 6.7	29.9 ± 5.6	0.4073, t-test
Normal (<25.0), n (%)	40 (23.8)	21 (52.5)	19 (47.5)	
Overweight (25.0-29.9), n (%)	67 (39.9)	26 (38.8)	41 (61.2)	
Obese (≥30), n (%)	61 (36.3)	30 (49.2)	31 (50.8)	
Family History of CRC, n (%)				
No	116 (69.1)	55 (47.4)	61 (52.6)	0.5404, CMH
Yes	52 (30.9)	22 (42.3)	30 (57.7)	
Procedure MD, n (%)				
TJD	105 (62.5)	45 (42.9)	60 (57.1)	0.3190, CMH
JCA	46 (27.4)	22 (47.8)	24 (52.2)	
BB	17 (10.1)	10 (58.8)	7 (41.2)	
Race, n (%)				
Caucasian	135 (80.3)	59 (43.7)	76 (56.3)	0.2639, CMH
African American	26 (15.5)	13 (50.0)	13 (50.0)	
Other	7 (4.2)	5 (71.4)	2 (28.6)	
Indication, n (%)				
Screening	125 (74.4)	63 (50.4)	62 (49.6)	0.0434*, CMH
Surveillance	43 (25.6)	14 (32.6)	29 (67.4)	
No. of ACF, mean ± S.D.	15.5 ± 14.6	11.4 ± 11.1	18.9 ± 16.3	0.0006**, t-test
Proximal ACF	0.9 ± 1.2	N/A	1.7 ± 1.2	
Distal ACF	14.6 ± 14.3	11.4 ± 11.1	17.2 ± 16.2	
Synchronous Polyps, mean ± S.D.	1.1 ± 1.5	0.7 ± 1.3	1.4 ± 1.6	0.0017**, t-test
No Polyps, n (%)	77 (45.8)	45 (58.4)	32 (41.6)	0.0026**, CMH
≥1 Polyps, n (%)	91 (54.2)	32 (35.2)	59 (64.8)	

†Denotes Cochran-Mantel-Haenszel Statistic.

5.3.2. Proximal ACF are Rare and Predict the Occurrence of Synchronous Neoplasia

A total of 2,598 ACF were counted in the subjects' proximal and distal colons with a mean of 15.5 ACF/subject. Only 5.8% of these ACF were in the proximal colon (mean = 0.9 proximal ACF /subject), while distal ACF contribute greatly to this number (14.6 distal ACF/patient; range) (**Table 13**). ACF multiplicity within the population was modeled using negative binomial regression while adjusting for age, gender, smoking status, BMI, and procedure MD (**Table 14**). Age (p=0.0026), smoking status (p=0.0269) and procedure MD (0.0008), were all significantly associated with higher ACF counts.

Approximately 54% of the population (n=91) had at least one proximal ACF. The study population was stratified according to those that had at least one proximal ACF and those that only had distal ACF. Pair-wise comparisons were performed between the two groups. Subjects with a proximal ACF were significantly older (mean = 57.6 years; t-test, p = 0.0245) and more likely to be undergoing surveillance colonoscopy (Cochran-Mantel-Haenzel χ^2, p = 0.0434) than patients with no proximal ACF. Additionally, those harboring a proximal ACF have significantly more ACF throughout their colon than those that do not (**Figure 17A**; p=0.0006, t-test). Distal ACF numbers using negative binomial regression were modeled while adjusting for other significant covariates in order to examine proximal ACF number as a predictor variable (**Table 15**). The model confirms that higher distal ACF counts are significantly associated with proximal ACF number (p=0.0184).

Table 14. Negative binomial model of total ACF. (* = p<0.05; ** = p<0.01)

Variable	Estimate (95% CL)	S.E.	*P* value	(*)
Age	0.0263 (0.01, 0.04)	0.0089	0.0032	**
Gender (M)	0.0354 (-0.24, 0.31)	0.1392	0.7992	
Smoker (Ever)	0.2929 (0.03, 0.55)	0.1328	0.0274	*
BMI	-0.0015 (-0.02, 0.02)	0.0108	0.8882	
Procedure MD (TJD)	0.5018 (0.22, 0.78)	0.1424	0.0004	**

Intercept = 0.7659 (-0.43, 1.97), SE = 0.61, p=0.2110; Dispersion = 0.6396 (0.51, 0.81), SE = 0.08

Figure 17. Proximal ACF incidence may indicate a field defect. A.) Total colon ACF counts for subjects with and without proximal (prox) ACF. Subjects with at least one proximal ACF have significantly higher (t-test; $p<0.01$) total colon ACF counts than those without ACF. **B**.) Subjects with at least one proximal ACF are significantly more likely to harbor a synchronous adenoma or polyp than those without proximal ACF (OR=2.59 [1.38-4.84]; Cochran-Mantel-Haenzel χ^2, $p = 0.003$). **C&D**.)To adjust for other CRC risk-factors, negative binomial modeling is used to predict the expected number of proximal ACF in a subject according to their (**C**) distal ACF counts and (**D**) number of synchronous polyps. Other CRC risk factors were kept constant at baseline or average value to generate predicted outcomes: age = 56; gender = male; smoking history = never; BMI = 30; Procedure MD = TJD.

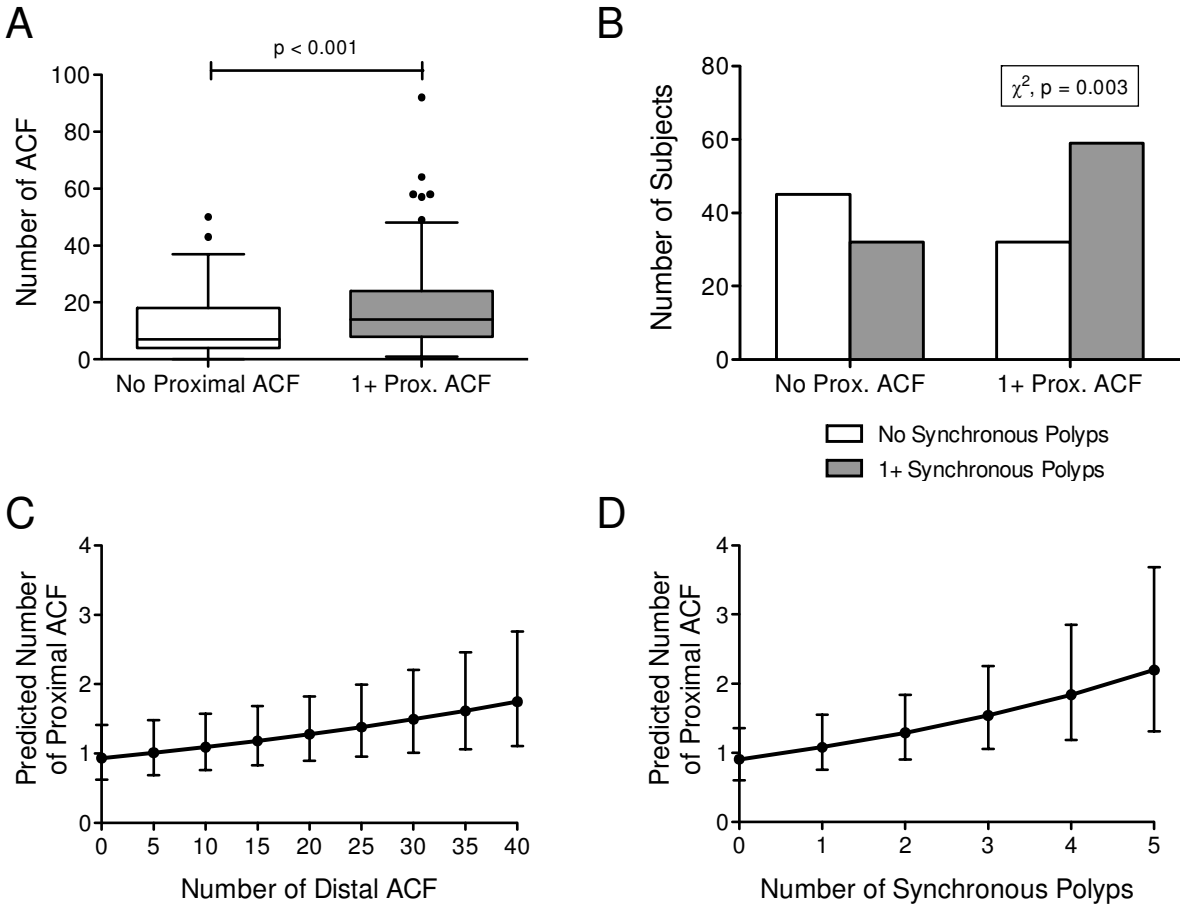
A
p < 0.001
Number of ACF
100
80
60
40
20
0
No Proximal ACF
1+ Prox. ACF
B
Number of Subjects
80
60
40
20
0
χ², p = 0.003
No Prox. ACF
1+ Prox. ACF
No Synchronous Polyps
1+ Synchronous Polyps
C
Predicted Number of Proximal ACF
4
3
2
1
0
0
5
10
15
20
25
30
35
40
Number of Distal ACF
D
Predicted Number of Proximal ACF
4
3
2
1
0
0
1
2
3
4
5
Number of Synchronous Polyps

This suggests that proximal ACF may indicate a possible field-defect within the colonic mucosa. Therefore, we examined whether these lesions associated with a firmly established CRC risk factor: the presence of one or more polyp or adenoma. The study population was further stratified according to whether or not they had a synchronous adenoma or polyp. Subjects with a proximal ACF are nearly three times as likely to have at least one synchronous polyp or adenoma somewhere within their colon (**Figure 17B**; OR=2.59 [1.38-4.84]; Cochran-Mantel-Haenzel χ^2, p=0.003). Negative binomial models predicting proximal ACF were used to confirm these findings, where separately, distal ACF number (**Table 16**) and synchronous polyp counts (**Table 17**) were included as predictor variables in addition to the covariates of age, gender, smoking status, indication, and procedure MD. Both distal ACF (p=0.018) and synchronous polyps (p=0.014) are strongly associated with proximal ACF. Expected proximal ACF counts were determined according to distal ACF count (**Figure 17C**) and the number of synchronous neoplasia (**Figure 17D**). Subjects are likely to have at least one proximal ACF if they have five or more distal ACF or at least one polyp, assuming they are at baseline or average risk for the other risk factors included in the model.

5.3.3. Proximal ACF are frequently dysplastic

A total of 760 ACF biopsies were subjected to routine pathologic assessment for histologic characteristics of ACF. The frequency of ACF pathologies by location is presented in **Table 18.** Of these biopsy specimens, 518 were confirmed to have an underlying ACF pathology (68.2%, positive hit-rate). False positives (e.g. the presence of a lymphoid follicle), contributed slightly more (19.2%) than missed biopsies (12.6%) to the negative hit rate. Additionally, there is no significant difference in these rates between colonic locations.

Table 15. Negative binomial model of distal ACF. (* = p<0.05; ** = p<0.01)

Variable	Estimate (95% CL)	S.E.	*P* value	(*)
Age	0.0247 (0.01, 0.04)	0.0091	0.0068	**
Gender (M)	-0.0194 (-0.30, 0.27)	0.1453	0.8935	
Smoker (Ever)	0.3676 (0.09, 0.64)	0.1396	0.0084	**
BMI	-0.0003 (-0.02, 0.02)	0.0111	0.9783	
Procedure MD (TJD)	0.4287 (0.13, 0.72)	0.1424	0.0044	**
Proximal ACF Number	0.1393 (0.02, 0.25)	0.0591	0.0184	*

Intercept = 0.6603 (-0.57, 1.89), SE = 0.63, p=0.2926; Dispersion = 0.6834 (0.54, 0.86), SE = 0.08

Table 16. Negative binomial model of proximal ACF with distal ACF as a predictor variable. (* = p<0.05; ** = p<0.01)

Variable	Estimate (95% CL)	S.E.	*P* value	(*)
Age	0.0018 (-0.02, 0.03)	0.0134	0.8930	
Gender (M)	0.3338 (-0.07, 0.74)	0.2060	0.1052	
Smoker (Ever)	-0.1780 (-0.57, 0.21)	0.1986	0.3701	
BMI	0.0068 (-0.03, 0.03)	0.0164	0.6763	
Procedure MD (TJD)	0.2604 (-0.17, 0.69)	0.2215	0.2398	
Distal ACF Number	0.0156 (0.003, 0.03)	0.0064	0.0141	*

Intercept = -0.9673 (-2.74, 0.81), SE = 0.63, p=0.2926; Dispersion = 0.4084 (0.18, 0.94), SE = 0.17

Table 17. Negative binomial model of proximal ACF with synchronous polyps as a predictor variable. (* = p<0.05; ** = p<0.01)

Variable	Estimate (95% CL)	S.E.	*P* value	(*)
Age	0.0084 (-0.02, 0.03)	0.0130	0.5163	
Gender (M)	0.1642 (-0.25, 0.27)	0.2090	0.4323	
Smoker (Ever)	-0.1417 (-0.52, 0.24)	0.1951	0.4676	
BMI	-0.0004 (-0.03, 0.03)	0.0164	0.9828	
Procedure MD (TJD)	0.3507 (-0.07, 0.77)	0.2142	0.1015	
Total Polyp Number	0.1771 (0.06, 0.29)	0.0589	0.0026	***

Intercept = -1.0752 (-2.84, 0.69), SE = 0.90, p=0.2329; Dispersion = 0.3779 (0.16, 0.90), SE = 0.17

Table 18. ACF pathologies by colonic location.

Pathology	ACF Location	
	Proximal Colon (n = 91)	Distal Colon (n = 427)
Dysplastic†	52 (57.1†)	56 (13.1)
Hyperplastic		
Serrated‡	11 (12.1)	271 (63.5‡)
Non-serrated	28 (30.8)	100 (23.4)
Hit Rate*	66.9%	68.4%
False-Positive Rate	16.9%	19.7%

*False Positive rate and hit rate calculated from pathologic analysis performed on 760 biopsies (136 proximal and 624 distal)

† OR[(*proximal, distal*) vs. (*dysplastic, hyperplastic)*] = 8.8 (95% CI: 5.4-14.6); χ^2 p<0.0001

‡ OR[(*proximal, distal*) vs. (*serrated, non-serrated)*] = 6.9 (95% CI: 3.3-14.4); χ^2 p<0.0001

Sampled ACF are more frequently hyperplastic (79%) throughout the colon, rather than dysplastic (**Table 18**). However, in context of colonic location, proximal ACF are frequently dysplastic (57%) and rarely serrated (12%). This is the opposite case in the distal colorectum, where the majority of ACF are serrated (64%) and dysplastic ACF are firmly the minority (13%). Non-serrated hyperplastic ACF are slightly more frequent in the proximal colon (31%) than the distal colorectum (23%).

Odds ratios were calculated for pathology and location. The odds of a dysplastic ACF being proximally located are approximately nine times more likely than it occurring in the distal colon or being hyperplastic (**Table 18**,†; OR=8.83 [95% CI: 5.35-14.58]; χ^2, $p<0.0001$). Among hyperplastic ACF, the serrated histology is approximately seven times more likely to occur in the distal colon than the proximal colon compared to non-serrated ACF (**Table 18**,‡; OR=6.90 [95% CI: 3.31-14.38, χ^2, $p<0.0001$).

5.3.4. Dysplastic ACF frequently have APC mutations, while hyperplastic ACF associate with MAPK activating mutations.

We have previously demonstrated the ability to use DNA mass spectrometry to reliably detect somatic mutations in microdissected ACF samples[75]. A custom mutation panel for CRC-specific tumor suppressors and proto-oncogenes was developed (**Table 19**). Genomic DNA was extracted from 42 microdissected proximal ACF, and 6 microdissected normal samples and subjected to DNA-MS analyses. HAPMAP genomic DNA was used as a negative control. Forty percent of the proximal ACF assayed were positive for a mutation covered by the panel.

Table 19. Mutations screened for using the custom ACF DNA-MS panel.

Gene (# mutations)	**Mutation Screened**
APC (11)	E1306*, E1379*, N1661*, Q1338*, Q1367*, Q1378*, Q1429*, R1114*, R1450*, R876*, S1465*
BRAF (5)	D594G, V600E/G/L/M
CDKN2A (7)	D84Y, E61*, E69*, E88*, H83Y, R58*, R80*
EGFR (15)	G719SC, L858R, L861Q, E746delGGA, E746delAAT, E746delATT, L747delTTA, L747delTAA, S752IF, A750P, T751I, P753Q, T751PAS, R108K, T790M
ERBB2 (8)	A775_G776insYVMA, D769H, G776SLC, G776VC, L755P, P780_Y781insGSP, S779_P780insVGS, V777L
FLT3 (2)	D835del, D835HY
HRAS (5)	G12VD, G13CRA, Q61H/K/LRP
KRAS (11)	A59T, G12A/C/D/R/S/V, G13V/D, Q61H/LRP
MET (5)	M1268T, R988C, T1010I, Y1248C, Y1253D
NRAS (19)	A18T, G12V/A/D/C/R/S, G13V/A/D/C/R/S, Q61E/K/L/R/P/H
PIK3CA (14)	C420R, C901F, E542K, E545K, H1047R/L/Y, H701P, M1043I, N345K, P539R, Q546K, R38H, R88Q
TP53 (9)	D281G/Y/H, G245SRC, G248GW, R273C/H/L, V143A

Positive mutation calls appear in **Table 20**. *APC* mutations were most frequent (14.3%) followed by mutations to *KRAS* (11.9%) and *BRAF* (7.1%), respectively and these mutations associate with specific pathologies. *APC* mutations are exclusively observed in dysplastic ACF (6 of 6) while mutations implicated in mitogen-activated protein kinase (MAPK) activation (*KRAS, BRAF, NRAS, ERBB2*) are primarily observed in hyperplastic ACF (9 of 11). No ACF were positive for more than one mutation.

Eight of 19 dysplastic ACF (42.1%) were positive for a mutation as detected by the panel. Five of these ACF were positive for non-sense point mutations to APC, either APC^{R876*} (*c.2626C>T*; n=3) or APC^{R1450*} (*c.4348C>T*; n=2). One ACF was positive for a deletion frameshift ($p.APC^{S1465fs*3}$) resulting in a premature stop codon downstream of Ser(1465). Additionally, a dysplastic ACF was positive for a $BRAF^{V600E}$ (*c.1799T>A*) mutation and another was positive for a $KRAS^{G12D}$ (*c.35G>A*) mutation.

Of the 23 hyperplastic ACF (serrated, n=8; non-serrated, n=15) assayed, 39.1% were positive for a MAPK-associated gene mutation. Four non-serrated hyperplastic ACF were positive for mutations within codon 12 of *KRAS*, one with *p.G12D* and three with *p.G12V* (*c.35G>T*) mutations. Two additional non-serrated hyperplastic ACF were positive for *ERBB2* mutations; one was positive for a missense mutation *p.G776S* (*c.2326G>A*) and the other an insertion, *p.A775_G776insYVMA* (*c.2324_2325insATACGTGATGGC*). Two serrated ACF were positive for $BRAF^{V600E}$ mutations while a third was positive for a $NRAS^{G13D}$ (*c.38G>A*) mutation.

Table 20. Mutations detected by DNA-MS panel in microdissected proximal ACF.

ACF ID #	Pathology	Gene	Mutation
077-1	Dysplastic	*APC*	R876*
149-2	Dysplastic	*APC*	R876*
152-1	Dysplastic	*APC*	R876*
230-1	Dysplastic	*APC*	R1450*
237-1	Dysplastic	*APC*	R1450*
240-1	Dysplastic	*APC*	S1465fs*3
076-1	Serrated	*BRAF*	V600E
121-1	Serrated	*BRAF*	V600E
229-1	Dysplastic	*BRAF*	V600E
115-1	Distended	*ERBB2*	A775_G776insYVMA
150-1	Distended	*ERBB2*	G776S
122-1	Distended	*KRAS*	G12D
151-1	Dysplastic	*KRAS*	G12D
121-4	Distended	*KRAS*	G12V
225-2	Distended	*KRAS*	G12V
230-3	Distended	*KRAS*	G12V
026-1	Serrated	*NRAS*	G13D

5.3.5. MSI is significantly associated with hyperplastic ACF, but not a colonic location.

We analyzed 35 proximal ACF (19 hyperplastic ACF; 16 dysplastic ACF) and 92 distal ACF (79 hyperplastic ACF; 13 dysplastic ACF) for MSI. Samples positive for instability in two or more microsatellite markers were considered MSI-H (**Figure 18A**, *bottom*), in only a single marker, MSI-L, and no markers, MSS (**Figure 18A**, *top*). Thirty percent of ACF were found to be MSI-H, with the majority of the MSI-H lesions being hyperplastic (89%) and distal (82%) (**Figure 18B**). For group comparisons MSS and MSI-L were grouped together as there are no established clinical, survival or prognostic, differences between MSI-L and MSS CRC[140-142]. MSI-H is more than three times more likely to be associated with a hyperplastic pathology rather than dysplasia (**Figure 18C**; OR [hyperplastic, MSI-H] = 3.32 [95%CI: 1.07-10.33]; χ^2, p = 0.03). There is no significant difference between the rates of MSI-H in serrated versus non-serrated hyperplastic ACF (χ^2, p = 0.43). There is also no difference between the rates of MSI according to colonic location (χ^2, p = 0.13).

5.4 Discussion

Since being first described nearly 30 years ago [58], ACF have been carefully examined in human and murine colons as surrogate markers of colorectal cancer risk or as endpoints for chemoprevention trials [80,82,88,143,144]. Classically and especially in chemoprevention trials, studies of ACF have been focused on endoscopic counts of distal ACF. As a result, gastroenterologist interrater variability has undoubtedly clouded their practicality in providing individual risk assessment[84], leading some to question their utility as a surrogate marker and, ultimately, their role in tumorigenesis [83,86,87].

Figure 18. Microsatellite instability in microdissected ACF. A.) *Top*; Allele size, in base pairs, frequency spectrum of five microsatellite markers (NR-27, NR-21, NR-24, BAT-25, BAT-26) in a microsatellite stable (MSS) ACF sample. *Bottom*; Four of five microsatellite markers (all but NR-24) show signs of instability in a microdissected ACF, as measured by a decrease in allele size (**arrows**). Two or more instable microsatellite markers indicate high microsatellite instability (MSI-H), as shown here, while instability measured in a single marker indicates low instability (MSI-L). **B**.) Rates of MSS (white bars), MSI-L (grey bars), and MSI-H (black bars) in microdissected ACF, grouped by colonic location and lesion pathology. **C**.) MSI-H significantly associates with hyperplastic ACF (35% of all hyperplastic ACF; n=98) compared to dysplastic ACF (14% of all dysplastic ACF; n=29); OR (hyperplastic, MSI-H) = 3.32 [95%CI: 1.07-10.33; (Fisher's Exact test, p=0.037)].

A

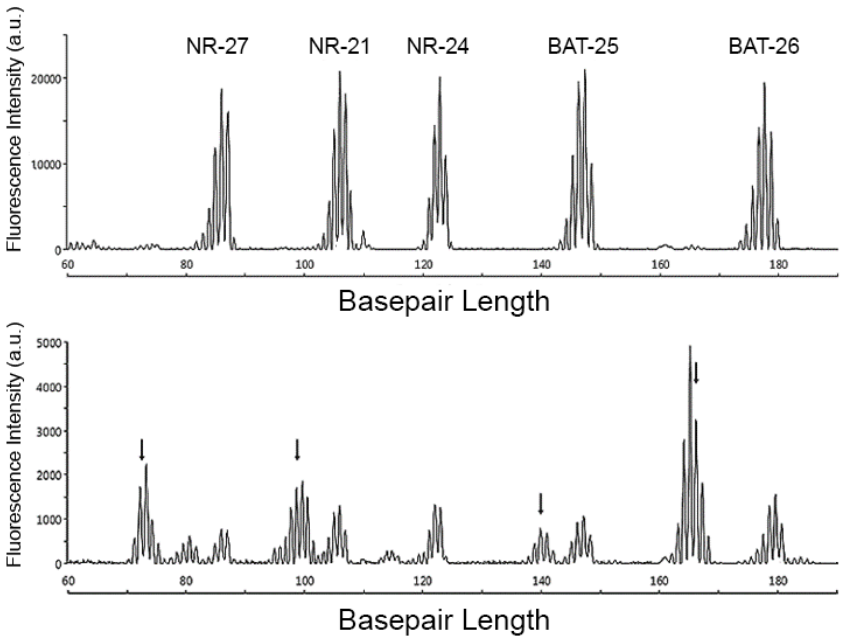
NR-27
NR-21
NR-24
BAT-25
BAT-26
Fluorescence Intensity (a.u.)
Basepair Length
Fluorescence Intensity (a.u.)
Basepair Length

B

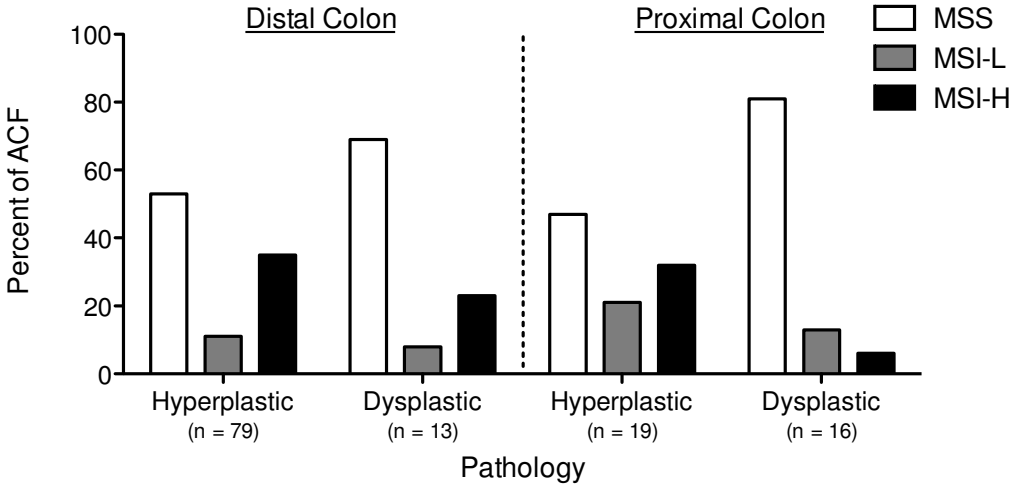
Distal Colon
Proximal Colon
MSS
MSI-L
MSI-H
Percent of ACF
Hyperplastic
(n = 79)
Dysplastic
(n = 13)
Hyperplastic
(n = 19)
Dysplastic
(n = 16)
Pathology

C

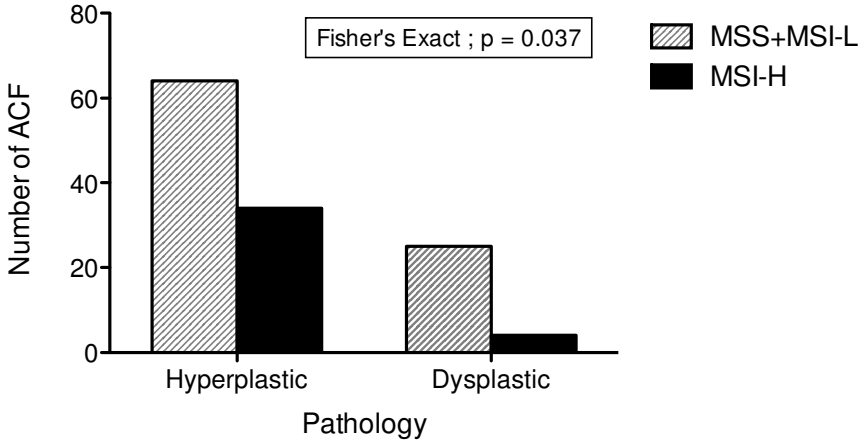
Fisher's Exact ; p = 0.037
MSS+MSI-L
MSI-H
Number of ACF
Hyperplastic
Dysplastic
Pathology

We demonstrate in this study that the procedure endoscopist does have a significant effect on ACF counts even within the same clinical setting. However, after carefully adjusting for this effect, there are still significant associations between ACF numbers and other CRC risk factors such as age and smoking history (**Tables 13 & 14**), as previously described[145]. Furthermore, the high hit-rate and low false-positive rate demonstrates that an ACF's endoscopic appearance is a reliable measure of an underlying pathology (**Table 18**), not unlike the endoscopic identification of polyps or adenomas.

The disproportionate incidence of ACF between regions of the colon may mean that the presence of a proximal ACF may be a distinct surrogate marker of CRC. This is not intended to imply that distal ACF are not important CRC biomarkers, as we have recently shown that increased distal ACF counts significantly associate with increased risk of advanced neoplasia upon five-year follow-up[74]; This study demonstrates that proximal ACF are associated with other markers of CRC risk including the incidence of synchronous neoplasia as well as elevated distal ACF counts (**Figure 18**). The presence of a proximal ACF may indicate a potential field effect or a 'fertile field' for neoplastic initiation.

Additionally, the high rate of dysplasia in proximal ACF further implicates their importance in CRC tumorigenesis and as a surrogate marker. Compared to the distal colon where ACF are primarily hyperplastic, the discretionary line between a proximal ACF and a "micro-adenoma" may be much less clear[146,147], especially considering the frequency of significant *APC* mutations. APC^{R876*} and APC^{R1450*} are non-sense mutations resulting in premature truncations to the APC gene. Another dysplastic ACF was positive for a deletion frameshift

(*APC*^{S1465fs*3}). Both APC^{R1450*} and this deletion occur in the gene region commonly referred to as the "mutation cluster region" (region spanning base pairs 1263-1589) and have been detected in colorectal cancers. These two mutations result in truncation of the APC protein and impaired beta-catenin binding capacity [13]. The APC^{R876*} mutation, while detected rarely in CRC, has previously been detected in ACF and although located outside the mutation cluster region, results in a truncated protein product and nuclear beta-catenin accumulation[75]. These ACF meet two of the criteria of traditional (tubular/villous) adenomas: aberrant Wnt activation and cytological dysplasia, and should be considered "pre-cancerous" lesions. Combined with the fact that surveillance of these lesions is not routinely included as a part of screening endoscopy and its possible that proximal ACF may significantly contribute to the incidence of interval CRC.

The high frequency of a detected mutation in proximal hyperplastic ACF suggests that a subset of these lesions may be primed for CRC development as well. We previously demonstrated (Chapter 3) the high frequency of *KRAS* (codons 12 and 13) and BRAF^{V600E} [60,76,148] mutations and the subsequent activation of the MAPK signaling cascade [130] in distal hyperplastic ACF. The identification of additional drivers of MAPK signaling, a hallmark of the serrated or alternative colon carcinogenesis pathway[4], such as *ERBB2* and *NRAS* in proximal hyperplastic ACF may have important implications in understanding serrated carcinogenesis. To our knowledge this is the first description of these two genes being mutated in human ACF, but not in CRC[118].

Importantly, MSI was significantly associated with hyperplastic ACF (**Figure 18**). MSI has previously been determined to have an important role in colon carcinogenesis especially in

cancers arising via the serrated pathway. The presence of MSI in ACF was first detected in patients with concurrent CRC [68,69] and later in ACF endoscopic biopsy specimens[70]. Cancers arising from the proximal colon are associated with the serrated pathway and are more likely to be microsatellite instable [4,149]. The association between hyperplastic ACF and MSI was not found to be location dependent in the present study. However, considering the high frequency of oncogenic mutation detected in these lesions and the increased risk for MSI, it is apparent that a subset of these lesions may be at increased risk for neoplastic progression and may warrant careful surveillance.

CHAPTER 6

SUMMARY, CONCLUSIONS, & FUTURE DIRECTIONS

Screening colonoscopy and subsequent polypectomy has become the frontline CRC prevention tool in the United States. However, modest CRC mortality and morbidity reduction following its wide-spread implementation and the observation of interval cancers have highlighted inherent limitations with routine or standard-of-care endoscopy. Routine lower endoscopy consists of either sigmoidoscopy (endoscope only advances to, and not beyond, the proximal sigmoid colon) or total colonoscopy (screened from cecum to anus) and has been credited with a lowering of CRC risk in multiple studies [26-28]. However, endoscopy is significantly more successful in preventing distal CRC compared to proximal CRC [25]. Needless to say, there are obvious reasons why sigmoidoscopy may be limited in preventing proximal CRC; even though, numerous epidemiological studies have shown that compared to no screening, sigmoidoscopy does reduce overall CRC risk [25]. Therefore, for the purposes of this discussion, 'colonoscopy' or 'endoscopy' will be used interchangeably to refer to total colonoscopy.

There are a few possible, non-mutually exclusive, explanations for the observed preventative differences between colonic locations.

1. Cancers arising in the proximal colon may acquire an aggressive molecular phenotype causing their rapid progression from precancerous lesions to malignancy; or,
2. Precancerous lesions within the proximal colon are difficult to detect or completely resect using routine endoscopy.

The traditional adenoma-carcinoma sequence provides a paradigm for explaining the success of colonoscopy. The step-wise accumulation of molecular aberrations described takes considerable time, years or even a decade, between the first initiating mutation and malignant transformation[2]. Cells maintain many mechanisms to respond to stressors, such as oncogene activation or DNA damage. Under normal conditions these cells will undergo senescence, quiescence or apoptosis, to prevent the propagation of damaged and potentially harmful cells. Therefore, for an initiated, precancerous cell to ultimately form a cancer, many of these protective mechanisms must be bypassed either through epigenetic silencing of the genes responsible or loss of function of the genes through mutation or chromosomal loss[150,151]. This explains why CRC cancers, but not precancerous polyps or adenomas, are typically negative for the expression of potent tumor suppressors such as p16 or p53 [3,124].

Oncogene induced senescence (OIS) is a phenomenon that has been described in cell and animal models of oncogene activation[124,152]. In response to oncogene activation, especially *KRAS* and *BRAF* mutations, tumor suppressors such as p16 are upregulated and cells enter a reversible, senescent state[122,123]. This effect has been observed in mouse models of *RAS* and *RAF* activation{Bennecke, 2010 #441;Carragher, 2010 #180}. OIS may partially explain the difference between proximal and distal ACF multiplicity. We hypothesize that distal ACF, which we report are primarily hyperplastic, frequently carry BRAF and KRAS mutations and significantly upregulate MAPK (Chapter 3), possess the appropriate characteristics to activate OIS. Initial attempts at quantifying p16 expression in ACF using conventional immunofluorescence proved difficult. While p16 expression was apparent, the changes between senescence-associated p16 expression and regular expression may be too slight to measure with

immunohistology. Additional studies, designed to sensitively measure RNA or protein expression of OIS pathway components should be performed to further implicate the role of OIS in ACF.

However, subsets of precancerous lesions may acquire molecular phenotypes that accelerate tumorigenesis and bypass protective mechanisms. Inherited defects in MMR genes are responsible for the CRC syndrome, HNPCC, in which 80% of all HNPCC patients will be diagnosed with CRC[140]. Somatic acquisition of defects to MMR genes either through point mutation or epigenetic silencing can cause a similar genomic instability phenotype, as measured by MSI[17]. Cells lose their ability to recognize and repair DNA damage without intact MMR function and may lose the ability to perpetuate pro-apoptotic signals[153]. Therefore, MSI-H lesions may more readily bypass protective apoptotic responses and accumulate genetic mutations at a significantly higher rate than MSS lesions. Importantly, MSI-H associates with SPs, especially SSAs, which have a predilection for the proximal colon[4,37,46]. Moreover, proximal CRCs are significantly more likely to be MSI-H than MSS[15,22].

We report here that 30% of ACF biopsy specimens were MSI-H consistent with early acquisition of a genomic instability phenotype (Chapter 5). While the rate of MSI-H in ACF did not significantly associate with a specific location in this study, MSI-H did specifically associate with hyperplastic ACF, the putative precursors to SPs. We acknowledge that the study may have been underpowered to measure site-specific associations of genomic instability (only 35 proximal ACF were available for MSI analysis). By increasing sample size, any relationship between colonic location and MSI within ACF may become more apparent.

Another proximally associated molecular phenotype of CRC is CIMP. While CIMP status was not investigated by these studies, CIMP has previously been associated with proximal cancers[17,22], SPs [15] and ACF[71]. Aberrant promoter methylation leading to loss of tumor suppressor gene expression, may also contribute to a rapid transformation from early precancerous lesion to malignancy [72]. Therefore it will be necessary to investigate epigenetic features of ACF, especially in context of their colonic location in future experiments. Because these are early lesions, to get an accurate representation of genome-wide epigenetic changes it may be necessary to expand beyond the limited scope of established CIMP panels.

Advances in epigenomics have provided sensitive tools, such as reduced representation bisulfite sequencing (RRBS)[154] or methylated CpG island recovery assay (MIRA)[155], which can provide comprehensive DNA methylation analysis in frozen biopsy samples. By doing so, insight may be obtained as to the earliest epigenetic changes resulting from or causing CRC initiation. Focus could be placed on those genes and signaling pathways involved in OIS. Proximal ACF, especially proximal hyperplastic ACF, may show early signs of the epigenetic signatures of advanced neoplasia or CRC and may have distinctly different methylation patterns compared to their distal or dysplastic counterparts.

These potential aggressive molecular phenotypes that may contribute to interval cancers all have clear associations with SPs. As discussed in the introduction, SSAs are the most accepted precancerous lesion of the serrated pathway and are very difficult to detect and resect due to their sessile morphology, the presence of a mucous cap obscuring endoscopic detection, and the lack of visually defined borders[12]. Furthermore, SSAs are likely to be proximally

located. Prevention of serrated carcinomas by polypectomy may be less trivial than reducing traditional carcinomas. Traditional adenomas are likely to be distally located and thus can be detected by either total colonoscopy or sigmoidoscopy. Moreover, their typical pedunculation and separation from the surrounding normal mucosa by a stalk-like projection may lead to easier identification and more complete resection[8].

Considering these morphologic features, it is not difficult to envision why interval cancers are more likely to be proximally located [31]. In fact, recent reports strongly implicate that the majority, up to 75% of iCRCs are the direct result of missed lesions during index colonoscopy[30-35]. While correlative, it appears the hardest to detect lesions and thus the most likely to be missed lesions, are the most likely to harbor aggressive molecular phenotypes, creating a potential perfect storm that may be responsible for interval cancers.

While gastroenterologists undoubtedly always perform careful endoscopic observation, we present risk factors for polyp occurrence that may identify patients who would benefit from the highest standard of care in an effort to reduce iCRC. Withdrawal time, for instance, is correlated with a clinician's adenoma detection rate[107] and thus inversely correlated with iCRC incidence[30]. We confirm a number of known risk factors for polyp occurrence including age, gender, and family history of CRC (Chapter 2). We also confirm the overall preventive effect of aspirin. Interestingly, however, we demonstrate a subset of the population that may be at increased risk for polyp occurrence: those that take aspirin daily and also have a history of smoking. This finding extends the recent results of Ishikawa *et al.,* who during a randomized

clinical trial of aspirin and CRC recurrence found that smoking abrogated the protective effect of aspirin and increased risk of CRC recurrence[105].

Once we stratified these results further according to polyp location and pathology, we found that the protective effect of aspirin was limited to traditional adenomas. While we were underpowered to study the interaction effect in the pathologic and location subtypes, smoking was positively associated with serrated polyp occurrence. NSAIDs, including ibuprofen and aspirin, have been shown to decrease total levels of cellular β-catenin and induce its phosphorylation in addition to inhibiting other downstream signaling effects within the Wnt pathway[57]. Since SPs are not associated with the canonical-Wnt signaling pathway, but instead the MAPK signaling cascade it follows that they may not be prevented by regular aspirin use and is consistent with our results. Therefore, a smoker who takes aspirin daily may not expect to be as protected as a non-smoker because of their increased risk for SPs. However, a biological explanation for the observed synergy between smoking and aspirin use leading to a higher risk of polyps than those who smoke, but do not take aspirin, is not readily apparent. Further investigation into this interaction is certainly warranted.

We also demonstrate that proximal lesions are significantly predicted by statin use and family history compared to distal lesions; and separately, that SPs are predicted by smoking status and BMI compared to traditional adenomas. Patients with these risk factors may be the most likely to benefit from shortened surveillance intervals, increased withdrawal times or advanced endoscopic techniques to increase the adenoma detection rate during index

colonoscopy. Prospective clinical studies could be performed to measure the added benefit of these different approaches in high-risk individuals.

Individuals who upon index colonoscopy had one or more precancerous lesion removed are at greater risk for iCRC compared to the those with clean colonoscopies[31]. This suggests that those patients with polyps upon index colonoscopy are likely to be harboring a precancerous lesion that goes undetected during the initial colonoscopy. This is consistent with our results showing that those patients in our study who were undergoing surveillance colonoscopy rather than a screening colonoscopy were significantly more likely to have a traditional adenoma somewhere within their colon (Chapter 2). It is possible that proximal ACF may represent the missed lesion that is contributing to the high rate of adenomas and iCRC in this high-risk population since ACF are routinely missed during standard endoscopy. Given the high frequency of dysplasia within proximal ACF, the identification of somatic, loss-of-function *APC* mutations, and their strong association with synchronous neoplasia, proximal ACF may be too important a lesion to ignore in high-risk individuals (Chapters 4&5).

While the reliability of ACF endoscopic appearance has been questioned, the present study demonstrates that the endoscopic appearance of an ACF is representative of an underlying, but not specific, pathology. Within the proximal colon, where ACF multiplicity is much lower, the frequency of dysplasia is considerably higher than previous studies that were limited to the distal colon[83]. Furthermore, they correlate with synchronous neoplasia and higher distal ACF counts, established markers of the colonic mucosa at risk. Therefore, proximal ACF may represent a distinctly different surrogate marker from distal ACF counts.

Additionally, the use of chromoendoscopic from the cecum to the hepatic flexure and identification of ACF should be more feasible than attempting to make total colon ACF screening a standard practice. By limiting ACF screening to the cecum and ascending colon, only a few additional minutes (<10) will be added to the standard colonoscopy procedure. Also, this measure may only be necessary in those individuals the clinician feels may be at risk for iCRC development. The presence of an adenoma or polyp on the way to the cecum during total colonoscopy could serve as an easily identifiable clinical indication for when this additional step may be warranted.

The addition of dye-spray and close surveillance of the proximal colon may have supplemental benefits for CRC prevention not specific to the identification and removal of proximal ACF. During careful proximal ACF screening, withdrawal times will certainly be extended thereby potentially increasing the adenoma detection rate. The use of dye-spray may also help in the identification and resection of SSAs by providing clearer visualization of the lesion and its borders; an observation that was made, but not specifically investigated, during the course of the clinical study.

In summary, proximal ACF are rare compared to their distal counterparts, but may signify the presence of a field defect or a colonic mucosa at higher risk for CRC development. Additionally, the high frequency of dysplasia and APC mutations, specifically, in biopsied proximal ACF, suggests that dye-spray and HD endoscopy may be warranted in certain cases, for example those with at least one synchronous polyp, of advanced age, or with a history of smoking. Given that proximal ACF are not included in routine screening, frequently possess

clinicopathologic and molecular features observed in neoplasia, and associate with other known CRC risk factors, it is clear that these lesions harbor some level of carcinogenic potential. As such they may represent a significant “missed” lesion and directly contribute to interval cancers.

APPENDIX

DETAILED PATHOLOGIC CHARACTERIZATION

We have used the following set of criteria for diagnosing polyps based on the recommendations of the World Health Organization[7]:

Serration is the presence of in-foldings of the surface epithelium of the crypt, creating micropapillations towards the lumen. It may or may not be associated with dysplasia. It is typically created as the result of alteration of proliferative zone of the crypts also leading to "hypermaturation" / accumulation of apoptotic cells / shedding of the aging cell. Serration leads to various morphologic patterns creating three main categories of lesions; hyperplastic polyp, sessile serrated adenoma and traditional serrated adenoma.

Hyperplastic polyps (HP) are serrated lesions with symmetrical normally placed proliferative zone leading to simple tubular crypts with serrated epithelium. The micro-vesicular subtype (MVHP) shows prominent serration with many cells containing numerous tiny mucin vacuoles; the epithelium of the mucinous type/ Goblet Cell rich type (GCHP) is filled with large goblet cells. The latter is exclusively left sides and seems not to have significant propensity for progression to cancer and typically show Kras mutation rather than BRAF that is characteristic of MVHP.

It has been suggested that MVHP can progress to SSA or dysplastic lesions. There is also suggestive evidence that MVHP may progress to cancer skipping SSA stage.

Sessile Serrated Adenomas (SSA) are serrated lesions with asymmetrically placed proliferative zone to the side of the crypt leading to complex, inverted, branched (inverted L or T) and dilated crypts yet maintaining orientation towards muscularis mucosa.

With progression to microsatellite instable (MSI) carcinomas, dysplasia develops and can be observed in combination with dysplastic-SSA adenomas.

Traditional Serrated Adenoma (TSA) are serrated lesions with multifocal asymmetrically placed proliferative zones along the side of the crypts leading to complex large crypts surrounded by numerous tiny ectopic crypt lumens along the sides as well as profuse micropapillary infolding towards the lumen.

The orientation towards the muscularis mucosa is lost similar to tubular adenomas. Conventional APC-mutated adenomas with a serrated growth pattern vs. serration in TSA is evident when comparing a TSA with a dysplastic adenoma.

Dysplastic (traditional) adenomas contain phenotypically altered cells that are typically, but not exclusively, found in advanced tumors that are part of the MSS-APC tumor suppressor pathway (TA, TVA, VA), but are also observed in CIMP, not APC-associated and MSI pathway (SSA) as well as less clearly understood dysplasia associated with TSA. Morphologically dysplastic crypts are lined by dysplastic cells that show elongated hyperchromatic nuclei with high N/C ratio and often little mucin.

Dysplasia can by classified into low-grade and high grade. High-grade dysplasia is architecturally characterized by complex gland architecture, with gland-in-gland formation, cross-bridging of epithelium and often shows epithelial cell stratification. Cytologically, cells possess hyper-chromatic nuclei and marked increased N/C ratio leading to marked crowding appearance. The orientation of nuclei towards the basement membrane is typically lost. Occasionally, the cytologic anaplasia is so severe that in the absence of architectural complexity described above the diagnosis of high-grade dysplasia is justified. Anything less severe than the above description is categorized as low-grade dysplasia. It should be emphasized that a typical TA / TVA / VA would have smooth non-serrated epithelial borders. However, occasionally serration may be present in these lesions, and this would not change the classification or diagnostic implications.

REFERENCES

1. Siegel R, Desantis C, Jemal A. Colorectal cancer statistics, 2014. CA: a cancer journal for clinicians 2014;64(2):104-117.
2. Fearon ER, Vogelstein B. A genetic model for colorectal tumorigenesis. Cell 1990;61(5):759-767.
3. Fearon ER. Molecular genetics of colorectal cancer. Annual review of pathology 2011;6:479-507.
4. Bettington M, Walker N, Clouston A, Brown I, Leggett B, Whitehall V. The serrated pathway to colorectal carcinoma: current concepts and challenges. Histopathology 2013;62(3):367-386.
5. Rustgi AK. The genetics of hereditary colon cancer. Genes & development 2007;21(20):2525-2538.
6. Rex DK, Lehman GA, Ulbright TM et al. Colonic neoplasia in asymptomatic persons with negative fecal occult blood tests: influence of age, gender, and family history. The American journal of gastroenterology 1993;88(6):825-831.
7. Bosman FT, World Health Organization., International Agency for Research on Cancer. WHO classification of tumours of the digestive system. Lyon: International Agency for Research on Cancer; 2010. 417 p. p.
8. Mansoor S, Dolkar T, El-Fanek H. Polyps and polypoid lesions of the colon. International journal of surgical pathology 2013;21(3):215-223.
9. Jass JR. Classification of colorectal cancer based on correlation of clinical, morphological and molecular features. Histopathology 2007;50(1):113-130.
10. Gill P, Wang LM, Bailey A, East JE, Leedham S, Chetty R. Reporting trends of right-sided hyperplastic and sessile serrated polyps in a large teaching hospital over a 4-year period (2009-2012). Journal of clinical pathology 2013;66(8):655-658.
11. Rex DK, Ahnen DJ, Baron JA et al. Serrated lesions of the colorectum: review and recommendations from an expert panel. The American journal of gastroenterology 2012;107(9):1315-1329; quiz 1314, 1330.

12. Tadepalli US, Feihel D, Miller KM et al. A morphologic analysis of sessile serrated polyps observed during routine colonoscopy (with video). Gastrointestinal endoscopy 2011;74(6):1360-1368.
13. Kohler EM, Derungs A, Daum G, Behrens J, Schneikert J. Functional definition of the mutation cluster region of adenomatous polyposis coli in colorectal tumours. Human molecular genetics 2008;17(13):1978-1987.
14. Malumbres M, Barbacid M. RAS oncogenes: the first 30 years. Nature reviews Cancer 2003;3(6):459-465.
15. O'Brien MJ, Yang S, Mack C et al. Comparison of microsatellite instability, CpG island methylation phenotype, BRAF and KRAS status in serrated polyps and traditional adenomas indicates separate pathways to distinct colorectal carcinoma end points. The American journal of surgical pathology 2006;30(12):1491-1501.
16. Issa JP. CpG island methylator phenotype in cancer. Nature reviews Cancer 2004;4(12):988-993.
17. Weisenberger DJ, Siegmund KD, Campan M et al. CpG island methylator phenotype underlies sporadic microsatellite instability and is tightly associated with BRAF mutation in colorectal cancer. Nature genetics 2006;38(7):787-793.
18. Goel A, Nagasaka T, Hamelin R, Boland CR. An optimized pentaplex PCR for detecting DNA mismatch repair-deficient colorectal cancers. PloS one 2010;5(2):e9393.
19. Suraweera N, Duval A, Reperant M et al. Evaluation of tumor microsatellite instability using five quasimonomorphic mononucleotide repeats and pentaplex PCR. Gastroenterology 2002;123(6):1804-1811.
20. Boland CR, Thibodeau SN, Hamilton SR et al. A National Cancer Institute Workshop on Microsatellite Instability for cancer detection and familial predisposition: development of international criteria for the determination of microsatellite instability in colorectal cancer. Cancer research 1998;58(22):5248-5257.
21. Li WQ, Kawakami K, Ruszkiewicz A, Bennett G, Moore J, Iacopetta B. BRAF mutations are associated with distinctive clinical, pathological and molecular features of colorectal cancer independently of microsatellite instability status. Molecular cancer 2006;5:2.
22. Ogino S, Nosho K, Kirkner GJ et al. CpG island methylator phenotype, microsatellite instability, BRAF mutation and clinical outcome in colon cancer. Gut 2009;58(1):90-96.

23. Winawer SJ, Zauber AG, Ho MN et al. Prevention of colorectal cancer by colonoscopic polypectomy. The National Polyp Study Workgroup. The New England journal of medicine 1993;329(27):1977-1981.
24. Robertson DJ, Lieberman DA, Winawer SJ et al. Colorectal cancers soon after colonoscopy: a pooled multicohort analysis. Gut 2013.
25. Kavanagh AM, Giovannucci EL, Fuchs CS, Colditz GA. Screening endoscopy and risk of colorectal cancer in United States men. Cancer causes & control : CCC 1998;9(4):455-462.
26. Lieberman DA, Williams JL, Holub JL et al. Colonoscopy utilization and outcomes 2000 to 2011. Gastrointestinal endoscopy 2014;80(1):133-143 e133.
27. Levin B, Lieberman DA, McFarland B et al. Screening and surveillance for the early detection of colorectal cancer and adenomatous polyps, 2008: a joint guideline from the American Cancer Society, the US Multi-Society Task Force on Colorectal Cancer, and the American College of Radiology. Gastroenterology 2008;134(5):1570-1595.
28. Lieberman DA, Rex DK, Winawer SJ et al. Guidelines for colonoscopy surveillance after screening and polypectomy: a consensus update by the US Multi-Society Task Force on Colorectal Cancer. Gastroenterology 2012;143(3):844-857.
29. Winawer SJ. Screening of colorectal cancer. Surgical oncology clinics of North America 2005;14(4):699-722.
30. Corley DA, Jensen CD, Marks AR et al. Adenoma Detection Rate and Risk of Colorectal Cancer and Death. New England Journal of Medicine 2014;370(14):1298-1306.
31. Samadder NJ, Curtin K, Tuohy TM et al. Characteristics of missed or interval colorectal cancer and patient survival: a population-based study. Gastroenterology 2014;146(4):950-960.
32. le Clercq CM, Bouwens MW, Rondagh EJ et al. Postcolonoscopy colorectal cancers are preventable: a population-based study. Gut 2013.
33. Bressler B, Paszat LF, Vinden C, Li C, He J, Rabeneck L. Colonoscopic miss rates for right-sided colon cancer: a population-based analysis. Gastroenterology 2004;127(2):452-456.

34. Bressler B, Paszat LF, Chen Z, Rothwell DM, Vinden C, Rabeneck L. Rates of new or missed colorectal cancers after colonoscopy and their risk factors: a population-based analysis. Gastroenterology 2007;132(1):96-102.
35. Erichsen R, Baron JA, Stoffel EM, Laurberg S, Sandler RS, Sorensen HT. Characteristics and survival of interval and sporadic colorectal cancer patients: a nationwide population-based cohort study. The American journal of gastroenterology 2013;108(8):1332-1340.
36. Rondagh EJ, Masclee AA, Bouwens MW et al. Endoscopic red flags for the detection of high-risk serrated polyps: an observational study. Endoscopy 2011;43(12):1052-1058.
37. Burnett-Hartman AN, Passarelli MN, Adams SV et al. Differences in epidemiologic risk factors for colorectal adenomas and serrated polyps by lesion severity and anatomical site. American journal of epidemiology 2013;177(7):625-637.
38. Potter JD, Slattery ML, Bostick RM, Gapstur SM. Colon cancer: a review of the epidemiology. Epidemiologic reviews 1993;15(2):499-545.
39. Choi SY, Kahyo H. Effect of cigarette smoking and alcohol consumption in the etiology of cancers of the digestive tract. International journal of cancer Journal international du cancer 1991;49(3):381-386.
40. Sandler RS, Sandler DP, Comstock GW, Helsing KJ, Shore DL. Cigarette smoking and the risk of colorectal cancer in women. Journal of the National Cancer Institute 1988;80(16):1329-1333.
41. Hoff G, Vatn MH, Larsen S. Relationship between tobacco smoking and colorectal polyps. Scandinavian journal of gastroenterology 1987;22(1):13-16.
42. Zahm SH, Cocco P, Blair A. Tobacco smoking as a risk factor for colon polyps. American journal of public health 1991;81(7):846-849.
43. Botteri E, Iodice S, Bagnardi V, Raimondi S, Lowenfels AB, Maisonneuve P. Smoking and colorectal cancer: a meta-analysis. JAMA : the journal of the American Medical Association 2008;300(23):2765-2778.
44. Botteri E, Iodice S, Raimondi S, Maisonneuve P, Lowenfels AB. Cigarette smoking and adenomatous polyps: a meta-analysis. Gastroenterology 2008;134(2):388-395.
45. Samadder NJ, Vierkant RA, Tillmans LS et al. Cigarette smoking and colorectal cancer risk by KRAS mutation status among older women. The American journal of gastroenterology 2012;107(5):782-789.

46. Burnett-Hartman AN, Newcomb PA, Potter JD et al. Genomic Aberrations Occurring in Subsets of Serrated Colorectal Lesions but not Conventional Adenomas. Cancer research 2013;73(9):2863-2872.
47. Martinez ME, McPherson RS, Annegers JF, Levin B. Cigarette smoking and alcohol consumption as risk factors for colorectal adenomatous polyps. Journal of the National Cancer Institute 1995;87(4):274-279.
48. Harriss DJ, Atkinson G, George K et al. Lifestyle factors and colorectal cancer risk (1): systematic review and meta-analysis of associations with body mass index. Colorectal disease : the official journal of the Association of Coloproctology of Great Britain and Ireland 2009;11(6):547-563.
49. Cotterchio M, Boucher BA, Manno M, Gallinger S, Okey AB, Harper PA. Red meat intake, doneness, polymorphisms in genes that encode carcinogen-metabolizing enzymes, and colorectal cancer risk. Cancer epidemiology, biomarkers & prevention : a publication of the American Association for Cancer Research, cosponsored by the American Society of Preventive Oncology 2008;17(11):3098-3107.
50. Din FV, Theodoratou E, Farrington SM et al. Effect of aspirin and NSAIDs on risk and survival from colorectal cancer. Gut 2010;59(12):1670-1679.
51. Chan AT, Arber N, Burn J et al. Aspirin in the chemoprevention of colorectal neoplasia: an overview. Cancer Prev Res (Phila) 2012;5(2):164-178.
52. Dube C, Rostom A, Lewin G et al. The use of aspirin for primary prevention of colorectal cancer: a systematic review prepared for the U.S. Preventive Services Task Force. Annals of internal medicine 2007;146(5):365-375.
53. Chan AT, Ogino S, Fuchs CS. Aspirin and the risk of colorectal cancer in relation to the expression of COX-2. The New England journal of medicine 2007;356(21):2131-2142.
54. Giardiello FM, Offerhaus GJ, DuBois RN. The role of nonsteroidal anti-inflammatory drugs in colorectal cancer prevention. Eur J Cancer 1995;31A(7-8):1071-1076.
55. Thun MJ, Henley SJ, Patrono C. Nonsteroidal anti-inflammatory drugs as anticancer agents: mechanistic, pharmacologic, and clinical issues. Journal of the National Cancer Institute 2002;94(4):252-266.
56. Chan TA. Nonsteroidal anti-inflammatory drugs, apoptosis, and colon-cancer chemoprevention. The lancet oncology 2002;3(3):166-174.

57. Greenspan EJ, Madigan JP, Boardman LA, Rosenberg DW. Ibuprofen inhibits activation of nuclear {beta}-catenin in human colon adenomas and induces the phosphorylation of GSK-3{beta}. Cancer Prev Res (Phila) 2011;4(1):161-171.
58. Bird RP. Observation and quantification of aberrant crypts in the murine colon treated with a colon carcinogen: preliminary findings. Cancer letters 1987;37(2):147-151.
59. Di Gregorio C, Losi L, Fante R et al. Histology of aberrant crypt foci in the human colon. Histopathology 1997;30(4):328-334.
60. Rosenberg DW, Yang S, Pleau DC et al. Mutations in BRAF and KRAS differentially distinguish serrated versus non-serrated hyperplastic aberrant crypt foci in humans. Cancer research 2007;67(8):3551-3554.
61. McLellan EA, Bird RP. Aberrant crypts: potential preneoplastic lesions in the murine colon. Cancer research 1988;48(21):6187-6192.
62. Pretlow TP, Barrow BJ, Ashton WS et al. Aberrant crypts: putative preneoplastic foci in human colonic mucosa. Cancer research 1991;51(5):1564-1567.
63. Roncucci L, Stamp D, Medline A, Cullen JB, Bruce WR. Identification and quantification of aberrant crypt foci and microadenomas in the human colon. Human pathology 1991;22(3):287-294.
64. Pretlow TP, O'Riordan MA, Pretlow TG, Stellato TA. Aberrant crypts in human colonic mucosa: putative preneoplastic lesions. J Cell Biochem Suppl 1992;16G:55-62.
65. Smith AJ, Stern HS, Penner M et al. Somatic APC and K-ras codon 12 mutations in aberrant crypt foci from human colons. Cancer research 1994;54(21):5527-5530.
66. Losi L, Roncucci L, di Gregorio C, de Leon MP, Benhattar J. K-ras and p53 mutations in human colorectal aberrant crypt foci. The Journal of pathology 1996;178(3):259-263.
67. Takayama T, Ohi M, Hayashi T et al. Analysis of K-ras, APC, and beta-catenin in aberrant crypt foci in sporadic adenoma, cancer, and familial adenomatous polyposis. Gastroenterology 2001;121(3):599-611.
68. Augenlicht LH, Richards C, Corner G, Pretlow TP. Evidence for genomic instability in human colonic aberrant crypt foci. Oncogene 1996;12(8):1767-1772.
69. Heinen CD, Shivapurkar N, Tang Z, Groden J, Alabaster O. Microsatellite instability in aberrant crypt foci from human colons. Cancer research 1996;56(23):5339-5341.

70. Greenspan EJ, Cyr JL, Pleau DC et al. Microsatellite instability in aberrant crypt foci from patients without concurrent colon cancer. Carcinogenesis 2007;28(4):769-776.
71. Chan AO, Broaddus RR, Houlihan PS, Issa JP, Hamilton SR, Rashid A. CpG island methylation in aberrant crypt foci of the colorectum. The American journal of pathology 2002;160(5):1823-1830.
72. Greenspan EJ, Jablonski MA, Rajan TV, Levine J, Belinsky GS, Rosenberg DW. Epigenetic alterations in RASSF1A in human aberrant crypt foci. Carcinogenesis 2006;27(7):1316-1322.
73. Yokota T, Sugano K, Kondo H et al. Detection of aberrant crypt foci by magnifying colonoscopy. Gastrointestinal endoscopy 1997;46(1):61-65.
74. Anderson JC, Swede H, Rustagi T et al. Aberrant crypt foci as predictors of colorectal neoplasia on repeat colonoscopy. Cancer causes & control : CCC 2012;23(2):355-361.
75. Drew DA, Devers TJ, O'Brien MJ, Horelik NA, Levine J, Rosenberg DW. HD Chromoendoscopy Coupled with DNA Mass Spectrometry Profiling Identifies Somatic Mutations in Microdissected Human Proximal Aberrant Crypt Foci. Molecular cancer research : MCR 2014;12(6):823-829.
76. Beach R, Chan AO, Wu TT et al. BRAF mutations in aberrant crypt foci and hyperplastic polyposis. The American journal of pathology 2005;166(4):1069-1075.
77. Stevens RG, Swede H, Rosenberg DW. Epidemiology of colonic aberrant crypt foci: review and analysis of existing studies. Cancer letters 2007;252(2):171-183.
78. Takayama T, Katsuki S, Takahashi Y et al. Aberrant crypt foci of the colon as precursors of adenoma and cancer. The New England journal of medicine 1998;339(18):1277-1284.
79. Corpet DE, Tache S. Most effective colon cancer chemopreventive agents in rats: a systematic review of aberrant crypt foci and tumor data, ranked by potency. Nutrition and cancer 2002;43(1):1-21.
80. Roncucci L, Pedroni M, Vaccina F, Benatti P, Marzona L, De Pol A. Aberrant crypt foci in colorectal carcinogenesis. Cell and crypt dynamics. Cell proliferation 2000;33(1):1-18.
81. Fenoglio-Preiser CM, Noffsinger A. Aberrant crypt foci: A review. Toxicol Pathol 1999;27(6):632-642.
82. Alrawi SJ, Schiff M, Carroll RE et al. Aberrant crypt foci. Anticancer research 2006;26(1A):107-119.

83. Gupta AK, Schoen RE. Aberrant crypt foci: are they intermediate endpoints of colon carcinogenesis in humans? Current opinion in gastroenterology 2009;25(1):59-65.
84. Gupta AK, Pinsky P, Rall C et al. Reliability and accuracy of the endoscopic appearance in the identification of aberrant crypt foci. Gastrointestinal endoscopy 2009;70(2):322-330.
85. Cho NL, Redston M, Zauber AG et al. Aberrant crypt foci in the adenoma prevention with celecoxib trial. Cancer Prev Res (Phila) 2008;1(1):21-31.
86. Lance P, Hamilton SR. Sporadic aberrant crypt foci are not a surrogate endpoint for colorectal adenoma prevention. Cancer Prev Res (Phila) 2008;1(1):4-8.
87. Stevens RG, Pretlow TP, Hurlstone DP, Giardina C, Rosenberg DW. Comment re: "Sporadic aberrant crypt foci are not a surrogate endpoint for colorectal adenoma prevention" and "Aberrant crypt foci in the adenoma prevention with celecoxib trial". Cancer Prev Res (Phila) 2008;1(3):215-216; author reply 216.
88. Wargovich MJ, Brown VR, Morris J. Aberrant crypt foci: the case for inclusion as a biomarker for colon cancer. Cancers 2010;2(3):1705-1716.
89. The Paris endoscopic classification of superficial neoplastic lesions: esophagus, stomach, and colon: November 30 to December 1, 2002. Gastrointestinal endoscopy 2003;58(6 Suppl):S3-43.
90. Soetikno R, Friedland S, Kaltenbach T, Chayama K, Tanaka S. Nonpolypoid (flat and depressed) colorectal neoplasms. Gastroenterology 2006;130(2):566-576; quiz 588-569.
91. Bettington M, Walker N, Rosty C et al. Critical appraisal of the diagnosis of the sessile serrated adenoma. The American journal of surgical pathology 2014;38(2):158-166.
92. Lawless JF. Negative Binomial and Mixed Poisson Regression. Can J Stat 1987;15(3):209-225.
93. Boroff ES, Gurudu SR, Hentz JG, Leighton JA, Ramirez FC. Polyp and adenoma detection rates in the proximal and distal colon. The American journal of gastroenterology 2013;108(6):993-999.
94. Siddiqui AA, Nazario H, Mahgoub A, Patel M, Cipher D, Spechler SJ. For patients with colorectal cancer, the long-term use of statins is associated with better clinical outcomes. Digestive diseases and sciences 2009;54(6):1307-1311.

95. Siddiqui A, Nazario HE, Patel M, Mahgoub A, Spechler SJ. Reduction in low-density lipoprotein cholesterol levels during statin therapy is associated with a reduced incidence of advanced colon polyps. Am J Med Sci 2009;338(5):378-381.
96. Liu Y, Tang W, Wang J et al. Association between statin use and colorectal cancer risk: a meta-analysis of 42 studies. Cancer causes & control : CCC 2014;25(2):237-249.
97. Ng K, Ogino S, Meyerhardt JA et al. Relationship between statin use and colon cancer recurrence and survival: results from CALGB 89803. Journal of the National Cancer Institute 2011;103(20):1540-1551.
98. Lee JE, Baba Y, Ng K et al. Statin use and colorectal cancer risk according to molecular subtypes in two large prospective cohort studies. Cancer Prev Res (Phila) 2011;4(11):1808-1815.
99. Limburg PJ, Mahoney MR, Ziegler KL et al. Randomized phase II trial of sulindac, atorvastatin, and prebiotic dietary fiber for colorectal cancer chemoprevention. Cancer Prev Res (Phila) 2011;4(2):259-269.
100. Coogan PF, Smith J, Rosenberg L. Statin use and risk of colorectal cancer. Journal of the National Cancer Institute 2007;99(1):32-40.
101. Bertagnolli MM, Hsu M, Hawk ET, Eagle CJ, Zauber AG, Adenoma Prevention with Celecoxib Study I. Statin use and colorectal adenoma risk: results from the adenoma prevention with celecoxib trial. Cancer Prev Res (Phila) 2010;3(5):588-596.
102. Rosty C, Hewett DG, Brown IS, Leggett BA, Whitehall VL. Serrated polyps of the large intestine: current understanding of diagnosis, pathogenesis, and clinical management. Journal of gastroenterology 2013;48(3):287-302.
103. Dodou D, de Winter JC. The relationship between distal and proximal colonic neoplasia: a meta-analysis. Journal of general internal medicine 2012;27(3):361-370.
104. Chan AT. Aspirin and chemoprevention of cancer: reaching beyond the colon. Gastroenterology 2012;143(4):1110-1112.
105. Ishikawa H, Mutoh M, Suzuki S et al. The preventive effects of low-dose enteric-coated aspirin tablets on the development of colorectal tumours in Asian patients: a randomised trial. Gut 2014.
106. Raju GS, Vadyala V, Slack R et al. Adenoma detection in patients undergoing a comprehensive colonoscopy screening. Cancer medicine 2013;2(3):391-402.

107. Butterly L, Robinson CM, Anderson JC et al. Serrated and adenomatous polyp detection increases with longer withdrawal time: results from the New Hampshire Colonoscopy Registry. The American journal of gastroenterology 2014;109(3):417-426.
108. O'Neill RA, Bhamidipati A, Bi X et al. Isoelectric focusing technology quantifies protein signaling in 25 cells. Proceedings of the National Academy of Sciences of the United States of America 2006;103(44):16153-16158.
109. Fan AC, Deb-Basu D, Orban MW et al. Nanofluidic proteomic assay for serial analysis of oncoprotein activation in clinical specimens. Nature medicine 2009;15(5):566-571.
110. Kedei N, Telek A, Czap A et al. The synthetic bryostatin analog Merle 23 dissects distinct mechanisms of bryostatin activity in the LNCaP human prostate cancer cell line. Biochemical pharmacology 2011;81(11):1296-1308.
111. Garber K. Beyond sequencing: new diagnostic tests turn to pathways. Journal of the National Cancer Institute 2011;103(4):290-292.
112. Yang S, Farraye FA, Mack C, Posnik O, O'Brien MJ. BRAF and KRAS Mutations in hyperplastic polyps and serrated adenomas of the colorectum: relationship to histology and CpG island methylation status. The American journal of surgical pathology 2004;28(11):1452-1459.
113. Vogelstein B, Fearon ER, Hamilton SR et al. Genetic alterations during colorectal-tumor development. The New England journal of medicine 1988;319(9):525-532.
114. Longacre TA, Fenoglio-Preiser CM. Mixed hyperplastic adenomatous polyps/serrated adenomas. A distinct form of colorectal neoplasia. The American journal of surgical pathology 1990;14(6):524-537.
115. O'Brien MJ. Hyperplastic and serrated polyps of the colorectum. Gastroenterol Clin North Am 2007;36(4):947-968, viii.
116. Leggett B, Whitehall V. Role of the serrated pathway in colorectal cancer pathogenesis. Gastroenterology 2010;138(6):2088-2100.
117. van der Weyden L, Adams DJ. The Ras-association domain family (RASSF) members and their role in human tumourigenesis. Biochimica et biophysica acta 2007;1776(1):58-85.
118. Network TCGA. Comprehensive molecular characterization of human colon and rectal cancer. Nature 2012;487(7407):330-337.

119. Lloyd AC. Distinct functions for ERKs? J Biol 2006;5(5):13.
120. Vantaggiato C, Formentini I, Bondanza A, Bonini C, Naldini L, Brambilla R. ERK1 and ERK2 mitogen-activated protein kinases affect Ras-dependent cell signaling differentially. J Biol 2006;5(5):14.
121. Roskoski R, Jr. ERK1/2 MAP kinases: structure, function, and regulation. Pharmacological research : the official journal of the Italian Pharmacological Society 2012;66(2):105-143.
122. Carragher LA, Snell KR, Giblett SM et al. V600EBraf induces gastrointestinal crypt senescence and promotes tumour progression through enhanced CpG methylation of p16INK4a. EMBO molecular medicine 2010;2(11):458-471.
123. Bennecke M, Kriegl L, Bajbouj M et al. Ink4a/Arf and oncogene-induced senescence prevent tumor progression during alternative colorectal tumorigenesis. Cancer cell 2010;18(2):135-146.
124. Collado M, Blasco MA, Serrano M. Cellular senescence in cancer and aging. Cell 2007;130(2):223-233.
125. Guo Y, Yuan C, Weghorst CM, Li J. IKKbeta specifically binds to P16 and phosphorylates Ser8 of P16. Biochemical and biophysical research communications 2010;393(3):504-508.
126. Gump J, Stokoe D, McCormick F. Phosphorylation of p16INK4A correlates with Cdk4 association. The Journal of biological chemistry 2003;278(9):6619-6622.
127. Rougier P, Mitry E. Epidemiology, treatment and chemoprevention in colorectal cancer. Annals of oncology : official journal of the European Society for Medical Oncology / ESMO 2003;14 Suppl 2:ii3-5.
128. Baxter NN, Goldwasser MA, Paszat LF, Saskin R, Urbach DR, Rabeneck L. Association of colonoscopy and death from colorectal cancer. Annals of internal medicine 2009;150(1):1-8.
129. Cooper GS, Xu F, Barnholtz Sloan JS, Schluchter MD, Koroukian SM. Prevalence and predictors of interval colorectal cancers in medicare beneficiaries. Cancer 2012;118(12):3044-3052.

130. Drew DA, Devers T, Horelik N et al. Nanoproteomic analysis of extracellular receptor kinase-1/2 post-translational activation in microdissected human hyperplastic colon lesions. Proteomics 2013;13(9):1428-1436.
131. Fumagalli D, Gavin PG, Taniyama Y et al. A rapid, sensitive, reproducible and cost-effective method for mutation profiling of colon cancer and metastatic lymph nodes. BMC Cancer 2010;10:101.
132. Kosaka T, Yatabe Y, Endoh H, Kuwano H, Takahashi T, Mitsudomi T. Mutations of the epidermal growth factor receptor gene in lung cancer: biological and clinical implications. Cancer research 2004;64(24):8919-8923.
133. Grundler R, Thiede C, Miething C, Steudel C, Peschel C, Duyster J. Sensitivity toward tyrosine kinase inhibitors varies between different activating mutations of the FLT3 receptor. Blood 2003;102(2):646-651.
134. Miyaki M, Konishi M, Kikuchi-Yanoshita R et al. Characteristics of somatic mutation of the adenomatous polyposis coli gene in colorectal tumors. Cancer research 1994;54(11):3011-3020.
135. Aretz S, Stienen D, Uhlhaas S et al. Large submicroscopic genomic APC deletions are a common cause of typical familial adenomatous polyposis. Journal of medical genetics 2005;42(2):185-192.
136. Kanter-Smoler G, Fritzell K, Rohlin A et al. Clinical characterization and the mutation spectrum in Swedish adenomatous polyposis families. BMC medicine 2008;6:10.
137. Siu IM, Robinson DR, Schwartz S et al. The identification of monoclonality in human aberrant crypt foci. Cancer research 1999;59(1):63-66.
138. De Rosa M, Scarano MI, Panariello L et al. The mutation spectrum of the APC gene in FAP patients from southern Italy: detection of known and four novel mutations. Human mutation 2003;21(6):655-656.
139. Orlando FA, Tan D, Baltodano JD et al. Aberrant crypt foci as precursors in colorectal cancer progression. Journal of surgical oncology 2008;98(3):207-213.
140. Popat S, Hubner R, Houlston RS. Systematic review of microsatellite instability and colorectal cancer prognosis. J Clin Oncol 2005;23(3):609-618.

141. Halling KC, French AJ, McDonnell SK et al. Microsatellite instability and 8p allelic imbalance in stage B2 and C colorectal cancers. Journal of the National Cancer Institute 1999;91(15):1295-1303.
142. Lin CC, Lin JK, Lin TC et al. The prognostic role of microsatellite instability, codon-specific KRAS, and BRAF mutations in colon cancer. Journal of surgical oncology 2014.
143. Gupta AK, Pretlow TP, Schoen RE. Aberrant crypt foci: what we know and what we need to know. Clinical gastroenterology and hepatology : the official clinical practice journal of the American Gastroenterological Association 2007;5(5):526-533.
144. Olivo S, Wargovich MJ. Inhibition of aberrant crypt foci by chemopreventive agents. In vivo 1998;12(2):159-166.
145. Sakai E, Takahashi H, Kato S et al. Investigation of the prevalence and number of aberrant crypt foci associated with human colorectal neoplasm. Cancer epidemiology, biomarkers & prevention : a publication of the American Association for Cancer Research, cosponsored by the American Society of Preventive Oncology 2011;20(9):1918-1924.
146. Archer MC, Bruce WR, Chan CC et al. Aberrant crypt foci and microadenoma as markers for colon cancer. Environmental health perspectives 1992;98:195-197.
147. Roncucci L, Medline A, Bruce WR. Classification of aberrant crypt foci and microadenomas in human colon. Cancer epidemiology, biomarkers & prevention : a publication of the American Association for Cancer Research, cosponsored by the American Society of Preventive Oncology 1991;1(1):57-60.
148. Pretlow TP, Pretlow TG. Mutant KRAS in aberrant crypt foci (ACF): initiation of colorectal cancer? Biochimica et biophysica acta 2005;1756(2):83-96.
149. Jass JR, Whitehall VL, Young J, Leggett BA. Emerging concepts in colorectal neoplasia. Gastroenterology 2002;123(3):862-876.
150. Hanahan D, Weinberg RA. The hallmarks of cancer. Cell 2000;100(1):57-70.
151. Hanahan D, Weinberg RA. Hallmarks of cancer: the next generation. Cell 2011;144(5):646-674.
152. Serrano M, Lin AW, McCurrach ME, Beach D, Lowe SW. Oncogenic ras provokes premature cell senescence associated with accumulation of p53 and p16INK4a. Cell 1997;88(5):593-602.

153. Lin B, Gupta D, Heinen CD. Human Pluripotent Stem Cells Have A Novel Mismatch Repair-Dependent Damage Response. The Journal of biological chemistry 2014.

154. Meissner A, Gnirke A, Bell GW, Ramsahoye B, Lander ES, Jaenisch R. Reduced representation bisulfite sequencing for comparative high-resolution DNA methylation analysis. Nucleic acids research 2005;33(18):5868-5877.

155. Hahn MA, Li AX, Wu X et al. Loss of the polycomb mark from bivalent promoters leads to activation of cancer-promoting genes in colorectal tumors. Cancer research 2014;74(13):3617-3629.